

Characterization of *TRAPPC11* and *GOSR2* mutations in human fibroblasts

Keshika Prematilake

A Thesis
in
The Department
of
Biology

Presented in Partial Fulfillment of the Requirements
for the Degree of Master of Biology at
Concordia University
Montreal, Quebec, Canada

October 2016

© Keshika Prematilake, 2016

CONCORDIA UNIVERSITY
School of Graduate Studies

This is to certify that the thesis prepared

By: Keshika Prematilake

Entitled: Characterization of *TRAPPC11* and *GOSR2* mutations in human fibroblasts

and submitted in partial fulfillment of the requirements for the degree of

Master of Science (Biology)

complies with the regulations of the University and meets the accepted standards with respect to originality and quality.

Signed by the final examining committee:

Dr. Grant Brown Chair

Dr. Vladimir Titorenko Examiner

Dr. Alisa Piekny Examiner

Dr. Michael Sacher Supervisor

Approved by Dr. Patrick Gulick
Chair of Department or Graduate Program Director

Dr. André Roy
Dean of Faculty

Date November 30, 2016

ABSTRACT

Characterization of *TRAPPC11* and *GOSR2* mutations in human fibroblasts

Keshika Prematilake

Eukaryotic cells consist of membrane-bounded organelles which communicate with each other through vesicles for the movement of proteins and lipids between them in a process called membrane traffic. It requires different types of proteins to facilitate docking and fusion of the cargo-containing vesicles to the correct compartment. Among them are a diverse group of membrane proteins called tethering factors including multi-subunit tethering complexes (MTCs). The transport protein particle (TRAPP) complexes are a family of related MTCs that are conserved from yeast to humans. Subunits of the mammalian TRAPP complexes are known to be involved in ER-to-Golgi and intra-Golgi trafficking while playing a fundamental role in Golgi morphology. The *TRAPPC11* subunit of the mammalian TRAPP III complex has been implicated in ER-to-ERGIC trafficking as well as autophagy. The mammalian TRAPP subunits are linked to a broad range of diseases of which the mechanism and the cause are not fully understood.

In this study, homozygous and compound heterozygous mutations in the *TRAPPC11* gene in human fibroblasts from five individuals were characterized using several biochemical, immunofluorescence and live cell microscopy techniques to identify the defective pathways and the effect of the mutations at the cellular level. Included in this study were two individuals with *GOSR2* mutations displaying similar clinical features to patients with *TRAPPC11* mutations. We hypothesized that the *TRAPPC11* mutations would result in a number of different defects at the cellular level given the number of pathways *TRAPPC11* has been suggested to function within. The current study suggests that some of the *TRAPPC11* mutations are linked to a variety of cellular phenotypes including hypoglycosylation of proteins, ER-to-Golgi trafficking defects, delay in the exit of proteins from the Golgi, Golgi fragmentation, defects in the autophagy pathway as well as partial disassembly of the complex. Golgi soluble N-ethylmaleimide-sensitive factor attachment protein receptor complex 2 (*GOSR2*) is a protein located in the cis-Golgi to facilitate docking and fusion of COPII vesicles from the ER. The current study also suggests that some of the *GOSR2*

mutations are linked to hypoglycosylation of proteins, ER-to-Golgi trafficking defects as well as a delay in the exit of proteins from the Golgi.

The affected individuals showed novel mutations in *TRAPPC11* and *GOSR2* as well as mutations seen in previous studies. Some of the earlier *TRAPPC11* mutations were in or near the foie gras domain, and these new *TRAPPC11* mutations cluster near that region. This suggests that the foie gras domain plays a critical role in the function of the TRAPPC11 protein. Since, *TRAPPC11* mutations affect the brain, eyes, liver, muscle, and bone, this suggests that the TRAPPC11 protein has a function in multiple tissue types and organs as well as homeostasis of the organism. This study and previous studies of *TRAPPC11* lead to the conclusion that *TRAPPC11* mutations, in general, result in neuromuscular phenotypes. In conclusion, these mutations can be added to the growing group of mutations in *TRAPPC11* and *GOSR2* causing neuromuscular and myopathy phenotypes. A better understanding of these mutations which result in neuromuscular phenotypes will allow for the screening of individuals who carry these mutations and further investigate the mechanism and treatment for these diseases.

ACKNOWLEDGEMENTS

I would like to express my deepest gratitude to teachers, friends, near and dear ones that I encountered during my Master's study who have shaped me and nurtured me to become who I am today. I would like to express my heartfelt gratitude to my supervisor, Dr. Michael Sacher, without whom I would not have been able to complete my thesis in high standards. I owe a debt of gratitude to Dr. Michael Sacher for constant guidance, support, and advice on experiments, presentations, and writings. I feel very much fortunate to learn from the best in the Department of Biology including Dr. Michael Sacher, my committee members, Dr. Alisa Piekny and Dr. Vladimir Titorenko, and professors such as Dr. Selvadurai Daya Dayanandan, Dr. Dylan Fraser, and Dr. William Zerges. I would like to express gratitude towards Dr. Christopher Brett and Dr. William Zerges for their support and reagents for experiments. I am grateful to CMCI for the use of equipment and Ms. Melina Jaramillo Garcia and Dr. Chloe Van Oostende for constant help and patience. My gratitude is extended to collaborators of my research without whom the work would not have been possible: Dr. Katrin Koehler, Dr. Angela Huebner, Dr. Austin A. Larson, Dr. Steven A. Moore and Dr. Cecilia Jimenez-Mallebrera for providing the fibroblasts and sharing genetic information of the subjects. I would also like to thank Dr. Martin Lowe and Dr. Kelley Moreman for reagents.

I wish to express my heartfelt gratitude to friends and senior lab mates; Dr. Miroslav P. Milev, Dr. Djenann Saint-Dic and Dr. Stephanie Brunet for training me in tissue culture work and gel filtration techniques. I am greatly indebted to Dr. Miroslav P. Milev for constant help in all aspects, constructive criticism on my work, helpful suggestions in carrying out the work and immense patience. I am deeply thankful to all of my colleagues and friends at Concordia University for helping me with my research and creating a cheerful environment to work. I would like to thank especially Benedeta, Daniela, Qingchuan, Alexandra, Amer, Thierry, Yehya, Sari, Nassim, Rodney, James, Vinitha, and Yu. This thesis is dedicated to my parents, Ananda and Kamanie, brothers, Sameera and Chamil, as well as my beloved husband, Shailesh, for their immense physical and mental support, encouragement and guidance.

I would like to show my appreciation to Ms. Kelly Pingel and Ms. Donna Stewart for the assistance in administrative work and help in meeting requirements for the program and scholarships. I am grateful to funding I received from Concordia University and GRASP (Groupe de Recherche Axé sur la Structure des Protéines) throughout my studies. Finally, I would like to express my gratitude to Concordia University for providing me the opportunity to pursue my Master's degree.

CONTRIBUTION OF AUTHORS

This thesis is comprised of three collaborative works which have been compressed into a chapter-based thesis according to Concordia University thesis preparation guidelines. The experimental settings provided here were completely designed by my supervisor, Dr. Michael Sacher, and myself. I have performed all the tissue culture work, ts045-VSV-G-GFP membrane trafficking assay, immunostaining, transfection, infection, western blotting, starvation experiments and statistical analysis of biochemical experiments. Dr. Miroslav P. Milev captured live-cell images and fixed cell images, helped in gel filtration experiments and performed quantification of data for the live-cell movies. Dr. Michael Sacher and I analyzed the data and I wrote the thesis with the guidance of Dr. Michael Sacher.

The manuscript for the first collaborative work (Subjects 1 and 2; Appendix I) was written by Dr. Katrin Koehler and Dr. Michael Sacher. Dr. Angela Huebner, Dr. Michael Sacher, and Dr. Katrin Koehler supervised the work and obtained funding support. Eda Utine and Filiz Hazan phenotyped the subjects. Markus Schuelke and Dr. Katrin Koehler processed, analyzed and validated the whole exome sequencing data. Susann Kutzner, Dana Landgraf, and Felix Reschke performed the Sanger sequencing. Dana Landgraf performed RNA and microsatellite analysis and Gulden Diniz performed the immunohistochemistry. Dr. Miroslav P. Milev and I performed western blotting, biochemical assays, immunostaining and time-lapse microscopy. Dr. Katrin Koehler, Dr. Miroslav P. Milev, myself, Ramona Jühlen and Dr. Michael Sacher analyzed and interpreted the data.

The manuscript for the second collaborative work (Subjects 3-5) is in preparation and was written by Dr. Austin A. Larson and Dr. Michael Sacher. Dr. Austin A. Larson, Dr. Steven A. Moore, and Peter R. Baker II designed the study. Dr. Steven A. Moore, Mary O. Cox, and Dr. Michael Sacher supervised the work and obtained funding support. Jacqueline K. Lekostaj, Aaron A. Stence, Aaron D. Bossler developed dystroglycanopathy sequencing panel and genetic evaluation of Subject 4. Dr. Steven A. Moore performed muscle biopsy, cultured fibroblast evaluation, and coordinated clinical groups. Mary O. Cox maintained fibroblast cultures and performed western blots. Dr. Miroslav P. Milev and I performed western blotting, biochemical

assays, immunostaining and time-lapse microscopy. Dr. Miroslav P. Milev, myself, and Dr. Michael Sacher analyzed and interpreted the data.

The manuscript for the third collaborative work (Subjects 6 and 7) is in preparation and the manuscript will be written by Dr. Cecilia Jimenez-Mallebrera and Dr. Michael Sacher. Dr. Cecilia Jimenez-Mallebrera and Dr. Michael Sacher designed this study, supervised the work and obtained funding support. Dr. Miroslav P. Milev and I performed western blotting, biochemical assays, gel filtration, immunostaining and time-lapse microscopy. Dr. Miroslav P. Milev, myself and Dr. Michael Sacher analysed and interpreted the data.

TABLE OF CONTENTS

List of figures.....	xi
List of tables.....	xii
List of abbreviations	xiii
Chapter 1: Introduction.....	1
1.1 Membrane trafficking.....	1
1.2 Tethering factors.....	3
1.2.1 TRAPP complexes of yeast.....	5
1.2.2 Mammalian TRAPP complexes.....	7
1.3 TRAPPC11 and TRAPPC12.....	11
1.3.1 <i>TRAPPC11</i> mutations reported to date.....	13
1.4 Autophagy.....	15
1.5 Neuromuscular diseases.....	17
1.6 Introduction to project: Characterization of <i>TRAPPC11</i> and <i>GOSR2</i> mutations in human fibroblasts.....	18
Chapter 2: Material and methods.....	20
2.1 Buffers and solutions.....	20
2.2 Cell culture conditions.....	21
2.3 Amino acid starvation.....	22
2.4 Transfection of mammalian cells.....	22
2.5 ts045-VSV-G-GFP membrane trafficking assay.....	23
2.5.1 Cell harvest and Western blotting.....	24
2.5.2 Immunofluorescence microscopy.....	25
2.5.3 Live-cell microscopy.....	27
2.6 Size exclusion chromatography.....	28
2.7 Statistical analysis.....	28
Chapter 3: Results.....	29
3.1 A <i>TRAPPC11</i> mutation results in a Triple A-like syndrome	29
3.2 <i>TRAPPC11</i> and <i>GOSR2</i> mutations cause α – dystroglycanopathy	30
3.3 Other cases with <i>TRAPPC11</i> mutations.....	31

3.4 TRAPPC11 protein levels are reduced in patients with certain <i>TRAPPC11</i> mutations.....	32
3.5 The effects of <i>TRAPPC11</i> and <i>GOSR2</i> mutations on the trafficking of VSV-G-GFP as assessed biochemically.....	34
3.6 Accumulation of VSV-G-GFP in the Golgi in individuals with different <i>TRAPPC11</i> mutations.....	37
3.7 VSV-G-GFP shows a significant delay in trafficking to and through the Golgi in individuals with <i>TRAPPC11</i> and <i>GOSR2</i> mutations	39
3.8 Altered LAMP1 and TGN46 localization in fibroblasts from an individual with <i>TRAPPC11</i> mutations.....	41
3.9 <i>TRAPPC11</i> mutations show reduced autophagy activity.....	42
3.10 Individuals with <i>TRAPPC11</i> mutations display altered TRAPP complex assembly.....	44
Chapter 4: Discussion.....	45
Chapter 5: Reference.....	51
Chapter 6: Appendix I.....	71

LIST OF FIGURES

Figure 1.1: Cartoon representation of the TRAPPC11 protein with mutations reported to date.....	15
Figure 1.2: Cartoon representation of the novel <i>TRAPPC11</i> mutations in this study.....	19
Figure 3.1: Western blot analysis of the lysates for TRAPPC11 and LAMP1.....	33
Figure 3.2: The ts045-vesicular stomatitis virus glycoprotein-GFP trafficking assay applied to HeLa cells.....	35
Figure 3.3: Affected individuals show a delay in endoglycosidase H resistance.....	36
Figure 3.4: The ts045-vesicular stomatitis virus glycoprotein-GFP in fibroblasts from affected individuals showed delayed kinetics of transport and accumulation in the Golgi..	38
Figure 3.5: Live-cell imaging of fibroblasts from affected individuals confirmed delayed kinetics of transport and accumulation of the ts045-vesicular stomatitis virus glycoprotein-GFP in the Golgi.	40
Figure 3.6: Altered LAMP1 and TGN46 localization in fibroblasts from control and the affected individual.....	42
Figure 3.7: Reduced autophagy activity in the fibroblasts from affected individuals.....	43
Figure 3.8: Subject 7 displays a shift in the TRAPPC12 subunit to a smaller molecular size.....	44
Figure 4.1: Cartoon representation of the current <i>TRAPPC11</i> mutations reported to date.....	49

LIST OF TABLES

Table 1.1 Yeast and mammalian TRAPP subunits and diseases associated with subunits...	10
Table 1.2 Mutations of <i>TRAPPC11</i> reported to date	14
Table 1.3 Novel mutations of <i>TRAPPC11</i> in this study.....	19
Table 2.1 Buffers and solutions used in the study.....	20
Table 2.2 siRNAs used in the study.....	23
Table 2.3 Primary antibodies used in the study.....	26
Table 2.4 Secondary antibodies used in the study.....	27
Table 3.1 Nomenclature of the subjects studied in the study.....	32
Table 4.1 Current mutations of <i>TRAPPC11</i> reported to date and mentioned in this study....	50

LIST OF ABBREVIATIONS

Amyotrophic lateral sclerosis	ALS
Autophagosome	AP
Autophagy-specific proteins	Atgs
Bafilomycin A1	Baf. A1
Centromere-associated protein E	CENP-E
Class C core vacuole/endosome tethering	CORVET
Coat protein complex I and II	COPI and II
Congenital disorders of glycosylation	CDG
Congenital muscular dystrophy	CMD
Conserved oligomeric Golgi complex	COG
Control	CTRL
Creatine kinase	CK
Cross-adsorbed	CA
Cycloheximide	CXM
Dimethyl-sulphoxide	DMSO
Distal myopathy with rimmed vacuoles	DMRV
Dithiothreitol	DTT
Dulbecco's modified Eagle's medium	DMEM
Earle's balanced salt solution	EBSS
Endoglycosidase H	EndoH
Endoplasmic reticulum	ER
Enhanced chemiluminescence	ECL
ER-Golgi intermediate compartment	ERGIC
Ethylenediaminetetraacetic acid	EDTA
Fetal bovine serum	FBS
Golgi apparatus	Golgi
Golgi soluble N-ethylmaleimide-sensitive factor attachment protein receptor complex 2	GOSR2

Golgi-associated retrograde protein	GARP
Green fluorescence protein	GFP
GTPase-activating proteins	GAPs
Guanine nucleotide exchange factors	GEFs
Guanosine triphosphate	GTP
Highly cross-adsorbed	HCA
Homotypic fusion and vacuole protein sorting	HOPS
Horseradish peroxidase	HRP
Human papillomavirus	HPV
Immunofluorescence	IF
Kilodaltons	kDa
Knockdown	KD
Limb-girdle muscular dystrophy	LGMD
Lipid-linked oligosaccharides	LLOs
Lysosome-associated membrane protein 1	LAMP1
Mammalian TRANsport Protein Particle	mTRAPP
Mannosidase II	ManII
MAP kinase kinase	MEK1
Microtubule-associated protein 1 light chain 3	LC3
Microtubule-organizing center	MTOC
Multisubunit tethering complexes	MTCs
National Institute of Health	NIH
N-ethylmaleimide	NEM
Normal goat serum	NGS
Oculopharyngeal muscular dystrophy	OPMD
Paraformaldehyde	PFA
Phosphate-buffered saline	PBS
Plasma membrane	PM
Pre-autophagosomal structure	PAS
Progressive myoclonus epilepsy	PME

<i>Schizosaccharomyces pombe</i>	<i>S. pombe</i>
Small interfering RNA	siRNA
Sodium dodecyl sulfate-polyacrylamide gel electrophoresis	SDS-PAGE
Soluble N-ethylmaleimide-sensitive factor attachment protein receptors	SNAREs
Spondyloepiphyseal dysplasia tarda	SED1 or SEDL
Standard error of the mean	SEM
Target SNAREs	t-SNAREs
Target-of-rapamycin	TOR
Temperature-sensitive vesicular stomatitis virus glycoprotein fused to GFP	ts045-VSV-G-GFP
Tetratricopeptide repeats	TPR
Trans-Golgi network	TGN
Translocon-associated protein	TRAP α
TRANsport Protein Particle	TRAPP
Vacuole protein sorting complex	VPS-C
Vesicle snares	v-SNAREs
Western blotting	WB
X-linked myopathy with excessive autophagy	XMEA
α -dystroglycan	α -DG

1 INTRODUCTION

1.1 Membrane trafficking

Eukaryotic cells consist of membrane-bound organelles which communicate with each other and the immediate environment surrounding the cells (Tokarev et al., 2009). The movement of proteins and lipids between these membrane-bounded compartments is mediated by transport of vesicles in a process called membrane traffic. The membrane traffic process includes the exocytic pathway which carries cargoes from the endoplasmic reticulum (ER) to the cell membrane and outside of the cell and the endocytic pathway which imports cargoes from the immediate environment bringing them into the cell. The membrane traffic pathways combined control the flow of cargo inside the cell by regulating the budding of cargo-containing vesicles, their transport along the cytoskeleton, and fusion with the acceptor membrane. Membrane trafficking is crucial for the viability and proper function of the cell as it allows the cell to communicate among its organelles and with its immediate environment to obtain nutrition and cellular signals (Tokarev et al., 2009).

During membrane trafficking, the cargo-containing vesicles bud from the donor compartments using specific coat and adaptor proteins such as coat protein complex I, II (COPI, II) and clathrin adaptor complexes which mediate endosomal trafficking. The COPII complex mediates anterograde transport from the ER to the Golgi apparatus (Golgi) while COPI mediates retrograde transport from the Golgi to the ER and intra-Golgi trafficking. The fusion of the vesicles at the correct acceptor compartment(s) involves vesicle capturing (or tethering) by a correct combination of vesicle-capturing equipment and membrane anchors such as soluble N-ethylmaleimide-sensitive factor attachment protein receptors (SNAREs) present at the vesicle (v-SNAREs) and the acceptor compartment(s) (t-SNAREs) (Sato and Nakano, 2005). The budding and fusion events are both governed by small GTPases which in turn are regulated by guanine nucleotide exchange factors (GEFs) and GTPase-activating proteins (GAPs). In combination, these proteins tightly regulate the directionality and reliability of the intracellular membrane trafficking.

In eukaryotic cells, newly synthesized proteins containing a signal sequence enter the ER during translation through a translocon pore via a signal recognition machinery. The proteins inside the ER or residing on the ER membrane are controlled for proper folding and assembly before exiting the ER at ER exit sites (Fewell and Brodsky, 2009). The newly formed vesicles travel from the ER to the Golgi via diffusion or by the help of microtubules and associated motor proteins (Presley et al., 1997). The ER-derived cargo-containing vesicles travel towards the microtubule-organizing center (MTOC) and fuse with the Golgi at the cis-Golgi cisterna and the cargo is subsequently processed in the medial- and trans-Golgi network (TGN). The TGN acts as a major sorting station for proteins and lipids. The proteins are directed to different organelles such as endosomes and lysosomes, embedded in the plasma membrane (PM) to facilitate membrane expansion during cell growth or secreted to the extracellular environment upon modifications by both ER and Golgi enzymes to include sugars and lipids in a highly ordered manner (Tokarev et al., 2009).

Early vesicle-mediated transport occurs between the ER and the Golgi via vesicles formed through the COPII and COPI machinery (Barlowe et al, 1994). The COPII vesicles contain a membrane bilayer with many proteins which allows it to be highly flexible to form positive membrane curvature to bud from the ER and to disassemble immediately after transport via GTP hydrolysis. (Barlowe et al, 1994; Sato and Nakano, 2005; Lord et al, 2011; Zanetti et al., 2013; Koreishi et al, 2013). The early intracellular membrane trafficking in mammalian cells differs from that in yeast as it involves fusion of COPII vesicles from the ER to form the ER-Golgi intermediate compartment (ERGIC) for further sorting of the cargoes before microtubule-dependent vesicle trafficking to the Golgi (Presley et al, 1997; Klumperman et al., 1998; Martinez-Menarguez et al, 1999; Breuza et al, 2004). During membrane trafficking, the organelle identity and size has to be maintained. This is accomplished by retrograde transport where molecules used for anterograde transport are recycled back to the original organelle. The retrograde transport from the Golgi to the ER occurs via Golgi-derived COPI vesicles involving the Dsl1 tethering complex and syntaxin 18 with the aid of the SNAREs at the ER.

The SNARE complexes play a major role in facilitating fusion at the acceptor compartment(s) by selectively locating at different compartments. However, SNAREs cannot

confirm all the selectivity as SNAREs form multiple complexes during multiple stages of membrane trafficking and have been shown to be promiscuous (Banfield, 2001). Therefore, other proteins have to partake in vesicle recognition to ensure selectivity.

1.2 Tethering factors

In order to facilitate SNAREs in docking and fusion of the cargo-containing vesicles to the correct compartment, a peripherally-associated diverse group of membrane protein complexes called tethering factors are required (Lupashin and Sztul, 2009). The tethering factors function either at a single step of the membrane trafficking pathway or at multiple steps such as the formation of SNAREs, cargo selection, and linking the vesicle to the neighboring membranes before fusion (Lupashin and Sztul, 2009). They acquire these functions by binding to coat proteins, activating specific Rab and Arl GTPases, and/or associating with different SNAREs (Bacon et al., 1989; Andag and Schmitt, 2003; Behnia et al., 2007; Cai et al., 2007; Zink et al., 2009). Tethering factors differ from tethers in a sense that tethers directly tether vesicles while tethering factors organize other factors needed for tethering (Brunet and Sacher, 2014). They act in homotypic fusion where two identical compartments fuse such as fusion of early endosomes, and/or in heterotypic fusion where two different compartments fuse such as fusion of COPI vesicles with the ER (Lupashin and Sztul, 2009).

Tethering factors are grouped into two general classes based on their structure called multisubunit tethering complexes (MTCs) and coiled-coil proteins. Recently, they have also been classified into three functional classes based on phylogeny and structure. The first are complexes which bind to SNAREs and function as the Rab effectors such as Dsl1 complex, conserved oligomeric Golgi (COG) complex, Golgi-associated retrograde protein (GARP) complex, homotypic fusion and vacuole protein sorting (HOPS), and Exocyst. The next group are complexes which act as GEFs for Rab proteins and consist of transport protein particle (TRAPP) complexes (I-III) and HOPS which may initiate tethering of coiled-coil tethers for fusion (Lupashin and Sztul, 2009). The last group is categorized into the coiled-coil tethers which include mammalian proteins p115, GM130, Giantin, Golgins, and early endosome antigen 1 (EEA1).

The MTCs were first characterized in budding yeast, *Saccharomyces cerevisiae*, and consist of eight different MTCs with homologs in higher eukaryotes. The MTCs include the above-mentioned complexes (Dsl1, COG, GARP, HOPS, TRAPP, and exocyst) as well as Class C core vacuole/endosome tethering (CORVET) complex and two vacuole protein sorting (VPS)-C complexes. Only CORVET, VPS-C, and HOPS are a heterogeneous family of proteins with interconvertible subunits, analogous to TRAPP complexes which have interconvertible subunits (Peplowska et al., 2007). MTCs contain 3 to 10 subunits which interact with vesicles over a short distance (up to 30 nm) to perform tethering of vesicles that are in close proximity. The ER-to-Golgi traffic requires MTCs such as Dsl1, COG, and TRAPPI and coiled-coil tethers, p115 and GM130. The COG and TRAPPII complexes play a role in intra-Golgi traffic as well as ER-to-Golgi traffic (Lupashin and Sztul, 2009). The TGN-endosomal-lysosomal pathway is regulated by TRAPPIII, HOPS, and GARP complexes.

In order to maintain the proper size and function of each cellular compartment, the budding and fusion events are coordinated to integrate anterograde and retrograde traffic, a process that involves tethering factors. The tethering factors proofread and aid assembly of SNAREs and act as effectors or activators for the Rab GTPases (Shestakova et al., 2007; Starai et al., 2008; Pérez-Victoria and Bonifacino, 2009; Ren et al., 2009). The GEF activity is the most upstream event in the tethering process. GEFs are recruited to membranes to generate guanosine triphosphate (GTP)-Rabs. The GTP-activated Rab then recruits oligomeric Rab effectors or long coiled-coil tethers and other membrane receptors to tether a vesicle while increasing selectivity (Lupashin and Sztul, 2009). For example, the fusion of COPII vesicles at the ERGIC is regulated by the mammalian TRAPP complexes which activate RAB1 to recruit p115 to the membrane (Nelson et al., 1998; Grabski et al., 2012). The subunits of the mammalian homolog of yeast Dsl1, ZW10, associate with the TGN SNAREs, the ER SNAREs such as syntaxin 18 (Ufe1), and the COG complex (Hirose et al., 2004; Aoki et al., 2009; Arasaki et al., 2013). Interestingly, depletion of ZW10 has been implicated not only in defects in membrane trafficking events but also in chromosome segregation in dividing cells due to its interaction with Beclin 1 (Williams et al., 1992; Chan et al., 2000; Xiao et al., 2001).

Mutations in many of the MTCs affect cellular functions as well as cause disease phenotypes. COG subunits affect the localization and function of Golgi glycosylation machinery resulting in congenital disorders of glycosylation (CDG) leading to many neurological and developmental diseases (Kingsley et al., 1986; Wu et al., 2004; Spaapen et al., 2005; Foulquier et al., 2006, 2007; Kubota et al., 2006; Shestakova et al., 2006; Kranz et al., 2007; Ng et al., 2007; Zeevaert et al., 2008; Paesold-Burda et al., 2009; Richardson et al., 2009; Reynders et al., 2009). Mutations in Vps54 and Vps53 subunits of the GARP complex affect motor neurons: the former destabilizes the complex and leads to neurodegenerative diseases and the latter cause progressive cerebello-cerebral atrophy type 2 (Pérez-Victoria et al., 2010; Feinstein et al., 2014). Loss-of-function mutations in HOPS or CORVET in mammalian cells have been linked to cancer and cause embryonic lethality or severe developmental defects (Gissen et al., 2004; Schonhaler et al., 2008; Messler et al., 2011; Roy et al., 2011; Aoyama et al., 2012; Kawamura et al., 2012). Like HOPS and CORVET, loss-of-function mutations in exocyst cause developmental delays in mammalian cells and *Drosophila melanogaster* (*Drosophila*) tracheal cells and affect synapse formation, cilia development, and axon growth (Jones et al., 2014).

1.2.1 TRAPP complexes of yeast

Similar to other MTCs discussed above, the TRAPP complexes were also first identified and studied using yeast genetics and protein biochemistry. The TRAPP complexes represent a family of related complexes that are conserved from yeast to humans (Sacher et al., 1998). Although initially proposed to form two related complexes (Sacher et al., 2001), in yeast the TRAPPs are organized into three complexes (Lipatova et al., 2016). TRAPPI, consisting of the core subunits Bet5, Trs20, Bet3, Trs23, Trs31, and Trs33 is involved in ER-to-Golgi traffic along with the long coiled-coil tether, Uso1 (Sacher et al., 1998, 2000, 2001; Jiang et al., 1998; Kim et al., 2006). TRAPPII with the additional subunits Trs120, Trs130 and Trs65, functions in endosome-to-Golgi and intra-Golgi traffic (Sacher et al., 2001). TRAPPIII with the additional subunit Trs85 mediates autophagosome (AP) formation during autophagy and the CVT pathway (Lynch-Day et al., 2010). All three complexes are GEFs and the structure of the core subunits bound to the Rab Ypt1 revealed their mechanism of action in performing the nucleotide exchange

reaction which is essential for their membrane trafficking functions (Jones et al., 2000; Wang et al., 2000; Cai et al., 2008).

The well-studied TRAPPI complex is 300kDa and its structure resembles a dumbbell shape. One of the lobes of the dumbbell has Trs20-Trs31-Bet3 subunits while the other lobe contains Bet3-Trs33-Bet5 subunits. The two lobes are bridged by Trs23 (Kim et al., 2006). The TRAPPI complex, containing subunits with mixed α/β topology, differs from long rod-like MTCs such as exocyst, COG, Dsl1 and GARP that are largely α -helical bundles, indicating a possible variation of the tethering function. The higher molecular weight of TRAPP II compared to TRAPPI is due to dimerization of the former as well as the addition of three high molecular size subunits. The yeast and mammalian TRAPPs are anchored to a Triton X-100 resistant fraction, indicating their stable association with membranes (Sacher et al., 2000, 2001). The TRAPPIII complex appears at a higher apparent molecular size compared to TRAPP II, suggesting that TRAPPIII more tightly associates with membranes (Brunet et al., 2013; Tan et al., 2013). Trs20p acts as an adaptor protein for Trs85 on one end of the TRAPPIII complex (Zong et al., 2011; Brunet et al., 2013; Taussig et al., 2013, 2014).

In vitro yeast transport assays have shown that TRAPPI is the initial interactor for the ER-derived COPII vesicle at the Golgi through the interaction between Bet3 present at both lobes of the TRAPPI complex and Sec23p, a component of the COPII vesicles (Lord et al., 2011). The interaction between TRAPPI and the COPII vesicles is followed by TRAPPI GEF activity towards Ypt1p to recruit its Rab effectors Uso1p, p115 and COG (in mammalian cells) (Wang et al., 2000; Morozova et al., 2006; Cai et al., 2008; Yamasaki et al., 2009).

The TRAPP II complex facilitates intra-Golgi trafficking as well as COPI-dependant endosome-to-Golgi retrograde trafficking in yeast (Sacher et al., 2001; Cai et al., 2005). Mutations of the Trs120 subunit disrupt retrograde trafficking from early endosomes in a COPI protein mislocalization manner (Sacher and Ferro-Novick, 2001; Cai et al., 2005; Yamasaki et al., 2009). The Bet3 subunit in the core of TRAPP is masked in TRAPP II by TRAPP II-specific subunits allowing TRAPP II to bind to the COPI vesicle coat, but not to COPII vesicles (Sacher et al., 2001; Cai et al., 2005; Yamasaki et al., 2009). It has been proposed that TRAPPI converts to TRAPP II

to assure a balance between the flow of materials in and out of the Golgi membranes (Morozova et al., 2006). Recently, a novel function of the TRAPP^{II} complex in fission yeast, *Schizosaccharomyces pombe* (*S. pombe*), has been reported where it is proposed to function during cytokinesis through the interaction of the Trs120 subunit with the Rab11 GTPase, Ypt3 (Wang et al., 2016).

The TRAPP^{III} complex is involved in a process called autophagy (see section 1.4). The complex is located at the site of assembly of the phagophores to assemble the membranes needed for autophagy as well as at the site of pre-autophagosomal structure (PAS) formation (Lynch-Day et al., 2010; Tan et al., 2013). Similar to TRAPP^{II}, TRAPP^{III} functions in endosome to Golgi retrograde traffic to recruit Atg9, a transmembrane protein required for AP formation, and the SNARE, Snc1, by activating Ypt1 in a Trs85 dependent manner (Meiling-Wesse et al., 2005; Nazarko et al., 2005; Lipatova et al., 2012; Shirahama-Noda et al., 2013). Ypt1 effectors such as the COG complex have also been shown to be required for AP formation (Yen et al., 2010). However, the exact mechanism of action of TRAPP^{III}, Ypt1, and COG in autophagy is still unknown.

1.2.2 Mammalian TRAPP complexes

In mammalian cells, two of the three TRAPP complexes were conserved from yeast; TRAPP^{II} and TRAPP^{III} (Sacher et al., 2000; Loh et al., 2005; Yamasaki et al., 2009; Bassik et al., 2013). Despite the fact that yeast subunits share 29 to 54% of sequence identity at the protein level with the mammalian subunits (Table 1.1), there is less known concerning the mammalian TRAPP (mTRAPP) complexes. Crystal structures have been solved for the TRAPPC1-TRAPPC3-TRAPPC4-TRAPPC6 and TRAPPC3-TRAPPC2-TRAPPC5 sub-complexes (Kim et al., 2006). All the mTRAPP complexes are ~670kDa in size (Meiling-Wesse et al., 2005; Nazarko et al., 2005). The mTRAPP^{II} complex consists of six core subunits (TRAPPC1-6a/b) (Aridon et al., 2016) as well as TRAPPC13, TRAPPC9, and TRAPPC10 (Bassik et al., 2013). In addition to the core subunits, the TRAPP^{III} complex contains TRAPPC8, TRAPPC11, TRAPPC12 and TRAPPC13 (Table 1.1; Bassik et al., 2013).

Like yeast TRAPP, the mTRAPP complexes consist of a conserved core upon which additional, and in some cases, metazoan-specific (see section 1.3), subunits bind (Bassik et al., 2013). Subunits of the mTRAPP complexes are present mainly in the cytosol or at the Golgi membranes and the ER/ERGIC interface and thus are involved in ER-to-Golgi and intra-Golgi trafficking, while playing a fundamental role in Golgi morphology (Yu et al., 2006; Scrivens et al., 2009; Choi et al., 2011; Zong et al., 2012). mTRAPP^{II} interacts with COPII vesicles by associating with the p150 motor protein, a subunit of dynactin that moves COPII vesicles along the microtubules as they mature into cis-Golgi (Zong et al., 2012). It also functions in intra-Golgi trafficking and acts as a GEF for the mammalian Ypt1 homolog, RAB1, while partially associating with COPI-coated vesicles at the cis-Golgi (Sacher and Ferro-Novick, 2001; Gwynn et al., 2006; Yamasaki et al., 2009). The activation of RAB1 is required to recruit other factors such as p115 and COG for the final fusion of the COPI vesicles with the early Golgi (Yamasaki et al., 2009).

The exact mechanism of action of mTRAPP^{III} is still unknown (Bassik et al., 2013). mTRAPP^{III} has been suggested to interact with COPII vesicles. However, the role of each subunit has been suggested to be more diverse with functions both within and outside of the complex (Ethell et al., 2000; Ghosh et al., 2001, 2003; Milev et al., 2015). For example, the role of TRAPPC4 has not yet been mapped to its association with the mTRAPP complex. TRAPPC4 recruits MAP kinase kinase (MEK1) for the phosphorylation of ERK1/2 and translocation of the phosphorylated ERK1/2 into the nucleus. Since TRAPPC4 expression is increased in the nuclei where the TRAPP complex is not located, its role in the ERK signaling pathway is independent of its role in the TRAPP complex. Since ERK2 interacts with Sec16, a COPII coat assembly protein, it is tempting to speculate that the role of TRAPPC4 in the ERK pathway may have an impact on membrane traffic (Farhan et al., 2010).

Since the subunits of mTRAPPs are ubiquitously expressed in every cell, mutations in TRAPP subunits which disable the complexes would be expected to be embryonic lethal. Nevertheless, the mammalian TRAPP subunits are linked to a broad range of diseases of which the mechanism and the cause are not fully understood (Table 1.1). Mutation in one of the subunits, *TRAPPC2*, common to both mTRAPPs, causes an X-linked disease called spondyloepiphyseal

dysplasia tarda (SEDT or SEDL) which results in short stature, barrel chest, and degenerative joint disease. It is due to bone growth defects caused by defects in trafficking of type II collagen in the Golgi and Golgi fragmentation in skeletal tissue (MacKenzie et al., 1996; Gedeon et al., 1999, 2001; Scrivens et al., 2009; Venditti et al., 2012). Recently, *TRAPPC2* mutations were also linked to miscarriage (Wen et al., 2015). *TRAPPC4* which is another core TRAPP subunit has been implicated in colorectal cancer and the mechanism is thought to involve its interaction with the mitogen-activated protein kinase, ERK2 (Zhao et al., 2011; Kong et al., 2013; Weng et al., 2014).

Additionally, mutations in *TRAPPC9* which give rise to a truncated protein cause mental retardation and, in some individuals, microcephaly due to defects in the NF- κ B pathway and neuronal differentiation (Khattak and Mir, 2014). *TRAPPC9* has been associated with cancer (Zhang et al., 2015) and schizophrenia (McCarthy et al., 2014). Mutation in *TRAPPC6A* causes mosaic loss of coat pigmentation in mice possibly due to impaired trans-Golgi trafficking and endocytosis (Gwynn et al., 2006). It is also involved in nonverbal reasoning and proposed to play a role in Alzheimer's disease (Hamilton et al., 2011; Chang et al., 2015). *TRAPPC6B* splicing variant has recently been associated with restless leg syndrome (Aridon et al., 2016). *TRAPPC8* has been shown to be significant for cell entry of the human papillomavirus (HPV) due to its possible role in endocytosis and ciliogenesis (Ishii et al., 2013; Schou et al., 2014). To date, there are a few TRAPP subunits which are involved in cancer: *TRAPPC1*, *TRAPPC4*, *TRAPPC9*, and *TRAPPC10* (Pongor et al., 2015; Zhang et al., 2015; Weng et al., 2014). Mutations in *TRAPPC11* will be discussed in detail below. Mutations in these proteins may lead to diseases by any number of mechanisms including interference with proper protein folding, protein-protein interactions and TRAPP complex integrity (Choi et al., 2009; Jeyabalan et al., 2010; Zong et al., 2011; Brunet et al., 2013; Taussig et al., 2014).

Table 1.1 Yeast and mammalian TRAPP subunits and diseases associated with subunits.

Yeast subunits	Mammalian subunits (size in kDa)	mTRAPP complex	Diseases associated with mTRAPP subunits
Bet5	TRAPPC1 (17)	II, III	Cancer
Trs20	TRAPPC2 (16)	II, III	SED1 (MacKenzie et al., 1996; Gedeon et al., 1999, 2001; Scrivens et al., 2009; Venditti et al., 2012); Miscarriage (Wen et al., 2015)
Tca17	TRAPPC2L (16)	II, III	Not found
Bet3	TRAPPC3 (20)	II, III	Not found
Trs23	TRAPPC4 (24)	II, III	Carcinogenesis (Weng et al., 2014)
Trs31	TRAPPC5 (21)	II, III	Not found
Trs33	TRAPPC6 a, b (19, 15)	II, III	(6a) Mosaic loss of coat pigmentation (Gwynn et al., 2006); Alzheimer's disease (Hamilton et al., 2011; Chang et al., 2015) (6b) Restless leg syndrome (Aridon et al., 2016)
Trs85	TRAPPC8 (161)	III	Needed for HPV entry (Ishii et al., 2013)
Trs120	TRAPPC9 (140)	II	Cancer (Zhang et al., 2015); Intellectual disability (Khattak and Mir, 2014); Schizophrenia (McCarthy et al., 2014)
Trs130	TRAPPC10 (142)	II	Cancer (Pongor et al., 2015)
N/A	TRAPPC11 (129)	III	Muscular dystrophy (Bögershausen et al., 2013); Fatty liver disease, steatosis, early onset of cataracts (Liang et al., 2015)
N/A	TRAPPC12 (79)	III	Not found
Trs65	TRAPPC13 (46)	III	Not found

kDa, kilodaltons; mTRAPP, mammalian TRAPP; N/A, not applicable.

1.3 TRAPPC11 and TRAPPC12

Mammalian TRAPPC11 and TRAPPC12 are the only subunits that have no apparent homologs in yeast. They are found mainly in the cytosol or in the Golgi membranes and the ER/ERGIC interface. They are present in all eukaryotic cells, including fungi (Scrivens et al., 2011; Bassik et al., 2013). They serve as components of the mTRAPPIII complex while also playing a pivotal role in Golgi morphology (Yu et al., 2006; Scrivens et al., 2009; Yamasaki et al., 2009; Choi et al., 2011; Zong et al., 2012). The TRAPPC11 subunit was co-precipitated with two different epitope-tagged TRAPP subunits; TRAPPC8 and TRAPPC12 (Scrivens et al., 2011). *TRAPPC11* codes for a 1,133 amino acid protein with a foie gras domain which is a central, highly conserved structural motif containing as many as six tetratricopeptide repeats (TPR) for protein-protein interactions, a gryzun domain, and non-overlapping regions of homology to human and yeast TRAPPC10 (Figure 1.1; Wendler et al., 2010). The functions of TRAPPC11 are not well characterized in mammalian cells but it has been implicated in ER-to-ERGIC trafficking as well as autophagy due to a decrease in AP formation upon TRAPPC11 knockdown (Behrends et al., 2010; Scrivens et al., 2011).

Studies by Wendler et al. (2010) and Sadler et al. (2005) showed that TRAPPC11 is crucial for development since depletion of *TRAPPC11* is lethal in both *Drosophila* and zebrafish. In the *Drosophila* studies, the depletion of *trappc11* by small interfering RNA (siRNA) caused Golgi fragmentation and rerouting of the marker protein CD8-green fluorescence protein (GFP) from apical to basal membranes of larval salivary glands as well as learning and memory defects (Wendler et al., 2010; Dubnau et al., 2003). In the study by Sadler et al. (2005), *trappc11* loss of function mutation, called *fgr*, caused enlarged livers, steatosis, developmental defects of the eye, gut, lower jaw and fin, and hepatocyte death, indicating a major role in the liver as well as other organs. In the study by DeRossi et al. (2016), a *trappc11* mutation in zebrafish caused Golgi fragmentation and blockage of protein secretion from hepatocytes. However, depletion of *TRAPPC11* by siRNA in HeLa cells resulted in membrane trafficking defects in post-ER compartments and partial disassembly of the TRAPP complex, indicating a potential role in stabilizing the TRAPP complex (Wendler et al., 2010; Scrivens et al., 2011). Interestingly, TRAPPC11 has been associated with protein glycosylation since siRNA knockdown of

TRAPPC11 in HeLa cells caused hypoglycosylation of translocon-associated protein (TRAP α) (DeRossi et al., 2016). Additionally, *TRAPPC11* knockdown caused an apparent decrease in levels of TRAPPC12 but not the levels of TRAPPC2, TRAPPC2L, or TRAPPC3, indicating a possible physical association of the TRAPPC11 and TRAPPC12 subunits (Scrivens et al., 2011).

TRAPPC12 has been identified to play a dual role in membrane trafficking and mitosis (Milev et al., 2015). Such so-called moonlighting proteins are known to acquire two or more unrelated functions at different times or at different cellular locations to increase the complexity of the cellular processes (Jeffery, 1999; Copley, 2012). There are many possible mechanisms for proteins to switch between various functions, including a change in cellular localization, ligand binding, variation in oligomerization, and post-translational modifications (Jeffery, 2003). Like TRAPPC11, TRAPPC12 contains a TPR domain which facilitates protein-protein interactions (Scrivens et al., 2011). The protein is mainly located in the Golgi (Scrivens et al., 2011) with a small amount present in the nucleus (Milev et al., 2015). TRAPPC12 associates with the kinetochore and plays a role in kinetochore assembly and stability by regulating recruitment of centromere-associated protein E (CENP-E) to the kinetochores (Milev et al., 2015). Depletion of TRAPPC12 activates the spindle assembly checkpoint.

During interphase, TRAPPC12 is localized to the Golgi where it can function in membrane traffic due to its interaction with the mTRAPP complex. The autophagy activity of TRAPPC12 has also been suggested by Behrends et al. (2010) who showed that depletion of TRAPPC12 caused an increase in APs and defects in autophagic flux (see section 1.4). During mitosis, TRAPPC12 disassociates from the mTRAPP complex and is phosphorylated outside of the TPR domain, a modification that is necessary for its interaction with CENP-E (Milev et al., 2015). These phosphates are removed before the onset of anaphase (Milev et al., 2015). The role of TRAPPC12 in membrane traffic and the exact mechanism of TRAPPC12 function in mitosis is yet to be determined.

1.3.1 *TRAPPC11* mutations reported to date

Currently, there are several documented *TRAPPC11* mutations causing disease in humans (Table 1.2; Figure 1.1). The study by Bögershausen et al. (2013) reported two different homozygous mutations, one in a Syrian pedigree and a second in two different Hutterite communities. The Hutterite mutation causes a deletion of exons 11 and 12 to produce an in-frame deletion of a portion of the foie gras domain (p.A372_S429del) while the Syrian mutation causes a missense mutation (p.G980R) within the N-terminal Gryzun domain. The affected individuals showed decreased levels of TRAPPC11 protein. The Golgi of fibroblasts taken from affected individuals had a fragmented phenotype while the trafficking of the marker protein, temperature-sensitive vesicular stomatitis virus glycoprotein fused to GFP (ts045-VSV-G-GFP), between ER and Golgi appeared normal in individuals with the p.A372_S429del mutation. However, post-Golgi trafficking was significantly delayed in these individuals, with the marker protein accumulating in the Golgi over time. This contrasts with the observations for the siRNA knockdown of TRAPPC11 which included an ER-to-ERGIC trafficking defect, suggesting a possible function of the foie gras domain in intra- or post-Golgi trafficking.

In the Bögershausen et al. (2013) study, a significant decrease in the late endosomal/lysosomal protein called lysosome-associated membrane protein 1 (LAMP1) in the individuals carrying the mutations was observed along with the remaining LAMP1 focused on a perinuclear region similar to the MTOC. This indicates a possible interaction of TRAPPC11 with motor proteins, similar to that seen for TRAPPC9 in the early secretory pathway (Zong et al., 2012). The individual with the mutation p.G980R showed a more prominent muscular phenotype similar to limb-girdle muscular dystrophy (LGMD). The patient also had increased creatine kinase (CK) levels due to the destruction of muscle fibers. Individuals affected with the p.A372_S429del mutation also showed muscle abnormalities with mild muscle weakness, ataxia and elevated levels of CK, as well as neurological abnormalities and intellectual disabilities. These phenotypes, mainly affecting the muscle and brain, have contrasted with the loss of function mutation in zebrafish which predominantly affected the liver. Recently, another study by DeRossi et al. (2016) has shown that the homozygous *TRAPPC11* mutation p.G980R in fibroblasts from affected individuals caused accumulation of lipid droplets.

Compound heterozygous mutations in *TRAPPC11* in one Asian individual have also been reported to cause congenital muscular dystrophy (CMD), fatty liver disease and early onset of cataracts (Liang et al., 2015). One mutation has been reported in the Syrian individual in the previous study (p.G980R), and the second mutation is a splice-site mutation which produced two different spliced transcripts, both possibly causing a frameshift and truncated protein (p.L240Afs*10 and p.L240Vfs*7). The 8-year old Han Chinese girl showed developmental delays and elevated levels of CK similar to the study by Bögershausen et al. (2013) and fatty liver disease, steatosis and impaired visual system similar to the zebrafish study by Sadler et al. (2005). The affected individual also showed altered forms of the lysosomal membrane glycoproteins such as LAMP1 and LAMP2 which indicates that the transport of proteins is affected by mutations in *TRAPPC11* which destabilize the protein, similar to that observed in the study by Bögershausen et al. (2013). The truncated protein appears as a loss of function mutation to cause severe phenotypes while recapitulating the zebrafish study. The diversified phenotypes of individuals with *TRAPPC11* mutations (i.e. brain, muscle, eye, liver, and bone) affirms the role of TRAPPC11 in multiple tissues in humans (Liang et al., 2015).

Table 1.2 Mutations of *TRAPPC11* reported to date.

Number of cases (families)	Family origin	<i>TRAPPC11</i> Genetic mutation	Mutation at protein level	Consanguinity (Yes/No)	Reference
3 (1 family)	Syrian	c.2938G>A/ c.2938G>A	p.G980R	Yes	Bögershausen et al., 2013
5 (2 families)	Hutterite	c.1287+5G>A/ c.1287+5G>A	p.A372_S429del	Yes	Bögershausen et al., 2013
1	Asian	c.2938G>A/ c.661-1G>T	p.L240Afs*10 and p.L240Vfs*7	No	Liang et al., 2015

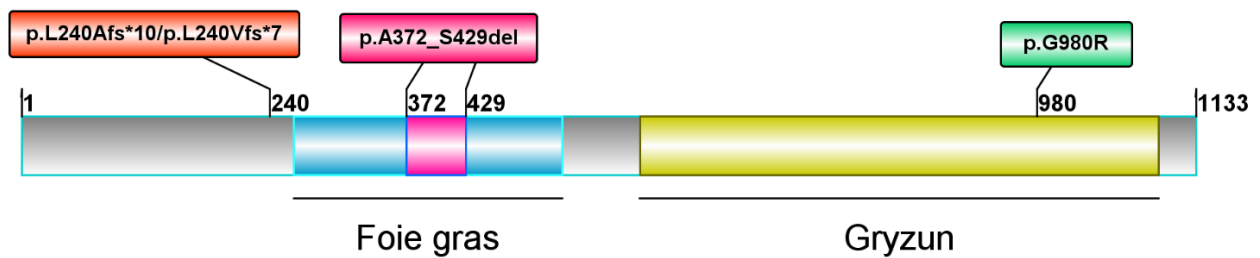


Figure 1.1: Cartoon representation of the TRAPPC11 protein with mutations reported to date. The protein sequence for TRAPPC11 is shown along with the location of the conserved foie gras (263-522) and gryzun (597-1097) domains. Currently reported *TRAPPC11* mutations causing disease in humans are shown based on their location along the protein sequence for TRAPPC11. The numbers represent the amino acid number in the protein sequence.

1.4 Autophagy

The mTRAPPIII complex is suggested to function in multiple tissues in humans as well as in multiple pathways, including autophagy (Lynch-Day et al., 2010; Tan et al., 2013). Similar to typical membrane trafficking pathways, autophagy also transports cargo and lipids to one compartment. It recycles proteins during cellular stresses such as nitrogen starvation or cell damage. The two forms of autophagy, macro- and microautophagy, are further subdivided into selective and non-selective autophagy. In microautophagy, cargo in the cytoplasm is directly internalized into the vacuoles or lysosomes without the need for pre-lysosomal compartments. During macroautophagy (hereafter autophagy), cargo in the cytoplasm is packaged into APs and is delivered to the lysosomes (Baba et al., 1994). Only macroautophagy is conserved from yeast to higher eukaryotes (Meijer et al., 2007).

Unfolded/ improperly folded/excess proteins in the ER are also delivered to lysosomes by APs for degradation and generation of energy by selective macroautophagy or ER-phagy (Lipatova et al., 2013; Bernales et al., 2007). The AP formation includes membrane formation around cytosolic cargo proteins at the PAS site by autophagy-specific proteins (Atgs) in yeast and at the ER and mitochondrial contact site in mammalian cells (Suzuki, 2001; Kim et al., 2002; Hamasaki

et al., 2013). The APs fuse with the vacuole or lysosome releasing material into the acidic lumen of the lysosomes for degradation by the lysosomal hydrolase enzymes. During nutrient starvation, the nonselective macroautophagy allows the “self-eating” process where cytosolic components are delivered to lysosomes for degradation and recycled for anabolic processes.

The cellular mechanism and components of the autophagy pathway were identified first in yeast. The autophagy pathway is regulated by the target-of-rapamycin (TOR) kinase that is active during normal cell growth conditions. Inactivation of TOR activity during starvation generates a novel AP for the activation of the autophagy pathway. The stages of the autophagy pathway and its players are well known. Nonetheless, less is known about the initial steps of the autophagy pathway, at the site of AP formation. An increase in APs does not signal an increase in autophagy, but a block in trafficking to lysosomes. An increase in autolysosomes (AP fused with lysosomes) indicates a decrease in protein degradation (autophagic flux). The autophagic flux is observed by monitoring synthesis and lipidation of autophagy markers such as LC3-II (microtubule-associated protein 1 light chain 3; protein from the cytosol [LC3-I] and lipidated form at the autophagosomal/ autolysosomal membrane [LC3-II]) (Germain et al., 2011; Klionsky et al., 2016). During formation of mammalian APs, LC3 is modified and incorporated into the membrane of APs and is later degraded by lysosomal hydrolytic enzymes (Kabeya et al., 2000).

Autophagy is critical in many instances such as programmed cell death (apoptosis), amino acid starvation, hypoxia, removal of growth factors, defense against pathogens as well as development and cell differentiation. Starvation-induced autophagy activity is clearer in skeletal and heart muscles, eye, and thymus tissue, and hepatocytes, but not as much in the brain cells (Schworer et al., 1981; Mizushima et al., 2004; Lünemann et al., 2007). When autophagy is disrupted, proteins build up in the ER causing ER stress and ER vesicle budding defects (Higashio and Kohno, 2002). Defects in autophagy lead to diseases such as SEDT, cancer, aging, bacterial infection and muscle and neurodegenerative disorders such as Parkinson’s disease and LGMD (Bursch et al., 1996; Anglade et al., 1997; Kegel et al., 2000; Brunet and Sacher, 2014).

1.5 Neuromuscular diseases

The accumulation of autophagic vacuoles (APs and autolysosomes) and cytoplasmic protein aggregates is a common feature in many neuromuscular diseases (Jongen et al., 1995; Kaneda et al., 2003; Nishino et al., 2005; Fujita et al., 2007; Lünemann et al., 2007; Raben et al., 2007; Nascimbeni et al., 2008). The accumulation of cytoplasmic protein aggregates indicates a defect in protein degradation. Hereditary neuromuscular diseases are primarily due to conformational changes in specific proteins due to mutations. The mutant proteins have a strong affinity to form insoluble aggregates which become sequestered inside autophagic vacuoles, but unable to be degraded by lysosomal enzymes. The insoluble proteins also aggregate in the cytoplasm and severely inhibit the ubiquitin-proteasome system. Inactivation of the protein degradative machinery, autophagy and ubiquitin-proteasome system, greatly affects the homeostasis to impair many cellular activities to eventually cause cell death. Impaired motor-nerve and/or skeletal muscle function due to cell death by apoptosis, necrosis and/or unregulated autophagy is the main characteristic of hereditary neuromuscular diseases (Pattingre et al., 2005).

In many neuromuscular diseases, genetic mutations and defects in the autophagy pathway are well characterized. For example, Danon disease is an X-linked myopathy and cardiomyopathy due to mutations of *LAMP2* which encodes for a highly glycosylated and expressed lysosomal membrane protein in the skeletal muscles and the heart (Nishino et al., 2000). Hereditary neuromuscular diseases caused by defects in autophagy are categorized into two groups; rimmed vacuolar myopathies and autophagic vacuolar myopathies (Nishino et al., 2005). The rimmed vacuolar myopathies are secondary lysosomal myopathies since autophagy is activated as a secondary effect of protein misfolding or aggregation. This group includes disorders such as distal myopathy with rimmed vacuoles (DMRV) and oculopharyngeal muscular dystrophy (OPMD). The autophagic vacuolar myopathies are due to the buildup of APs due to blockage or inhibition of the autophagy pathway. This group includes disorders such as Pompe disease and X-linked myopathy with excessive autophagy (XMEA) (Nishino et al., 2005).

Neuromuscular diseases affect both men and women of all ages and are characterized by mild functional impairment with progressive loss of muscle function that can extend to severe

disability and early death. Though genetic mutations responsible for inherited neuromuscular diseases have been identified, the molecular and cellular mechanisms that cause the muscle and nerve defects are not well known. Thus, it is critical to better understand the nature of these rare diseases to target therapies which are common to more than one neuromuscular disease (Darin and Tulinius, 2000). Since neuromuscular diseases are related to defects in autophagy, this study will also address the role of TRAPPC11 in autophagy.

1.6 Introduction to project: Characterization of *TRAPPC11* and *GOSR2* mutations in human fibroblasts

In this study, homozygous and compound heterozygous mutations in the *TRAPPC11* gene in human fibroblasts from five affected individuals will be characterized using several biochemical, immunofluorescence and live cell microscopy techniques to identify the defective pathway(s). A similar type of analysis was performed for two individuals with mutations in *GOSR2* gene to identify their defective pathway(s). The affected individuals showed novel mutations in *TRAPPC11* and *GOSR2* as well as one of the previously mentioned mutations in the Bögershausen et al. (2013) study (Table 1.2; Figure 1.2). We hypothesized that the *TRAPPC11* mutant phenotype would be similar to the cellular phenotypes of mutants observed in previous studies (see section 1.3 and 1.3.1), resulting in Golgi fragmentation, defects in protein glycosylation, delay in protein secretion and partial disassembly of the mTRAPP complex (Wendler et al., 2010; Scrivens et al., 2011; Bögershausen et al., 2013; DeRossi et al., 2016). The current study suggests that some of the *TRAPPC11* mutations are linked to a variety of cellular phenotypes including ER-to-Golgi trafficking defects, delay in the exit of proteins from the Golgi, Golgi fragmentation, defects in the autophagy pathway as well as partial disassembly of the mTRAPP complex. The current study also suggests that some of the *GOSR2* mutations are linked to ER-to-Golgi trafficking defects as well as a delay in the exit of proteins from the Golgi. This study and previous studies of *TRAPPC11* led to the conclusion that *TRAPPC11* mutations, in general, result in neuromuscular phenotypes.

Table 1.3 Novel mutations of *TRAPPC11* in this study.

Number of cases (families)	Family origin	<i>TRAPPC11</i> Genetic mutation	Mutation at protein level	Consanguinity (Y/N)
4 (2 families)	Turkish	c.1893+3A>G/ c.1893+3A>G	p.V588Gfs*16	Yes
1	Mixed European	c.851A>C/ c.965+5G>T	p.Q284P (c.851 A>C)	No
2 (2 families)	Subject 6: Pakistan Subject 7: Asian	Subject 6: Unavailable Subject 7: c.1287 +5G>A and c3379_3380insT	Subject 6: p.Q933H and p.F866I Subject 7: p.A372_S429del and p.N1127Vfs*45	Unknown

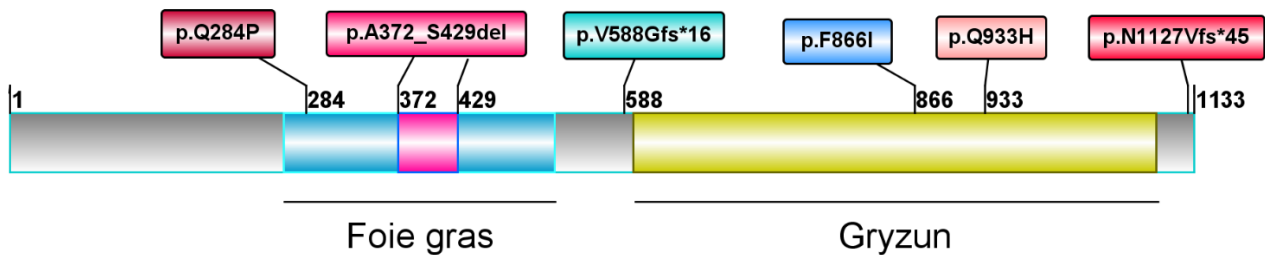


Figure 1.2: Cartoon representation of the novel *TRAPPC11* mutations in this study. Novel *TRAPPC11* mutations discussed in this study are shown based on their location along the protein sequence for TRAPPC11. The numbers represent the amino acid number in the protein sequence.

2 MATERIAL AND METHODS

2.1 Buffers and solutions

All buffers and solutions used in the study are listed in Table 2.1 below.

Table 2.1 Buffers and solutions used in the study.

Reagent	Components
Growth medium	Dulbecco's modified Eagle's medium (DMEM, Wisent) supplemented with 2 mM L-glutamine and 10% (vol/vol) fetal bovine serum (FBS, Wisent)
Gel filtration buffer	50 mM Tris-HCl pH 7.2, 150 mM NaCl, 0.5 mM Ethylenediaminetetraacetic acid (EDTA), 1 mM Dithiothreitol (DTT)
Freezing medium	DMEM containing 10% FBS with 10% dimethylsulphoxide (DMSO) (v/v)
Mammalian cell lysis buffer (1)	50 mM Tris-HCl pH 7.2, 150 mM NaCl, 0.5 mM EDTA, 1 mM DTT, 1% Triton X-100 (v/v), one tablet of protease inhibitor cocktail (Roche), and two tablets of Phospho-Stop (Roche) per 10 ml
Mammalian cell lysis buffer (2)	20mM HEPES pH 7.4, 0.1M KCl, 0.5% Triton X-100 (v/v), 5mM MgCl ₂ with one tablet of protease inhibitor cocktail (Roche) per 10 ml
Phosphate-buffered saline (PBS)	0.8% NaCl (w/v), 0.02% KCl (w/v), 0.061% Na ₂ HPO ₄ (w/v), 0.02% KH ₂ PO ₄ (w/v), pH 7.3
PBS-T	PBS containing 0.1% Tween-20 (v/v)
Sodium dodecyl sulfate-polyacrylamide gel electrophoresis (SDS-PAGE) running buffer	25 mM Tris-base, 200 mM glycine, 0.1% SDS
SDS sample buffer (4x)	80 mM Tris-HCl pH 6.8, 2% SDS (w/v), 10% glycerol (v/v), 0.1% bromophenol blue, 5% β-mercaptoethanol (v/v)

Western blotting transfer buffer	25 mM Tris-base, 200 mM glycine, 20% methanol
---	---

2.2 Cell culture conditions

Human fibroblasts were cultured and grown in growth medium at 37°C in a humidified incubator with 5% CO₂. The growth medium was pre-sterilised and stored at 4°C and pre-warmed to 37°C in a water bath unless mentioned otherwise. The passage numbers of fibroblasts were kept less than 15 passages and the medium was changed every two days to ensure freshness of the cell cultures while eliminating the formation of endogenous growth inhibitory proteins (Epifanova et al., 1982; Miyazaki and Horio, 1989). All the subjects from whom the fibroblasts were obtained or their legal representatives provided written informed consent to perform the study.

In order to subculture confluent cells, the medium was removed and 3 ml of 0.05% trypsin solution (Wisent) was added to the cells followed by careful removal of 2 ml of trypsin after 1 minute. The cells were then returned to the 37°C incubator for an additional 2 minutes. Immediately following the incubation, the cells were detached using growth medium to re-plate. The cells were plated on either 6-well dishes for western blotting or in 12-well dishes with sterile 18 mm glass coverslips pre-coated with poly-l-lysine (Thermo Fisher Scientific) for immunofluorescence or on 35 mm glass-bottom dishes (14 mm glass diameter, glass thickness of 1.5; MatTek) for live-cell microscopy.

The cryopreservation of the cells in liquid nitrogen was done by trypsinizing a confluent dish of cells as above and resuspending cells in an appropriate amount of cold freezing medium. Depending on the size of the dish, 4 to 6 aliquots of 1 ml of cells in the freezing medium were frozen in sterile ampules from each dish. The ampules were immediately stored overnight in a freezing box at -80°C to allow gradual cooling at a controlled rate of ~1°C/minute. The ampules were then transferred to a liquid nitrogen storage tank for prolonged storage.

The cells were thawed from the liquid nitrogen storage tank by thawing quickly in a 37°C water bath for 1 to 2 minutes and immediately transferring in a drop-wise manner to a dish containing growth medium and grown in a 37°C incubator overnight. The medium was changed with fresh growth medium the next day.

2.3 Amino acid starvation

Starvation of the cells was performed in Earle's balanced salt solution (EBSS; Wisent). The procedure for serum starvation included washing the cells three times with pre-warmed EBSS medium and then incubating them in EBSS medium for 1 hour or 4 hours. In some cases, Bafilomycin A1 at a final concentration of 100nM was used. After starvation in EBSS, cells were harvested at various time points in mammalian lysis buffer (1) and pelleted at 13,000 rpm for 10 minutes before freezing the supernatant or measuring the protein concentration.

2.4 Transfection of mammalian cells

Transfection of plasmid constructs and/or siRNA listed in Table 2.2 was performed using a polymer-based transfection reagent, JetPrime (Polyplus), following the manufacturer's protocol. The amount of DNA used per one well of 12- or 6-well plate was 0.5 μ g and 1 μ g of the purified plasmid, respectively, and the amount of siRNAs used per one well on a 6-well plate are listed in Table 2.2. The cells of passage number 2 or 3 were trypsinized and plated on 12- or 6-well plates to reach a density of 60-70% confluency 24 to 48 hours prior to the transfection. Cells were left with DNA or siRNA for 24 to 48 hours for the transient transfection to occur. Subsequently, the cells were used for the ts045-VSV-G-GFP trafficking assay (see section 2.5) or harvested and analyzed for transfection efficiency using western blotting (see section 2.5.1) or fixed for immunofluorescence (see section 2.5.2).

Table 2.2 siRNAs used in the study.

Target gene	Final concentration	Code	Sequence (5' to 3')	Source
<i>TRAPPC2</i>	20 nM	s12673 (Ambion)	CAAUUCUCCUAUUC GAUCAtt	Life Technologies
<i>TRAPPC11</i>	20nM	s226950 (Ambion)	GGAUUUAUAAACUA CAAGAtt	Life Technologies
<i>TRAPPC12</i>	10 nM	s27465 (Ambion)	CGGACAAGCUGAAC GAACAtt	Life Technologies
<i>SYNTAXIN5</i>	20 nM	N/A	UAGCCUCAACAAAC AAAUUt	Life Technologies

2.5 ts045-VSV-G-GFP membrane trafficking assay

HeLa cells or human fibroblasts were incubated with 50 μ L of the diluted virus encoding the ts045-VSV-G-GFP protein (1:5 in sterile 1xPBS) per well in a 6-well dish for 1 hour at 37°C with occasional tilting. Upon completion of 1 hour of infection, 2 mL of growth medium pre-warmed to 40°C was added to each well on a 6-well dish and shifted to 40°C for 16 to 18 hours to ensure retention of the ts045-VSV-G-GFP protein in the ER (Knipe et al., 1977; Lodish and Weiss, 1979; Bergmann et al., 1981; Lodish and Kong, 1983; Kreis and Lodish, 1986; Beckers et al., 1987). In order to release the ts045-VSV-G-GFP protein from the ER, the cells were shifted to 32°C 45 minutes after the addition of cycloheximide (CXM) to a final concentration of 10 μ g/ml. The temperature downshift was done by changing the medium with fresh growth medium pre-warmed to 32°C containing CXM. At different time points, the cells were either fixed (see section 2.5.2) or quickly harvested in ice-cold lysis buffer (2) using a cell scraper to lift the cells off the plate. The protein concentrations were measured as in section 2.5.1. Endoglycosidase H (EndoH) treatment was performed on a portion of the total cell lysate (TCL; 5-20 μ g/ μ l) according to the manufacturer's protocol (New England Biolabs, Cat. # P0702L and Cat. # P0703L) except only 10 Units of the EndoH or EndoH_f enzyme was used per reaction. Western blotting was performed

on EndoH-treated and -untreated lysates to detect the ts045-VSV-G-GFP protein using mouse-anti-GFP (1:3000; Table 2.3). Quantification of the intensity of western blot bands was done using ImageJ 1.48v software (National Institute of Health (NIH)) after background subtraction and expressed as a ratio of pixels from the EndoH resistant band/ (pixels from the EndoH resistant band+ pixels from the EndoH sensitive band). For immunofluorescence microscopy, mouse-anti-GFP (1:200; Table 2.3) and rabbit-anti-mannosidase II (ManII) (1:200; Table 2.3) was used.

2.5.1 Cell harvest and Western blotting

HeLa lysates from control or treated/knockdown HeLa cells and fibroblast lysates from cultured control or affected individuals were harvested in mammalian cell lysis buffer (1) for TCL preparation and in mammalian cell lysis buffer (2) for the ts045-VSV-G-GFP trafficking assay (see section 2.5). The lysates were cleared at 13,000 rpm for 10 minutes and the supernatant was frozen or protein concentration was measured. The protein concentrations of TCLs were measured using a Coomassie Brilliant Blue G-250 dye-based Bradford assay (Bradford, 1976). 1 μ l of the TCL was carefully diluted in dH₂O (1:100) and mixed with 1 ml of 1x Bradford reagent (BioRad). The absorbance of prepared samples was measured using an Ultrospec 2100pro spectrophotometer at 595 nm along with a blank containing 1 ml of Bradford reagent and 1 μ l of the mammalian cell lysis buffer (1 or 2) diluted in dH₂O (1:100). The absorbance was used to obtain protein concentrations in μ g/ μ l by deriving a standard calibration curve prepared using known amounts of BSA (0-10 μ g).

Total protein from each TCL (5-30 μ g) was loaded on an 8% and/or 15% SDS-PAGE gel after boiling the samples in 4x SDS sample buffer at \sim 95°C for 5 minutes and separated using electrophoresis at 120V in SDS-PAGE running buffer. For the ts045-VSV-G-GFP trafficking assay, 10-20 μ g of protein was loaded onto an 8% SDS-PAGE gel containing 30% acrylamide/bis-acrylamide, 29:1 (3.3% crosslinker) solution (BioShop) in order to better separate EndoH sensitive and EndoH resistant bands in EndoH/EndoH_f treated samples. The proteins in the SDS-PAGE gel were transferred to nitrocellulose membrane using standard procedures (Sambrook and Russel, 2001) for 1 hour at 100V or overnight at 30V using western blotting transfer buffer. The

membranes were blocked for 1 hour with tilting using 5% skim milk powder (w/v) in 1xPBS-T and incubated for 1 hour with primary antibodies in 1xPBS-T followed by secondary antibodies in 1xPBS-T for 45 minutes with tilting. The membrane was washed 3 times with 1xPBS-T, with a final wash being 5 minutes, before secondary antibody incubation. The primary and secondary antibodies are listed in Table 2.3 and Table 2.4, respectively, along with their dilutions. Upon completion of antibody incubation, the membrane was washed three times with 1xPBS-T, 10 minutes each, and the signal was detected by applying enhanced chemiluminescence (ECL) Western Blotting Detection reagents (GE Healthcare) on the membrane for 1 minute and detecting the signal on a GE Amersham Imager 600.

2.5.2 Immunofluorescence microscopy

HeLa or fibroblasts were fixed in 3-4% paraformaldehyde (PFA) in 1xPBS, pH 7.2, for 20 minutes after removing the medium and washing the coverslips gently twice with 1xPBS pre-warmed to 37⁰C. For endogenous LAMP1 and tubulin staining, coverslips were fixed in cold methanol at -20°C for 3 minutes. After removal of PFA (or methanol), the coverslips were gently washed once with 1xPBS and the excess PFA (or methanol) was quenched with 0.1 M glycine for 10 minutes. The coverslips were washed once with 1xPBS and then the cells were permeabilized with 0.1% Triton X-100 (in 1xPBS) for 10 minutes. The cells were rinsed with 1xPBS to remove residual Triton X-100 and washed in 1xPBS for 10 minutes. Subsequently, the cells were blocked with 5% normal goat serum (NGS, Cell Signaling Technology) in 1xPBS for 45 minutes at room temperature. Upon completion, the cells were incubated with primary antibodies (Table 2.3) diluted in 5% NGS in 1xPBS overnight at 4°C for anti-LAMP1 and anti-tubulin or for 1 hour at room temperature for anti-GFP and anti-ManII. The cells were gently washed three times with 1xPBS for 5 minutes each. The cells were then incubated with secondary antibodies (Table 2.4) and DAPI (1:500) diluted in 5% NGS in 1xPBS for 1 hour at room temperature while reducing exposure to light. The coverslips were gently washed three times with 1xPBS, mounted with Prolong Gold AntiFade reagent (Life Technologies) and sealed with nail polish. The immunofluorescence signal was detected under 1024 x 1024-pixel resolution on a Nikon C2 laser

scanning confocal microscope equipped with a 63x Plan Apo I, NA1.4 objective (Nikon) and controlled by NIS Element C4.4 software. Z-stacks were acquired with 0.2 μ m increments.

Table 2.3 Primary antibodies used in the study.

Antigen	Type	Host	Dilution (IF)	Dilution (WB)	Size (kDa)	Cat. #	Source
GFP	M	m	1:200	1:3000	27	11814460001	Sigma-Aldrich
LAMP1	M	r	1:200	1:3000	120	H4A3	Santa Cruz, Biotechnology
LC3B	P	r	1:250	1:3000	15	ab48394	Abcam
ManII	P	r	1:200	N/A	N/A	N/A	Kelley Moreman, University of Georgia
p115	M	m	1:250	N/A	115	7D1	Dr. Dennis Shields
TUBULIN	M	m	1:500	1:8000	50	61603	Abcam
TGN46	P	r	1:200	N/A	51	16052	Abcam
TRAPPC12	P	m	1:50	1:2000	78	H000511112- B01P	Abnova
TRAPPC12	P	r	1:200	1:2500	78	N/A	Sacher laboratory
TRAPPC11	P	r	N/A	1:500	129	N/A	Sacher laboratory

kDa, kilodaltons; N/A, not applicable; M, monoclonal; P, polyclonal; r, rabbit; m, mouse; g, goat; h, human; IF, immunofluorescence; WB, Western blotting.

Table 2.4 Secondary antibodies used in the study.

Secondary IgGs	Host	Dilution (IF)	Dilution (WB)	Cat. #	Source
Alexa Fluor 488 (α-m)	g	1:500	N/A	A.11013	Life Technologies
Alexa Fluor 647 (α-m)	g	1:500	N/A	A.21236	Life Technologies
Alexa Fluor 647 (α-r)	g	1:500	N/A	A.21245	Life Technologies
HRP-labeled (α-m)	g	N/A	1:5000	KP-474-1806	KPL
HRP-labeled (α-r)	g	N/A	1:5000	KP-474-1506	KPL

kDa, kilodaltons; N/A, not applicable; r, rabbit; m, mouse; g, goat; HRP, horseradish peroxidase; IF, immunofluorescence; WB, Western blotting.

2.5.3 Live-cell microscopy

Fibroblasts from control and affected individuals were placed on 35 mm glass-bottom dishes (14 mm glass diameter, glass thickness of 1.5; MatTek) and treated as for the ts045-VSV-G-GFP trafficking assay (see section 2.5) except the infection of fibroblasts from control and affected individuals was performed with a 2-hour interval to ensure equal incubation time at 40°C. CXM was added for 45 minutes at 40°C and the dishes for fibroblasts from affected individuals followed by the dishes for control fibroblasts were placed in a temperature controlled chamber heated to 32°C with 5% CO₂. Time-lapse microscopy was performed 3 minutes after the temperature downshift (the time required to appoint cells for imaging) using a 40x or 60x oil objective (NA 1.3), no binning, on an inverted confocal microscope (LiveScan Swept Field; Nikon), Piezo Z stage (Nano-Z100N; Mad City Labs, Inc.), and an electron-multiplying charge-coupled device camera (512 x 512; iXon X3; Andor Technology). Images were acquired with NIS-

Elements Version 4.0 acquisition software every 1 minute with 20% laser power using a 500msec exposure time at 0.2- μm increments with a slit size of 50 μm for the duration of 2.5 hours. Note that these settings were first determined using control samples and kept constant for experimental conditions. The original images were viewed and analyzed on ImageJ 1.48v software (NIH). Cropped images from the videos at different time points were assembled in Illustrator CS6 (Adobe) for representation.

2.6 Size exclusion chromatography

Fibroblasts from control or affected individuals were grown to full confluency in two 15cm dishes and lysed in mammalian cell lysis buffer (1). Cell lysates were cleared at 13,000 rpm for ~15 minutes and protein concentrations were measured as above. An ÄKTA FPLC chromatography system (GE) was used to fractionate ~5 mg of the TCL on a Superose 6 preparation grade column (GE Healthcare) at a flow rate of 0.5 ml/min. The Superose 6 column was pre-equilibrated with 2 volumes of gel filtration buffer prior to loading the lysates. Fractions of 0.5 ml were collected and fractionated by SDS-PAGE for Western blotting for different subunits of the mTRAPPIII complex using antibodies mentioned in Table 2.3.

2.7 Statistical analysis

All data were expressed as means \pm S.E.M. To establish significance, data were subjected to unpaired two-tailed student's *t*-tests with Welch's correction while assuming unequal variance, or one-way ANOVA using the GraphPad Prism software statistical package 6.0 (GraphPad Software). For one-way ANOVA, post-hoc differences were made using Fisher's probability of least squared differences. The criterion for significance was set at $P \leq 0.05$. For live-cell microscopy, the GFP fluorescence in the Golgi region was measured using ImageJ 1.48v software (NIH) in the original movies after combining stacks. The GFP fluorescence from the Golgi region was marked at the time point where the maximum intensity of the GFP fluorescence in the Golgi region (~30 minutes for control) was observed and the GFP fluorescence in the marked Golgi

region at each time point was measured. The percentage of the GFP fluorescence in the Golgi region at each time point over the maximum intensity of the GFP fluorescence in the Golgi region was calculated for fibroblasts from control or affected individuals.

3 RESULTS

Note: The clinical characterization and DNA sequencing for individuals described in sections 3.1, 3.2 and 3.3 were performed by our collaborators.

3.1 A *TRAPPC11* mutation results in a Triple A-like syndrome

Recently, four affected individuals from two unrelated and consanguineous Turkish families presented with a triple A-like syndrome. The affected individuals displayed a combination of neurological defects such as cerebral atrophy, therapy-refractory epilepsy, global retardation (developmental delays and intellectual disability) as well as scoliosis, achalasia, and alacrima. Mild muscle dystrophic changes were seen in the muscle histology data. Triple A syndrome (also known as Allgrove syndrome) is a rare, autosomal recessive disease which mainly consists of three symptoms; achalasia, alacrima and adrenal insufficiency (Allgrove et al., 1978). It is associated with homozygous or compound heterozygous mutations in a gene called *AAAS* located on chromosome 12q13. There have been less than 100 cases of triple A disease that have been reported since 1978 (Misgar et al., 2015). Due to genetic heterogeneity, mutations in genes other than *AAAS* have been reported for ~30% of the cases. The disease has an early onset in childhood with a broad spectrum of phenotypes ranging from severe neurological abnormalities, ataxia and muscle weakness (Grant et al., 1993; Houlden et al., 2002).

Genome-wide linkage analysis and whole-exome sequencing were used by our collaborators to discover a homozygous splice mutation in *TRAPPC11* (c.1893+3A>G, [NM_021942.5]) in two affected individuals (Subject 1 and Subject 2; Table 3.1). This splice mutation leads to a loss of exon 18 (131bp) resulting in a frameshift mutation (p.V588Gfs*16). The predicted shorter protein of 70 kDa is expressed to a level only 12% that of control in fibroblasts from affected individuals. The fibroblasts from affected individuals also contain 20%

of the normal WT transcript of *TRAPPC11* (loss of 80% of WT transcript of *TRAPPC11*) compared to control fibroblasts indicating an incomplete penetrance in the affected individuals due to partial loss of function.

3.2 *TRAPPC11* and *GOSR2* mutations cause α – dystroglycanopathy

Consequently, another set of collaborators identified three individuals with CMD of different severity in individuals aged 11 to 24 months from two different families. These individuals have α - dystroglycanopathy based on dystrophic muscle biopsies and abnormal hypoglycosylation of α -dystroglycan (α -DG). α - dystroglycanopathy is caused by mutations occurring in more than 15 genes that lead to various muscular dystrophies and hypoglycosylation of α -DG resulting in decreased binding to laminin, a fibrous protein in the basal lamina, by the extracellular matrix-binding glycan of α -DG. This is likely due to defects in glycosyltransferase protein activity in the ER or the Golgi that attach extracellular matrix-binding glycan to α -DG (Michele et al., 2002). Clinically, the phenotypes of α - dystroglycanopathy consist of CMD, brain and eye dysfunction and adult-onset of LGMD (Bönnemann et al., 2014).

Whole exome sequencing and sequencing of a dystroglycanopathy gene panel were conducted and identified compound heterozygous mutations in the three affected individuals. The first individual (Subject 3; Table 3.1) was diagnosed with congenital hypotonia, hyporeflexia, elevated CK levels, seizures, and hepatopathy (liver dysfunction due to heart failure). Subject 3 also displayed symptoms of severe developmental delay and microvesicular steatosis as well as cerebral atrophy and retinopathy. This affected individual is from a non-consanguineous mixed European family and carries compound heterozygous splice mutations in *TRAPPC11* (c.851A>C and c.965+5G>T, [NM_021942.5]) of which the first leads to a point mutation (p.Q284P) and the second genetic mutation has not been mapped to the protein sequence but is presumed to result in a splicing defect.

The second and third affected individuals (Subject 4 and Subject 5; Table 3.1) have mutations in the *GOSR2* gene, which plays a role in Golgi vesicle transport, and has been

associated with progressive myoclonus epilepsy (PME), hypotonia, weakness, developmental delay, and seizures. Clinically, they were diagnosed with CMD and epilepsy. Subject 4 has ventriculomegaly (dilation of the lateral ventricles of the brain), periventricular white matter changes, and thin corpus callosum, whereas Subject 5 showed mild dystroglycanopathy with thinning of the corpus callosum and optic nerve hypoplasia or underdevelopment of the optic nerve. Both affected individuals (Subjects 4 and 5) conserve the founder mutation in North Sea PME (c.430G>T; [NM_001012511]) which leads to a loss of function point mutation at the protein level (p.G144W) resulting in mislocalization of Golgi soluble N-ethylmaleimide-sensitive factor attachment protein receptor complex 2 (GOSR2) protein from the cis-Golgi where it functions in ER-to-Golgi trafficking (Corbett et al., 2011). The other mutations present in each affected individual are c.2T>G (Subject 4) and c.336+1G>A (Subject 5) of which the first has been mapped to a point mutation (p.M1R) resulting in the use of an alternative start codon eliminating 18 amino acids from the amino-terminus of the protein. The second genetic mutation in Subject 5 has not been mapped to the protein sequence yet. There was a deceased fourth affected individual who was a sibling of Subject 4 and thus preserved the same mutations as Subject 4. In this study, the characterization of fibroblasts from patients with *GOSR2* mutations was also performed since they possess similar clinical features to *TRAPPC11*-mutated individuals such as CMD, epilepsy, dystroglycanopathy and underdevelopment of the eye.

3.3 Other cases with *TRAPPC11* mutations

As mentioned in Table 3.1, other cases with *TRAPPC11* mutations analyzed in this study include two compound heterozygous mutations (Subject 6 and Subject 7). Subject 6 is a 15-year-old boy from Pakistan with CMD, microcephaly, and cataracts. At the protein level, the mutation has been mapped to p.Q933H and p.F866I with a frequency of 0.2 and 0.006, respectively (Figure 1.2, section 1.6). The frequency of the former mutation suggests it would not likely affect protein function. In addition, subject 6 has an unaffected sibling with identical *TRAPPC11* mutations and thus, the phenotype of this subject is likely not due to *TRAPPC11* mutations. This patient can be considered as another type of control. Subject 7 is a 7-year-old Asian boy with an intellectual disability, muscular weakness, microcephaly, epilepsy, and elevated CK. Subject 7 harbours a

previously described *TRAPPC11* mutation by Bögershausen et al. (2013) in the intron region (c.1287 +5G>A [NM_021942.5]) giving rise to p.A372_S429del in the protein level (Figure 1.2, section 1.6). The second mutation (c3379_3380insT) causes a frameshift and a C-terminal extension in the protein level (p.N1127Vfs*45).

Table 3.1 Nomenclature of the subjects studied in the study.

Subject	Gene and genetic mutation	Mutation at protein level
1 and 2	<i>TRAPPC11</i> c.1893+3A>G and c.1893+3A>G	p.V588Gfs*16
3	<i>TRAPPC11</i> c.851A>C and c.965+5G>T	p.Q284P (c.851 A>C)
4	<i>GOSR2</i> c.430G>T and c.2T>G	p.G144W and p.M1R
5	<i>GOSR2</i> c.430G>T and c.336+1G>A	p.G144W (c.430G>T)
6	<i>TRAPPC11</i> Unavailable	p.Q933H and p.F866I
7	<i>TRAPPC11</i> c.1287 +5G>A and c3379_3380insT	p.A372_S429del and p.N1127Vfs*45

3.4 TRAPPC11 protein levels are reduced in patients with certain *TRAPPC11* mutations

We determined the effect of mutations on the cellular levels of TRAPPC11 protein in fibroblasts from affected individuals compared to that in control fibroblasts. Lysates prepared from fibroblasts from control and affected individuals were subjected to western blotting using rabbit antiserum raised against the human TRAPPC11 protein (Scrivens et al, 2011). For Subjects 1, 2, 3, 6 and 7, the truncated protein was not detected using the TRAPPC11 antiserum which was raised against an epitope in the extreme carboxyl terminus of the protein. As a result, a truncated product was not detected. Instead, a decrease in the level of basal TRAPPC11 protein in fibroblasts from affected individuals with *TRAPPC11* mutations was observed (Figure 3.1A, B, and D). A small trace of full-length TRAPPC11 is visible on the western blot for Subject 1 and 2 due to the reduced mRNA levels of the regular splice product and incomplete splicing defect (Figure 3.1A; see section 3.1). Subjects 4 and 5 had similar levels of basal TRAPPC11 compared to control due to lack of mutation in *TRAPPC11* that would reduce the TRAPPC11 protein expression (Figure 3.1C; see section 3.2).

As suggested by Bogershausen et al. (2013), the *TRAPPC11* mutations p.G980R and p.A372_S429del are associated with hyperglycosylated LAMP1. In this study, we showed that LAMP1 was hypoglycosylated in fibroblast from Subjects 1-7 (Figure 3.1E-H). The hypoglycosylation of LAMP1 in fibroblasts from affected individuals indicated a possible defect in membrane trafficking or a possible *TRAPPC11* function in glycosylation as recently shown in the study by DeRossi et al. (2016). The *GOSR2* affected individuals (Subjects 4 and 5) also showed similar results as *TRAPPC11* affected individuals. The expression levels of *GOSR2* protein is not shown in these individuals due to lack of antibody to *GOSR2*.

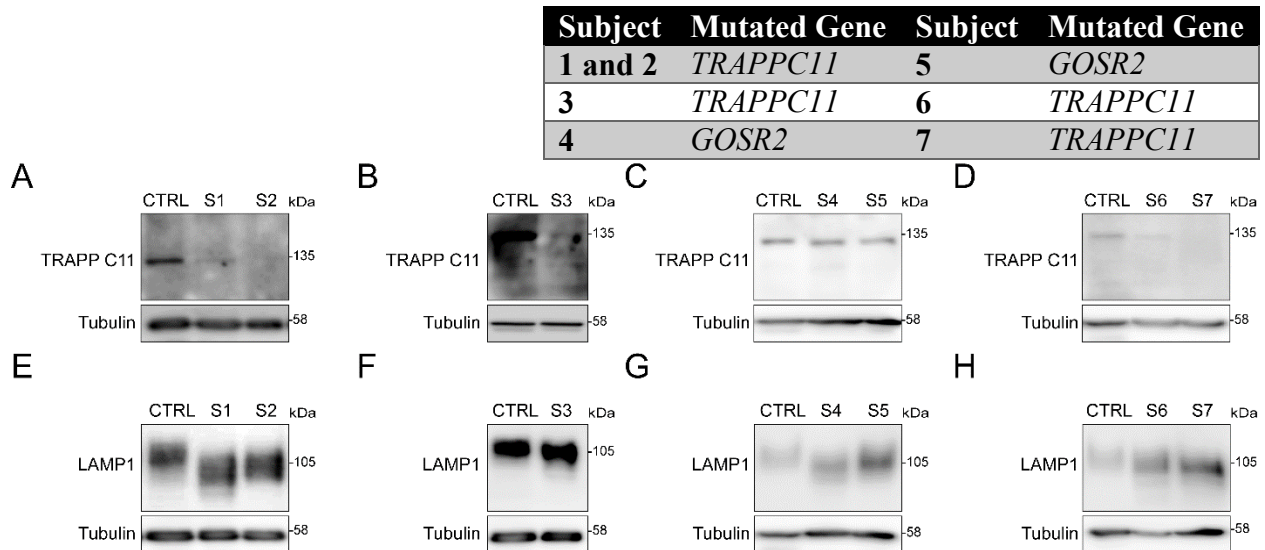


Figure 3.1: Western blot analysis of the lysates for *TRAPPC11* and *LAMP1*. Lysates prepared from control (CTRL) and Subjects 1-7 (S1-7) fibroblasts were probed for *TRAPPC11* (A-D), *LAMP1* (E-H) and tubulin as a loading control. The predicted truncated *TRAPPC11* in fibroblasts from affected individuals cannot be detected since the antibody was raised against an epitope in the extreme carboxyl-terminus of the protein. The molecular mass is indicated in kilodaltons (kDa) next to the blots. The description of Subjects 1-7 is shown.

3.5 The effects of *TRAPPC11* and *GOSR2* mutations on the trafficking of VSV-G-GFP as assessed biochemically

Previously, TRAPPC11 has been implicated in ER-to-Golgi transport (Scrivens et al, 2011; Wendler et al, 2010). Thus, we utilized a well-established membrane trafficking assay to monitor the movement of the ts045-VSV-G-GFP protein from the ER through the Golgi and on to the PM (Etchison et al, 1977; Katz et al, 1977; Rothman and Lenard, 1977; Scales et al., 1997). The ts045-VSV-G-GFP protein is retained in the ER at the restrictive temperature (40°C) and as the temperature decreases (32°C), in the presence of the protein synthesis inhibitor CXM, the protein is synchronously released from the ER. Once the protein is in the Golgi, it is processed by Golgi enzymes to be resistant to EndoH. Samples were collected prior to the downshift of temperature (0 min) and at time points shown in figures 4 and 5. The sensitivity of the protein to EndoH can be utilized to assess whether the protein has been modified in the Golgi.

The trafficking assay was first applied to HeLa cells following knockdown of TRAPPC11, TRAPPC12, or SYNTAXIN5, a t-SNARE involved in the fusion of transport vesicles with the cis-Golgi (Dascher et al., 1994), or addition of an alkylating agent, N-Ethylmaleimide (NEM), to inhibit membrane traffic (Balch et al., 1984; Glick and Rothman, 1987; Malhotra et al., 1988). TRAPPC11 and TRAPPC12 knockdown showed a delay in acquisition of EndoH resistance, though not as severe as either the SYNTAXIN5 knockdown or the NEM treatment (Figure 3.2). Thus, the ts045-VSV-G-GFP trafficking assay is sensitive to identify delays in the processing of the ts045-VSV-G-GFP protein.

I next applied this assay to fibroblasts from control or affected individuals. Quantification of upper (EndoH resistant) and lower (EndoH sensitive) bands for the EndoH assay for affected individuals showed a slight difference between the affected individuals (Subjects 1, 3 and 5) and control. The delay in the appearance of the EndoH resistant band was significant at 40 minutes for Subject 2 and at 40 minutes and 90 minutes for Subjects 3 and 7. Note that the quantification for the EndoH assay for Subject 2 was omitted. Subjects 4 and 6 showed no apparent difference in phenotype compared to control at the cellular level. For Subject 5, the EndoH resistance was acquired earlier than control and appeared to be significantly higher at 20 minutes. The slight

difference in the appearance of the EndoH resistant form in affected individuals suggests a defect in the trafficking of the ts045-VSV-G-GFP protein out of the ER or delay in traffic through the Golgi complex (Figure 3.3B-E).

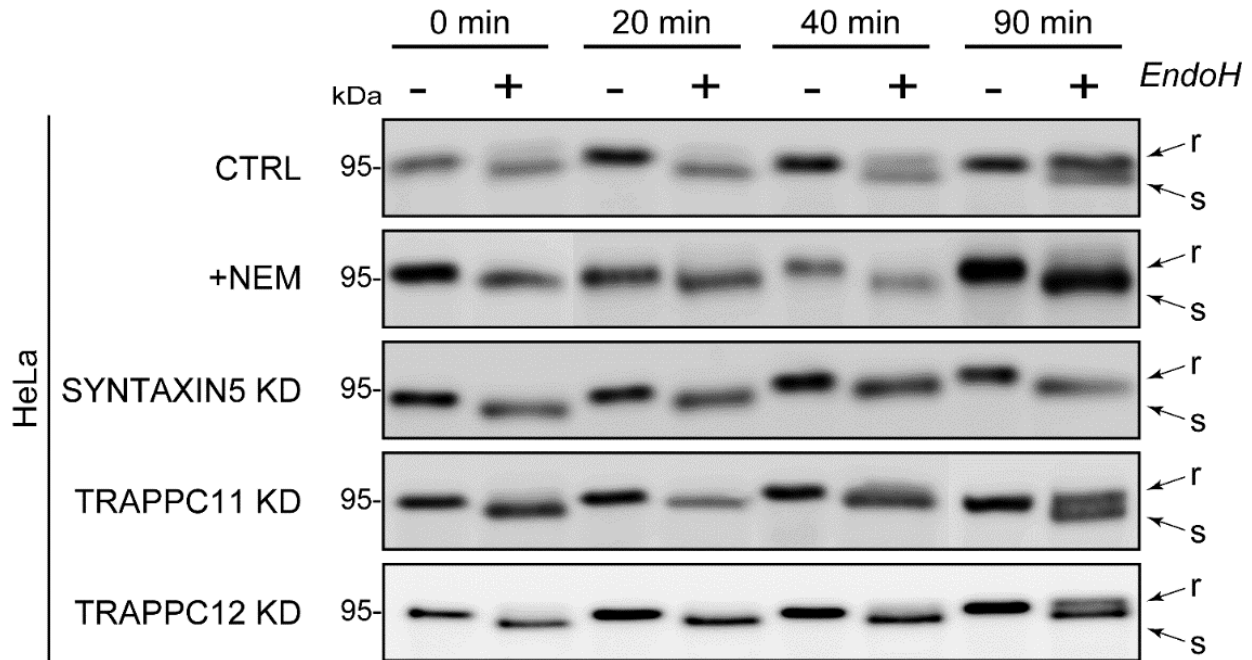


Figure 3.2: The ts045-vesicular stomatitis virus glycoprotein-GFP trafficking assay applied to HeLa cells. HeLa cells transfected with siRNA specific for SYNTAXIN5, TRAPPC11, or TRAPPC12, or treated with N-Ethylmaleimide (NEM), were subjected to the temperature-sensitive vesicular stomatitis virus glycoprotein fused to GFP (ts045-VSV-G-GFP) trafficking assay by infecting the cells with the virus. The ts045-VSV-G-GFP protein was retained in the ER by shifting the cells to non-permissive temperature overnight. Samples were collected at various time points. A portion of each sample was treated with Endoglycosidase H (EndoH) and analyzed by Western blotting for the ts045-VSV-G-GFP protein using anti-GFP. The sensitivity of the ts045-VSV-G-GFP protein to EndoH indicates whether ts045-VSV-G-GFP protein has reached the Golgi. Arrows indicate the EndoH resistant form (r) and the EndoH sensitive form (s) of ts045-VSV-G-GFP. The molecular mass is indicated in kilodaltons (kDa) next to the blots. KD, Knockdown; CTRL, Control.

Subject	Mutated Gene	Subject	Mutated Gene
1 and 2	<i>TRAPPC11</i>	5	<i>GOSR2</i>
3	<i>TRAPPC11</i>	6	<i>TRAPPC11</i>
4	<i>GOSR2</i>	7	<i>TRAPPC11</i>

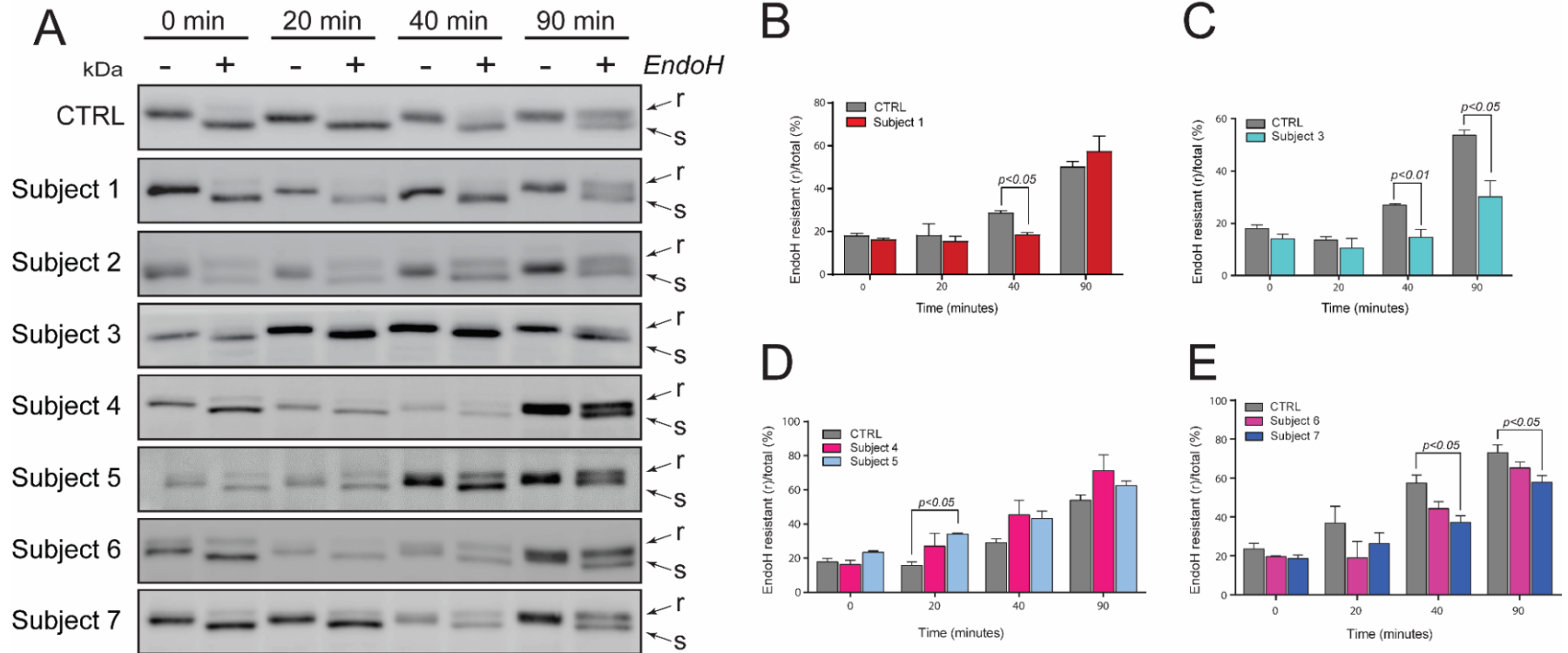


Figure 3.3: Affected individuals show a delay in endoglycosidase H resistance. (A) Fibroblasts from control (CTRL) and affected individuals were subjected to the ts045-VSV-G-GFP trafficking assay as described for Figure 3.2. A representative blot for each is shown. Arrows indicate the EndoH resistant form (r) and the EndoH sensitive form (s) of ts045-VSV-G-GFP. The molecular mass is indicated in kilodaltons (kDa) next to the blots. (B) Data from three or more independent experiments described in (A) were quantified and are displayed as mean \pm SEM. Statistical significance between control and affected individuals was assessed using a Student's t-test or one-way ANOVA. Post-hoc differences were made using Fisher's probability of least squared differences. The description of Subjects 1-7 is shown.

3.6 Accumulation of VSV-G-GFP in the Golgi in individuals with different *TRAPPC11* mutations

In order to distinguish between the above two possibilities (i.e. a delay in ER exit or a delay in Golgi trafficking since EndoH resistance occurs in a medial-Golgi compartment), we used confocal microscopy on fixed cells at various time points (Figure 3.4) to determine the location of the ts045-VSV-G-GFP protein and the point of delay in trafficking. As seen in Figure 3.4, the control fibroblasts showed the ts045-VSV-G-GFP protein in the ER by staining the cytoplasm at the zero-minute time point. At the 30-minute time point, the GFP fluorescence shifted to a singular point giving rise to colocalization with the Golgi marker ManII. The overlap of the GFP and ManII signal gradually decreased as the ts045-VSV-G-GFP protein traveled to the PM by 90 minutes. The fibroblasts from Subject 1 showed ManII and GFP signal overlap at a later time (60 minutes) and the overlap was persistent even after 120 minutes. Some of the cells of Subject 1 lacked this delayed trafficking phenotype and thus showed the overlap of the ts045-VSV-G-GFP protein with the Golgi marker protein at 30 minutes and the gradual disappearance of it afterward, similar to the control fibroblasts. Thus, there are two different populations of fibroblasts with different kinetics of transport in Subject 1 due to the incomplete splicing defect (see section 3.1).

For Subjects 3 and 7, the overlap of the GFP and ManII signal occurred as early as 20 minutes but was kept consistent over the time frame up to 120 minutes. Subjects 4 and 6 showed no apparent difference in phenotype to control at the cellular level during the biochemical assay (see section 3.5) and thus were omitted from the immunostaining study. Note that Subjects 2 and 5 were also omitted from this assay. It is important to note that fibroblasts from affected individuals (Subjects 1, 3 and 7) showed Golgi fragmentation compared to control (Figure 3.4). The ts045-VSV-G-GFP trafficking assay applied to fixed fibroblasts with *TRAPPC11* mutations (Figure 3.4) indicates that there is a defect in protein trafficking out of the Golgi and a delay in the arrival of the protein to the Golgi, similar to that observed in the biochemical assay (Figure 3.3).

GFP (VSV-G) Man II DAPI

Subject	Mutated Gene
1	<i>TRAPPC11</i>
3	<i>TRAPPC11</i>
7	<i>TRAPPC11</i>

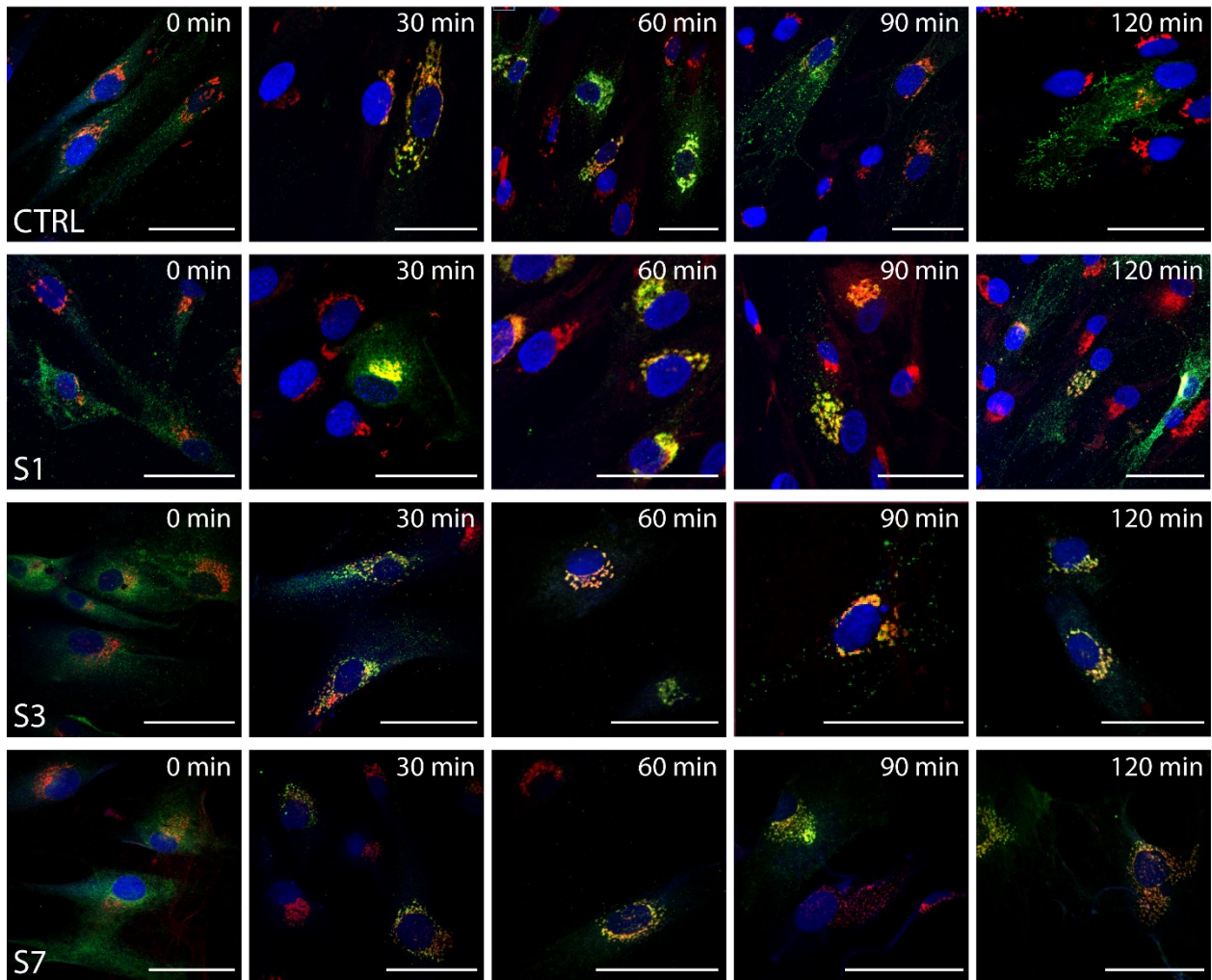
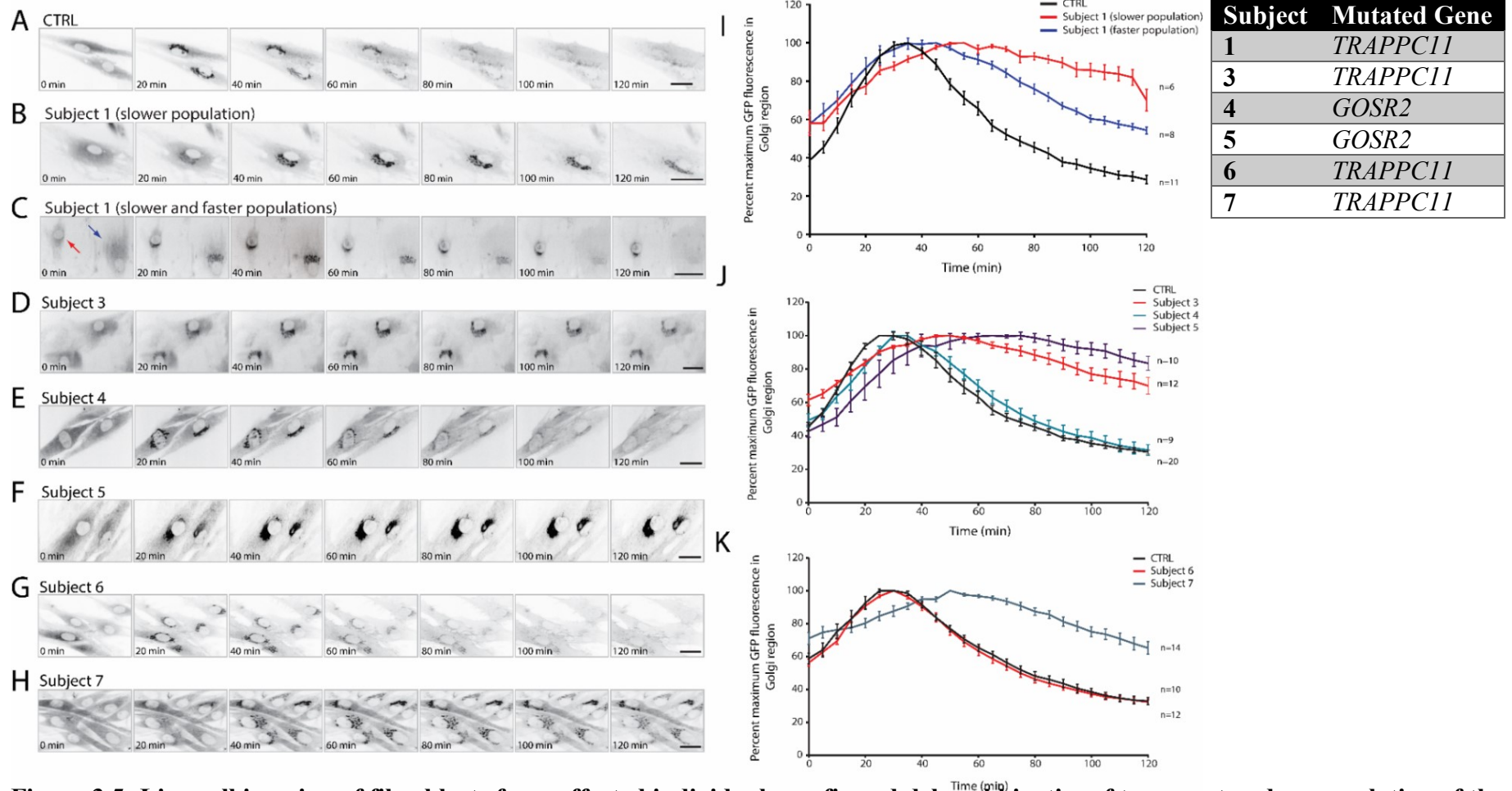


Figure 3.4: The ts045-vesicular stomatitis virus glycoprotein-GFP in fibroblasts from affected individuals showed delayed kinetics of transport and accumulation in the Golgi. Fibroblasts from control (CTRL) and affected individuals (Subject 1 (S1), S3 and S7) were subjected to the ts045-VSV-G-GFP trafficking assay as described in Figure 3.2. Samples were removed at various time points and fixed before staining for mannosidase II (ManII), GFP and DAPI. Immunostaining showed a delay in transport of ts045-VSV-G-GFP to the PM in fibroblasts from affected individuals, with the protein accumulating in the Golgi. Note the disrupted Golgi morphology in affected individuals. The scale bars represent 50 μ m. The description of Subjects 1, 3 and 7 is shown.

3.7 VSV-G-GFP shows a significant delay in trafficking to and through the Golgi in individuals with *TRAPPC11* and *GOSR2* mutations

Since microscopy of fixed cells was performed on groups of different cells for a given time point, live-cell microscopy was performed to visualize the movement of the ts045-VSV-G-GFP protein during trafficking inside a particular cell as shown in Figure 3.5A-H. Similar to observations for the fixed cells, an apparent delay in the release of the ts045-VSV-G-GFP protein from the Golgi was observed for Subjects 1, 3 and 7. Quantification of the live cells (Figure 3.5I-K) suggested a slight delay in the arrival of the ts045-VSV-G-GFP protein to the Golgi (20-25 minutes) in Subjects 1, 3 and 7 compared to control cells (30 minutes), and further retention of the ts045-VSV-G-GFP protein in the Golgi for these subjects, consistent with the biochemical assay (Figure 3.3). For Subject 1, quantification of the two different populations with different kinetics in the movies showed ~70% of cells with a delay in trafficking and ~30% with trafficking kinetics similar to the control fibroblasts (Figure 3.5C and I). The ratio of the two different populations agrees with the incomplete penetrance due to splicing defect which produced a small quantity of full-length TRAPPC11 in affected individuals sufficient to induce kinetics similar to that in control (see section 3.1). Note that the trafficking assay for Subject 2 was omitted.

Subjects 4 and 6 showed no apparent difference in phenotype to control during the biochemical assay (see section 3.5) and during the time-lapse microscopy (Figure 3.5E and G). In contrast to the data from the biochemical assay for Subject 5, the kinetics of transport of the marker protein from the ER to the Golgi was delayed (10-15 minute delay), possibly due to analysis of the entire cell population in the biochemical assay (Figure 3.3) compared to analysis of a single cell during live-cell imaging (Figure 3.5F and J). The data for all the subjects were not pooled to perform one-way ANOVA since different controls were used for subjects 3, 4 and 5 versus subjects 6 and 7. Live-cell analysis suggested a possibility that either two steps in membrane traffic are affected simultaneously (i.e. ER-to-Golgi and intra-Golgi) or the delay in arrival at the Golgi is a secondary consequence of the reduced transport through the Golgi.



3.8 Altered LAMP1 and TGN46 localization in fibroblasts from an individual with *TRAPPC11* mutations

In an attempt to understand the consequences of an intra-Golgi trafficking delay, fibroblasts from control and Subject 7 with *TRAPPC11* mutations were stained for p115 (cis-Golgi), ManII (medial-Golgi), TGN46 (trans-Golgi), LAMP1 (lysosomes), and tubulin (microtubules). Subject 7 was chosen since it displayed the most severe cellular phenotype in terms of Golgi morphology. Any aberration in the location and/or structure of these marker proteins can possibly give away the defective mechanism along the secretory pathway of the ts045-VSV-G-GFP protein. As seen in Figure 3.6, immunostaining of fibroblasts from Subject 7 indicated an apparent difference in the localization pattern of TGN46 and LAMP1 marker proteins compared to control. TGN46 was observed as organized stacks in the Golgi while LAMP1 was observed as puncta ubiquitously in the cell for the control (red arrows in Figure 3.6), similar to previous studies (Prescott et al., 1997; Humphries et al., 2011). In contrast, fibroblasts from Subject 7 showed a noticeable perinuclear staining for TGN46 and LAMP1 in a large population of cells (red arrows in Figure 3.6; quantifications not shown). Also, the Golgi morphology was disrupted in the affected individual compared to control, as shown by the p115 and ManII staining. Note that the microtubules are not altered in Subject 7 (red arrow pointing to MTOC in Figure 3.6). These observations indicate a possible role for *TRAPPC11* in the structure and formation of the Golgi complex and late endosomal/lysosomal compartments. A possible explanation is that *TRAPPC11* interacts with a motor protein to regulate the formation of these altered structures by affecting the transport of the vesicles along the microtubules.

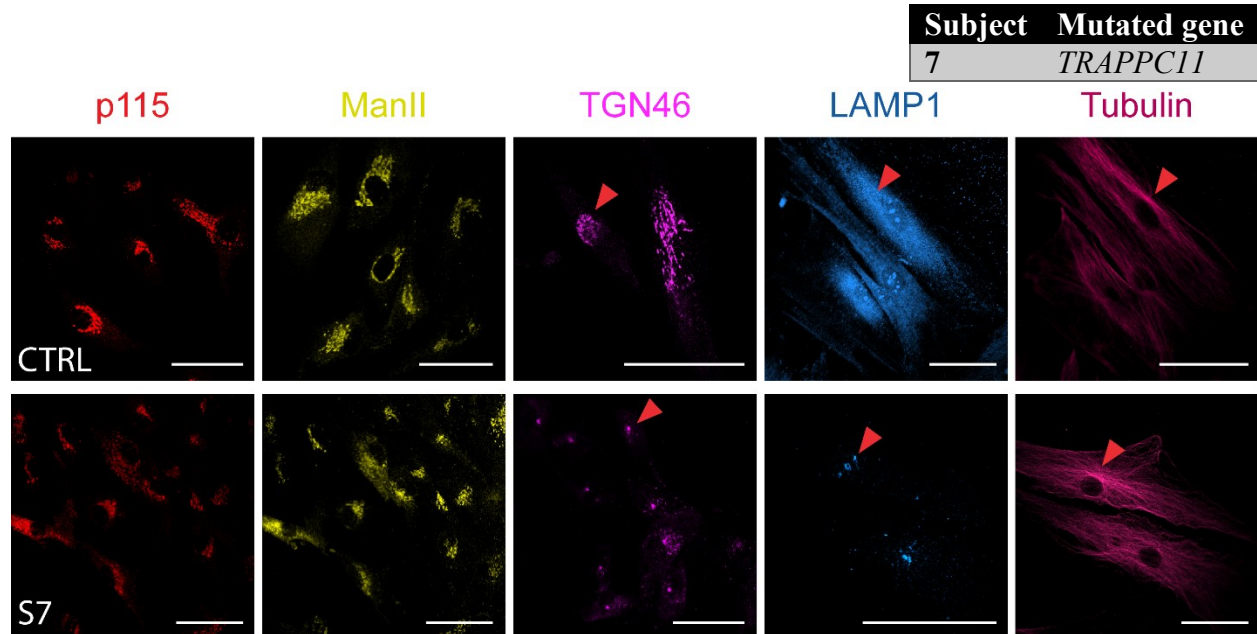


Figure 3.6: Altered LAMP1 and TGN46 localization in fibroblasts from Subject 7. Immunostaining with a trans-Golgi marker, TGN46, and lysosome marker, LAMP1, displayed a typical diffuse pattern for both proteins in control fibroblasts. An apparent perinuclear accumulation of TGN46 and LAMP1 was observed in fibroblasts from an affected individual, Subject 7 (S7), with *TRAPPC11* mutations. Note the disrupted Golgi morphology in the affected individual as shown by p115 (cis-Golgi) and ManII (medial-Golgi) staining. Tubulin immunostaining showed unaffected microtubules in both control and Subject 7. The red arrows point to the trans-Golgi or lysosomes or microtubule-organizing center (MTOC). The mutated gene in Subjects 7 is shown. The scale bars are 50 μ m.

3.9 *TRAPPC11* mutations show reduced autophagy activity

Since the structure and formation of the late endosomal/lysosomal compartments are affected by *TRAPPC11* mutations, I was interested in observing whether *TRAPPC11* mutations in the affected individuals had any effect on the autophagy pathway, as reported by a previous study (Behrends et al., 2010). In contrast to suggestions by the Behrends et al. (2010) study, the lipidated form of LC3 (LC3-II) accumulated in affected individuals (Subjects 1, 2 and 3) during nutrient deprivation whereas, in the control fibroblasts, the levels of LC3-II decreased over time (Figure 3.7A). The accumulation of LC3-II in affected individuals indicates an increase in autophagosomes and/or autolysosomes due to a defect in the degradation of LC3-II by lysosomal enzymes. This dysfunction could be due to an inability of autophagosomes to fuse with lysosomes

or the defects in structure and formation of late endosomal/lysosomal compartments (see section 3.8). Quantification of the levels of LC3-II normalized to the tubulin control further supported this observation since at 4 hours, the fibroblasts from affected individuals contained significantly more LC3-II levels compared to control. The levels were close to the levels of LC3-II that accumulate in Bafilomycin A1 (Baf. A1)-treated cells, a molecule that inhibits autophagic flux (Figure 3.7B).

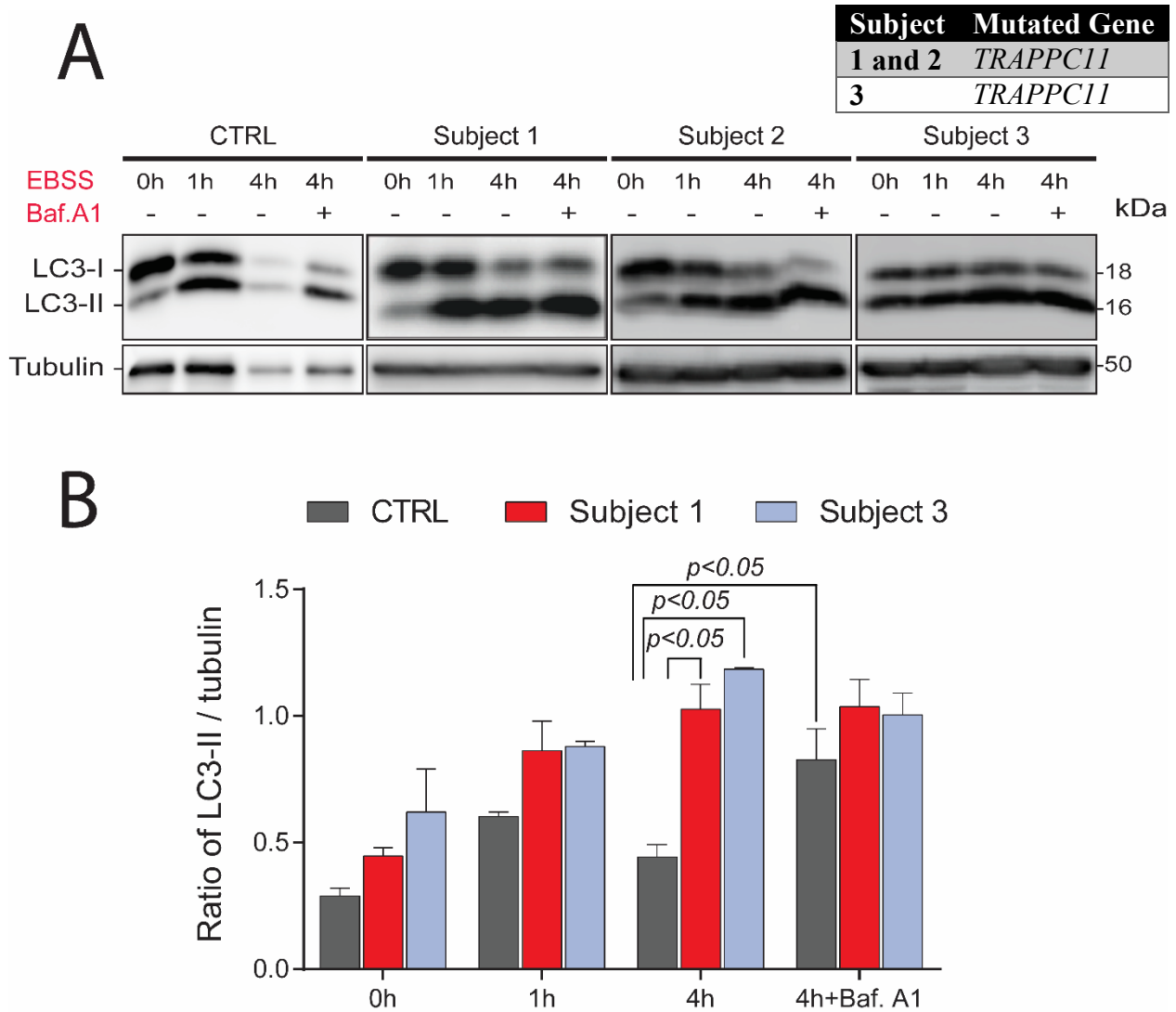


Figure 3.7: Reduced autophagy activity in the fibroblasts from affected individuals. (A) Fibroblasts from control or affected individuals (Subjects 1, 2, and 3) were non-treated or treated with the autophagy inhibitor Bafilomycin A1 (Baf.A1) for 4 hours and/or EBSS for 1 hour (1h) or 4 hours (4h) to induce autophagy. The fibroblasts were harvested in lysis buffer and subjected to western blotting for microtubule-associated protein 1 light chain 3 (LC3; isoforms I and II). Tubulin was used as a loading control. The molecular mass is indicated in kilodaltons (kDa) next

to the blots. (B) Data from three or more independent experiments described in (A) were quantified and are displayed as mean \pm SEM. Statistical significance between control and affected individuals and +/- Baf. A1 conditions were assessed using a Student's t-test. The mutated genes in Subjects are shown.

3.10 Individuals with *TRAPPC11* mutations display altered TRAPP complex assembly

In order to determine whether the effect of *TRAPPC11* mutations on different pathways is due to its ability to disrupt the mTRAPP complex, size exclusion chromatography was performed on cells from subject 7, the subject with the most dramatically affected Golgi. As seen in Figure 3.8, when immunoblotted for the mTRAPP subunit TRAPPC12, the control fibroblasts displayed a broad size distribution (fractions 19-25) with the larger molecular size fractions contributing to the mTRAPP complex (Bassik et al., 2013). Subject 7 displayed a slight shift to a lower molecular weight with peaks appearing in fractions 24/25 possibly due to disassociation from the complex. This suggests a possible disruption of the mTRAPP complex (or disassociation of one of the subunits, TRAPPC12, from the complex) due to mutations in *TRAPPC11*. These results shed light on the role of TRAPPC11 in stabilizing the mTRAPP complex since mutations in *TRAPPC11* cause disassociation of at least one of the TRAPP subunits, TRAPPC12, as it shifts to a lower molecular size fraction (Figure 3.8). Effects on the entire complex require assessment of the fractionation of other TRAPP subunits.

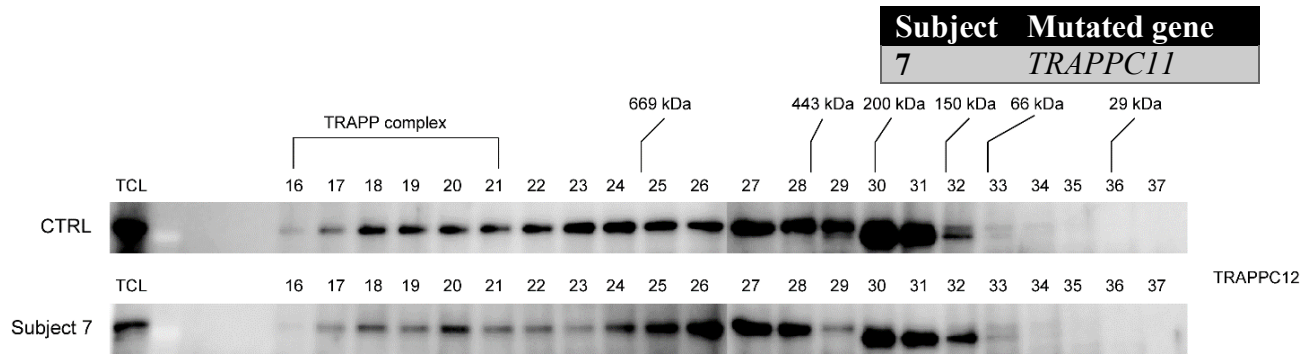


Figure 3.8: Subject 7 displays a shift in the TRAPPC12 subunit to a smaller molecular size. Fibroblasts from control or Subject 7 were lysed and the lysates were fractionated on a Superose 6 size exclusion column and fractions (16-37) were subjected to western blotting using antibodies against TRAPPC12. The migration of standards is indicated above the top panel along with the molecular sizes indicated in kilodaltons (kDa). The mutated gene in Subject 7 is shown.

4 DISCUSSION

In this study, homozygous and compound heterozygous mutations in the *TRAPPC11* and *GOSR2* genes in human fibroblasts from seven individuals were characterized and have been added to the growing group of mutations in *TRAPPC11* and *GOSR2* causing neuromuscular and myopathy phenotypes. The affected individuals showed novel mutations in *TRAPPC11* as well as mutations seen in previous studies (Table 4.1 and Figure 4.1). Previous studies on the *TRAPPC11* mutations in human fibroblasts have shown fragmented Golgi, protein accumulation in the Golgi, decreased LAMP1 levels, accumulation of LAMP1 at the MTOC and accumulation of lipid droplets. In this study, I have shown that *TRAPPC11* mutations in human fibroblasts cause hypoglycosylation of LAMP1, ER-to-Golgi trafficking defects, delay in the exit of proteins from the Golgi, Golgi fragmentation, defects in the autophagy pathway as well as partial disassembly of the mTRAPP complex. This study greatly contributes to the characterization of the growing group of *TRAPPC11* mutations to identify the defective pathways which cause a neuromuscular phenotype. This study is the first study to show reduced autophagy activity in *TRAPPC11*-mutated individuals, which is a characteristic of many neuromuscular diseases. Thus, this study will greatly shed light on the future work which identifies the mechanism of action of TRAPPC11 with relation to neuromuscular diseases that affect multiple organs and the homeostasis of the organism.

Five out of seven individuals studied in this study with *TRAPPC11* or *GOSR2* mutations showed defects at the cellular level (Figure 3.1). Two of these five affected individuals (Subjects 1 and 2) are from a Turkish background and have a homozygous mutation in *TRAPPC11* leading to a Triple-A-like disorder with scoliosis, alacrima, achalasia, muscle dystrophic changes and cerebral atrophy. The third individual (Subject 3) is from a European background and has CMD, α -dystroglycanopathy, brain, eye, and liver involvement, due to a mutation in *TRAPPC11*. The fourth individual (Subject 5) with the *GOSR2* mutation was clinically diagnosed with CMD, epilepsy, mild dystroglycanopathy and defect in eye development. The fifth individual with *TRAPPC11* mutation (Subject 7) is Asian and showed cognitive impairment, muscular weakness, and microcephaly. Combined with previous studies (Bögershausen et al., 2013; Liang et al., 2015), *TRAPPC11* mutations affect the brain, eyes, liver, muscle, and bone, indicating its role in multiple tissue types and organs (Liang et al., 2015). Moreover, the *TRAPPC11* mutations mentioned in

this study which displayed changes at the cellular level include frameshifts, point mutations or deletions at or near the foie gras domain (Figure 4.1). Thus, we can conclude that the foie gras domain is a common site for TRAPPC11 mutations that lead to the cellular phenotypes mentioned in this study.

LAMP1 and LAMP2 make up ~50% of the lysosomal membrane proteins (Eskelinen, 2006). They are critical for the maintenance of lysosomal structure, pH, and function. They are also involved in lysosomal exocytosis, movement of the lysosomes along the microtubules and the fusion of APs with lysosomes (Schwake et al., 2013). Based on our findings, LAMP1 was hypoglycosylated in all the affected individuals. Immunostaining of fibroblasts from Subject 7 indicated a noticeable perinuclear staining for LAMP1 possibly due to the inability of lysosomes to move along the microtubules. This study is consistent with the Bögershausen et al. (2013) study where LAMP1 focused on a perinuclear region similar to the MTOC. In contrast to the Behrends et al. (2010) study, the lipidated form of LC3 (LC3-II) accumulated in affected individuals (Subject 1, 2 and 3; Figure 3.7) during nutrient deprivation possibly due to the hypoglycosylation of LAMP1, which may inhibit fusion of APs with lysosomes. This study also contrasts with the Bögershausen et al. (2013) study which showed hyperglycosylation of LAMP1 and LAMP2 in affected individuals. In the study by DeRossi et al. (2016), glycosylation in a zebrafish model of *TRAPPC11*-related diseases showed defects in synthesizing lipid-linked oligosaccharides (LLOs) as the mechanism of defective protein glycosylation. Thus, we can conclude that TRAPPC11 mutations affect the autophagy pathway possibly due to defective LAMP1 glycosylation that might interfere with the fusion of APs with lysosomes, leading to neuromuscular diseases.

α -DG is hypoglycosylated in skeletal muscle cells of the individuals with *TRAPPC11* or *GOSR2* mutations (Subjects 3-5). It is tempting to speculate that TRAPPC11 causes α -dystroglycanopathy by inhibiting glycosyltransferase function(s) important for the synthesis of the extracellular matrix-binding glycan of the α -DG, consistent with the roles of TRAPPC11 in LLO synthesis (DeRossi et al., 2016). GOSR2 is located in the cis-Golgi to facilitate docking and fusion of COPII vesicles from the ER. SNARE complexes with GOSR2 are known to interact with the COG complex (Kudlyk et al., 2013). Since CDGs and neurological diseases are caused by mutations in *COG* genes which affect protein glycosylation, *GOSR2* mutations can also be linked

to defects in protein glycosylation. Alternatively, since GOSR2 is a SNARE protein that functions in ER-to-Golgi transport (Fusella et al., 2013), α -DG hypoglycosylation in those patients may result from membrane trafficking defects.

The defect in glycosylation of LAMP1 and/or α -DG in TRAPPC11 patients can also be due to defects in membrane trafficking pathways as suggested by Figures 3.3-3.5. In Figures 3.3-3.5, the delayed arrival of the ts045-VSV-G-GFP protein to the Golgi could be a secondary effect due to the defect in transport through the Golgi. It is also possible that the delay in the arrival of the ts045-VSV-G-GFP protein to the Golgi is independent of the delay in transport through the Golgi. In order to distinguish between these two possibilities, fibroblasts from Subject 7 was stained with an ER marker (data not shown) as well as cis-, medial-, and trans-Golgi markers. While the ER structure was intact in this individual (not shown), the cis-, medial-, and trans-Golgi were affected by the *TRAPPC11* mutations. Our observations are consistent with those of the Bögershausen et al. (2013) study which showed abnormally fragmented and diffused Golgi in fibroblasts from affected individuals.

Many cellular stresses such as autophagy can affect Golgi structure. Golgi morphology disruption is related to many neurodegenerative diseases such as amyotrophic lateral sclerosis (ALS), Alzheimer's disease, and Parkinson's disease (Haase and Rabouille, 2015; Joshi et al., 2015; Machamer, 2015). Since ER and Golgi are the major compartments for protein glycosylation, atypical Golgi morphology and/or dynamics in affected individuals could be responsible for the hypoglycosylation of LAMP1 in all the individuals and α -DG in Subject 3-5. In individuals with *TRAPPC11* mutations, the mTRAPP complex integrity appears to be compromised since the size exclusion chromatography experiments showed a shift of the TRAPPC12 protein to lower molecular size fractions, possibly due to disassembly of the TRAPP complex. These findings are inconclusive as further investigations are required to observe the effect on other TRAPP subunits and the integrity of the mTRAPP complex function.

Since altered Golgi morphology was not observed in individuals with *GOSR2* mutations, a possible explanation for the defects in protein secretion would be the inhibition of intra-Golgi transport by blockage of the inter-cisternal connections (Fusella et al., 2013). The study by Fusella

et al. (2013) also suggests inhibition of COPI vesicle formation due to a deficit of GOSR2 and acceleration of cis-to-trans-Golgi transport of the ts045-VSV-G-GFP protein. It is possible that the increased rate of acquisition of EndoH resistance in an individual with a *GOSR2* mutation (Subject 5) was observed due to incomplete protein glycosylation in the Golgi (Xiang et al., 2013). The delay in protein secretion from the Golgi in these individuals can be due to improper sorting at the TGN, similar to that for GRASP55/65 depletion (Xiang et al., 2013). Thus, we can conclude that mutations in *TRAPPC11* and *GOSR2* may cause muscular dystrophy due to hypoglycosylation of LAMP1 and α -DG due to abnormal Golgi morphology and/or protein secretion out of the Golgi.

Protein trafficking out of the Golgi was also significantly delayed in individuals with *TRAPPC11* mutations that also had abnormal Golgi morphology and hypoglycosylation of LAMP1 and/or α -DG. The study by Bögershausen et al. (2013) also reported defects in protein trafficking out of the Golgi and abnormal glycosylation of both LAMP1 and LAMP2. Thus, this study underscores the role of *TRAPPC11* in membrane trafficking and glycosylation since the newly-discovered mutations show multiple defects including ER-to-Golgi and intra-Golgi trafficking delays. In conclusion, *TRAPPC11* and *GOSR2* are membrane trafficking proteins that are associated with ER-to-Golgi trafficking as well as intra-Golgi trafficking. *TRAPPC11* plays a role in multiple trafficking pathways including ER-to-Golgi trafficking, protein secretion out of the Golgi, Golgi morphology, protein glycosylation, autophagy, and integrity of the mTRAPP complex. These genes should be considered in the diagnostic evaluation of patients with neuromuscular diseases with unknown genetic mutations.

The relationship between *TRAPPC11* mutations and neuromuscular phenotypes is very complex and needs further investigation for a better understanding of the mechanism of action of *TRAPPC11*. Identifying the mechanism by which *TRAPPC11* affects protein secretion, glycosylation and Golgi morphology should be the focus of future studies. In order to accomplish this, one can look into interacting partners of *TRAPPC11*, specifically in or around the foie gras domain where most of the mutations that lead to cellular phenotypes are located. The deficit of another Golgi-associated protein, dymeclin, was recently reported to be associated with similar clinical phenotypes to *TRAPPC11* mutations. These individuals displayed postnatal microcephaly, defects in the nervous system and eye, and ER-to-Golgi trafficking defects in mice and humans

(Dupuis et al., 2015). Thus, dymeclin could be a possible candidate to examine its interaction and pathomechanism with relation to TRAPPC11, though it is not known as an interacting partner of the TRAPP complex (Liang et al., 2015). The carriers and the target membranes of the exact stage of trafficking which TRAPPC11 is involved have to be investigated. Generation of a global interacting map of all the tethers and tethering factors will allow us to identify possible interacting partners of TRAPPC11 and additional functions of TRAPPC11 and other tethering factors.

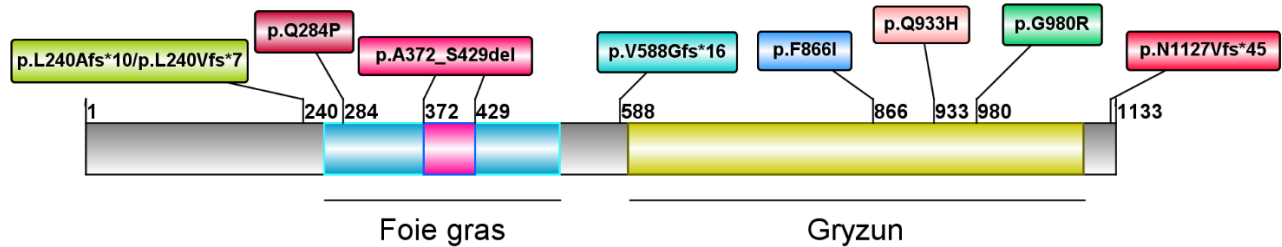


Figure 4.1: Cartoon representation of the current *TRAPPC11* mutations reported to date. Novel *TRAPPC11* mutations discussed in this study and previously mentioned *TRAPPC11* mutations are shown based on their location along the protein sequence for TRAPPC11. The numbers represent the amino acid number in the protein sequence.

Table 4.1 Current mutations of *TRAPPC11* reported to date and mentioned in this study.

Number of cases (families)	Family origin	<i>TRAPPC11</i> Genetic mutation	Mutation at protein level	Consanguinity (Yes/No)	Reference
3 (1 family)	Syrian	c.2938G>A/ c.2938G>A	p.G980R	Yes	Bögershausen et al., 2013
5 (2 families)	Hutterite	c.1287+5G>A/ c.1287+5G>A	p.A372_S429del	Yes	Bögershausen et al., 2013
1	Asian	c.2938G>A/ c.661-1G>T	p.L240Afs*10 and p.L240Vfs*7	No	Liang et al., 2015
4 (2 families)	Turkish	c.1893+3A>G/ c.1893+3A>G	p.V588Gfs*16	Yes	Koehler et al., 2016
1	Mixed European	c.851A>C/ c.965+5G>T	p.Q284P (c.851 A>C)	No	Larson et al., Unpublished work
2 (2 families)	Subject 6: Pakistan Subject 7: Asian	Subject 6: Unavailable Subject 7: c.1287 +5G>A/ c3379_3380insT	Subject 6: p.Q933H and p.F866I Subject 7: p.A372_S429del and p.N1127Vfs*45	Unknown	Jimenez-Mallebrera et al., Unpublished work

5 REFERENCE

- Allgrove, J., Clayden, G. S., Grant, D. B., and Macaulay, J. C. (1978). Familial glucocorticoid deficiency with achalasia of the cardia and deficient tear production. *Lancet (London, England)*, *1*(8077), 1284–1286.
- Andag, U., and Schmitt, H. D. (2003). Dsl1p, an essential component of the Golgi-endoplasmic reticulum retrieval system in yeast, uses the same sequence motif to interact with different subunits of the COPI vesicle coat. *The Journal of Biological Chemistry*, *278*(51), 51722–51734. <https://doi.org/10.1074/jbc.M308740200>
- Anglade, P., Vyas, S., Javoy-Agid, F., Herrero, M. T., Michel, P. P., Marquez, J., ... Agid, Y. (1997). Apoptosis and autophagy in nigral neurons of patients with Parkinson's disease. *Histology and Histopathology*, *12*(1), 25–31.
- Aoki, T., Ichimura, S., Itoh, A., Kuramoto, M., Shinkawa, T., Isobe, T., and Tagaya, M. (2009). Identification of the neuroblastoma-amplified gene product as a component of the syntaxin 18 complex implicated in Golgi-to-endoplasmic reticulum retrograde transport. *Molecular Biology of the Cell*, *20*(11), 2639–2649. <https://doi.org/10.1091/mbc.E08-11-1104>
- Aoyama, M., Sun-Wada, G.-H., Yamamoto, A., Yamamoto, M., Hamada, H., and Wada, Y. (2012). Spatial restriction of bone morphogenetic protein signaling in mouse gastrula through the mVam2-dependent endocytic pathway. *Developmental Cell*, *22*(6), 1163–1175. <https://doi.org/10.1016/j.devcel.2012.05.009>
- Arasaki, K., Takagi, D., Furuno, A., Sohda, M., Misumi, Y., Wakana, Y., ... Tagaya, M. (2013). A new role for RINT-1 in SNARE complex assembly at the trans-Golgi network in coordination with the COG complex. *Molecular Biology of the Cell*, *24*(18), 2907–2917. <https://doi.org/10.1091/mbc.E13-01-0014>
- Aridon, P., De Fusco, M., Winkelmann, J. W., Zucconi, M., Arnao, V., Ferini-Strambi, L., and Casari, G. (2016). A TRAPPC6B splicing variant associates to restless legs syndrome. *Parkinsonism and Related Disorders*, *31*, 135–138. <https://doi.org/10.1016/j.parkreldis.2016.08.016>
- Baba, M., Takeshige, K., Baba, N., and Ohsumi, Y. (1994). Ultrastructural analysis of the autophagic process in yeast: detection of autophagosomes and their characterization. *The Journal of Cell Biology*, *124*(6), 903–913.

- Bacon, R. A., Salminen, A., Ruohola, H., Novick, P., and Ferro-Novick, S. (1989). The GTP-binding protein Ypt1 is required for transport in vitro: the Golgi apparatus is defective in ypt1 mutants. *The Journal of Cell Biology*, 109(3), 1015–1022.
- Balch, W. E., Glick, B. S., and Rothman, J. E. (1984). Sequential intermediates in the pathway of intercompartmental transport in a cell-free system. *Cell*, 39(3 Pt 2), 525–536.
- Banfield, D. K. (2001). SNARE complexes--is there sufficient complexity for vesicle targeting specificity? *Trends in Biochemical Sciences*, 26(1), 67–68.
- Barlowe, C., Orci, L., Yeung, T., Hosobuchi, M., Hamamoto, S., Salama, N., ... Schekman, R. (1994). COPII: a membrane coat formed by Sec proteins that drive vesicle budding from the endoplasmic reticulum. *Cell*, 77(6), 895–907.
- Bassik, M. C., Kampmann, M., Lebbink, R. J., Wang, S., Hein, M. Y., Poser, I., ... Weissman, J. S. (2013). A systematic mammalian genetic interaction map reveals pathways underlying ricin susceptibility. *Cell*, 152(4), 909–922. <https://doi.org/10.1016/j.cell.2013.01.030>
- Beckers, C. J., Keller, D. S., and Balch, W. E. (1987). Semi-intact cells permeable to macromolecules: use in reconstitution of protein transport from the endoplasmic reticulum to the Golgi complex. *Cell*, 50(4), 523–534.
- Behnia, R., Barr, F. A., Flanagan, J. J., Barlowe, C., and Munro, S. (2007). The yeast orthologue of GRASP65 forms a complex with a coiled-coil protein that contributes to ER to Golgi traffic. *The Journal of Cell Biology*, 176(3), 255–261. <https://doi.org/10.1083/jcb.200607151>
- Behrends, C., Sowa, M. E., Gygi, S. P., and Harper, J. W. (2010). Network organization of the human autophagy system. *Nature*, 466(7302), 68–76. <https://doi.org/10.1038/nature09204>
- Bergmann, J. E., Tokuyasu, K. T., and Singer, S. J. (1981). Passage of an integral membrane protein, the vesicular stomatitis virus glycoprotein, through the Golgi apparatus en route to the plasma membrane. *Proceedings of the National Academy of Sciences of the United States of America*, 78(3), 1746–1750.
- Bernales, S., Schuck, S., and Walter, P. (2007). ER-phagy: selective autophagy of the endoplasmic reticulum. *Autophagy*, 3(3), 285–287.
- Bögershausen, N., Shahrzad, N., Chong, J. X., von Kleist-Retzow, J.-C., Stanga, D., Li, Y., ... Lamont, R. E. (2013). Recessive TRAPPC11 Mutations Cause a Disease Spectrum of Limb Girdle Muscular Dystrophy and Myopathy with Movement Disorder and Intellectual Disability.

- The American Journal of Human Genetics*, 93(1), 181–190.
<https://doi.org/10.1016/j.ajhg.2013.05.028>
- Bönnemann, C. G., Wang, C. H., Quijano-Roy, S., Deconinck, N., Bertini, E., Ferreiro, A., ... North, K. N. (2014). Diagnostic approach to the congenital muscular dystrophies. *Neuromuscular Disorders*, 24(4), 289–311. <https://doi.org/10.1016/j.nmd.2013.12.011>
- Breuza, L., Halbeisen, R., Jenö, P., Otte, S., Barlowe, C., Hong, W., and Hauri, H.-P. (2004). Proteomics of Endoplasmic Reticulum-Golgi Intermediate Compartment (ERGIC) Membranes from Brefeldin A-treated HepG2 Cells Identifies ERGIC-32, a New Cycling Protein That Interacts with Human Erv46. *Journal of Biological Chemistry*, 279(45), 47242–47253.
<https://doi.org/10.1074/jbc.M406644200>
- Brunet, S., and Sacher, M. (2014a). Are All Multisubunit Tethering Complexes Bona Fide Tethers? *Traffic*, 15(11), 1282–1287. <https://doi.org/10.1111/tra.12200>
- Brunet, S., and Sacher, M. (2014b). In Sickness and in Health: The Role of TRAPP and Associated Proteins in Disease. *Traffic*, 15(8), 803–818. <https://doi.org/10.1111/tra.12183>
- Brunet, S., Shahrzad, N., Saint-Dic, D., Dutczak, H., and Sacher, M. (2013). A trs20 mutation that mimics an SEDT-causing mutation blocks selective and non-selective autophagy: a model for TRAPP III organization. *Traffic (Copenhagen, Denmark)*, 14(10), 1091–1104.
<https://doi.org/10.1111/tra.12095>
- Bursch, W., Ellinger, A., Kienzl, H., Török, L., Pandey, S., Sikorska, M., ... Hermann, R. S. (1996). Active cell death induced by the anti-estrogens tamoxifen and ICI 164 384 in human mammary carcinoma cells (MCF-7) in culture: the role of autophagy. *Carcinogenesis*, 17(8), 1595–1607.
- Cai, H., Yu, S., Menon, S., Cai, Y., Lazarova, D., Fu, C., ... Ferro-Novick, S. (2007). TRAPP I tethers COPII vesicles by binding the coat subunit Sec23. *Nature*, 445(7130), 941–944.
<https://doi.org/10.1038/nature05527>
- Cai, H., Zhang, Y., Pypaert, M., Walker, L., and Ferro-Novick, S. (2005). Mutants in trs120 disrupt traffic from the early endosome to the late Golgi. *The Journal of Cell Biology*, 171(5), 823–833.
<https://doi.org/10.1083/jcb.200505145>
- Cai, Y., Chin, H. F., Lazarova, D., Menon, S., Fu, C., Cai, H., ... Reinisch, K. M. (2008). The structural basis for activation of the Rab Ypt1p by the TRAPP membrane-tethering complexes. *Cell*, 133(7), 1202–1213. <https://doi.org/10.1016/j.cell.2008.04.049>

- Chan, G. K., Jablonski, S. A., Starr, D. A., Goldberg, M. L., and Yen, T. J. (2000). Human Zw10 and ROD are mitotic checkpoint proteins that bind to kinetochores. *Nature Cell Biology*, 2(12), 944–947. <https://doi.org/10.1038/35046598>
- Chang, J.-Y., Lee, M.-H., Lin, S.-R., Yang, L.-Y., Sun, S. H., Sze, C.-I., ... Chang, N.-S. (2015). Trafficking protein particle complex 6A delta (TRAPPC6A Δ) is an extracellular plaque-forming protein in the brain. *Oncotarget*, 6(6), 3578–3589. <https://doi.org/10.18632/oncotarget.2876>
- Choi, C., Davey, M., Schluter, C., Pandher, P., Fang, Y., Foster, L. J., and Conibear, E. (2011). Organization and assembly of the TRAPPII complex. *Traffic (Copenhagen, Denmark)*, 12(6), 715–725. <https://doi.org/10.1111/j.1600-0854.2011.01181.x>
- Choi, M. Y., Chan, C. C. Y., Chan, D., Luk, K. D. K., Cheah, K. S. E., and Tanner, J. A. (2009). Biochemical consequences of sedlin mutations that cause spondyloepiphyseal dysplasia tarda. *The Biochemical Journal*, 423(2), 233–242. <https://doi.org/10.1042/BJ20090541>
- Copley, S. D. (2012). Moonlighting is mainstream: Paradigm adjustment required. *BioEssays*, 34(7), 578–588. <https://doi.org/10.1002/bies.201100191>
- Corbett, M. A., Schwake, M., Bahlo, M., Dibbens, L. M., Lin, M., Gandolfo, L. C., ... Berkovic, S. F. (2011). A mutation in the Golgi Qb-SNARE gene GOSR2 causes progressive myoclonus epilepsy with early ataxia. *American Journal of Human Genetics*, 88(5), 657–663. <https://doi.org/10.1016/j.ajhg.2011.04.011>
- Darin, N., and Tulinius, M. (2000). Neuromuscular disorders in childhood: a descriptive epidemiological study from western Sweden. *Neuromuscular Disorders: NMD*, 10(1), 1–9.
- Dascher, C., Matteson, J., and Balch, W. E. (1994). Syntaxin 5 regulates endoplasmic reticulum to Golgi transport. *The Journal of Biological Chemistry*, 269(47), 29363–29366.
- DeRossi, C., Vacaru, A., Rafiq, R., Cinaroglu, A., Imrie, D., Nayar, S., ... Sadler, K. C. (2016). trappc11 is required for protein glycosylation in zebrafish and humans. *Molecular Biology of the Cell*, 27(8), 1220–1234. <https://doi.org/10.1091/mbc.E15-08-0557>
- Dubnau, J., Chiang, A.-S., Grady, L., Barditch, J., Gossweiler, S., McNeil, J., ... Tully, T. (2003). The staufen/pumilio pathway is involved in Drosophila long-term memory. *Current Biology: CB*, 13(4), 286–296.
- Dupuis, N., Fafouri, A., Bayot, A., Kumar, M., Lecharpentier, T., Ball, G., ... El Ghouzzi, V. (2015). Dymeclin deficiency causes postnatal microcephaly, hypomyelination and reticulum-to-Golgi

- trafficking defects in mice and humans. *Human Molecular Genetics*, 24(10), 2771–2783.
<https://doi.org/10.1093/hmg/ddv038>
- Epifanova, O. I., Terskikh, V. V., and Polunovskii, V. A. (1982). [Active metabolic processes in resting cells]. *Tsitologiya*, 24(11), 1259–1273.
- Eskelinen, E.-L. (2006). Roles of LAMP-1 and LAMP-2 in lysosome biogenesis and autophagy. *Molecular Aspects of Medicine*, 27(5–6), 495–502. <https://doi.org/10.1016/j.mam.2006.08.005>
- Etchison, J. R., Robertson, J. S., and Summers, D. F. (1977). Partial structural analysis of the oligosaccharide moieties of the vesicular stomatitis virus glycoprotein by sequential chemical and enzymatic degradation. *Virology*, 78(2), 375–392.
- Ethell, I. M., Hagihara, K., Miura, Y., Irie, F., and Yamaguchi, Y. (2000). Synbindin, A novel syndecan-2-binding protein in neuronal dendritic spines. *The Journal of Cell Biology*, 151(1), 53–68.
- Farhan, H., Wendeler, M. W., Mitrovic, S., Fava, E., Silberberg, Y., Sharan, R., ... Hauri, H.-P. (2010). MAPK signaling to the early secretory pathway revealed by kinase/phosphatase functional screening. *The Journal of Cell Biology*, 189(6), 997–1011.
<https://doi.org/10.1083/jcb.200912082>
- Feinstein, M., Flusser, H., Lerman-Sagie, T., Ben-Zeev, B., Lev, D., Agamy, O., ... Birk, O. S. (2014). VPS53 mutations cause progressive cerebello-cerebral atrophy type 2 (PCCA2). *Journal of Medical Genetics*, 51(5), 303–308. <https://doi.org/10.1136/jmedgenet-2013-101823>
- Fewell, S. W., and Brodsky, J. L. (2009). Entry into the Endoplasmic Reticulum: Protein Translocation, Folding and Quality Control. In N. Segev, *Trafficking Inside Cells* (pp. 119–142). New York, NY: Springer New York. Retrieved from http://link.springer.com/10.1007/978-0-387-93877-6_7
- Foulquier, F., Ungar, D., Reynders, E., Zeevaert, R., Mills, P., García-Silva, M. T., ... Matthijs, G. (2007). A new inborn error of glycosylation due to a Cog8 deficiency reveals a critical role for the Cog1-Cog8 interaction in COG complex formation. *Human Molecular Genetics*, 16(7), 717–730. <https://doi.org/10.1093/hmg/ddl476>
- Foulquier, F., Vasile, E., Schollen, E., Callewaert, N., Raemaekers, T., Quelhas, D., ... Matthijs, G. (2006). Conserved oligomeric Golgi complex subunit 1 deficiency reveals a previously uncharacterized congenital disorder of glycosylation type II. *Proceedings of the National*

Academy of Sciences of the United States of America, 103(10), 3764–3769.

<https://doi.org/10.1073/pnas.0507685103>

- Fujita, E., Kouroku, Y., Isoai, A., Kumagai, H., Misutani, A., Matsuda, C., ... Momoi, T. (2007). Two endoplasmic reticulum-associated degradation (ERAD) systems for the novel variant of the mutant dysferlin: ubiquitin/proteasome ERAD(I) and autophagy/lysosome ERAD(II). *Human Molecular Genetics*, 16(6), 618–629. <https://doi.org/10.1093/hmg/ddm002>
- Fusella, A., Micaroni, M., Di Giandomenico, D., Mironov, A. A., and Beznoussenko, G. V. (2013). Segregation of the Qb-SNAREs GS27 and GS28 into Golgi vesicles regulates intra-Golgi transport. *Traffic (Copenhagen, Denmark)*, 14(5), 568–584. <https://doi.org/10.1111/tra.12055>
- Gedeon, A. K., Colley, A., Jamieson, R., Thompson, E. M., Rogers, J., Sillence, D., ... Géczy, J. (1999). Identification of the gene (SEDL) causing X-linked spondyloepiphyseal dysplasia tarda. *Nature Genetics*, 22(4), 400–404. <https://doi.org/10.1038/11976>
- Gedeon, A. K., Tiller, G. E., Le Merrer, M., Heuertz, S., Tranebjaerg, L., Chitayat, D., ... Mulley, J. C. (2001). The molecular basis of X-linked spondyloepiphyseal dysplasia tarda. *American Journal of Human Genetics*, 68(6), 1386–1397. <https://doi.org/10.1086/320592>
- Germain, M., Nguyen, A. P., Le Grand, J. N., Arbour, N., Vanderluit, J. L., Park, D. S., ... Slack, R. S. (2011). MCL-1 is a stress sensor that regulates autophagy in a developmentally regulated manner: Regulation of autophagy by MCL-1. *The EMBO Journal*, 30(2), 395–407. <https://doi.org/10.1038/emboj.2010.327>
- Ghosh, A. K., Majumder, M., Steele, R., White, R. A., and Ray, R. B. (2001). A novel 16-kilodalton cellular protein physically interacts with and antagonizes the functional activity of c-myc promoter-binding protein 1. *Molecular and Cellular Biology*, 21(2), 655–662. <https://doi.org/10.1128/MCB.21.2.655-662.2001>
- Gissen, P., Johnson, C. A., Morgan, N. V., Stapelbroek, J. M., Forshe, T., Cooper, W. N., ... Maher, E. R. (2004). Mutations in VPS33B, encoding a regulator of SNARE-dependent membrane fusion, cause arthrogyrosis-renal dysfunction-cholestasis (ARC) syndrome. *Nature Genetics*, 36(4), 400–404. <https://doi.org/10.1038/ng1325>
- Glick, B. S., and Rothman, J. E. (1987). Possible role for fatty acyl-coenzyme A in intracellular protein transport. *Nature*, 326(6110), 309–312. <https://doi.org/10.1038/326309a0>
- Grabski, R., Balklava, Z., Wyrozumska, P., Szul, T., Brandon, E., Alvarez, C., ... Sztul, E. (2012). Identification of a functional domain within the p115 tethering factor that is required for Golgi

- ribbon assembly and membrane trafficking. *Journal of Cell Science*, 125(Pt 8), 1896–1909.
<https://doi.org/10.1242/jcs.090571>
- Grant, D. B., Barnes, N. D., Dumic, M., Ginalska-Malinowska, M., Milla, P. J., von Petrykowski, W., ... Werder, E. (1993). Neurological and adrenal dysfunction in the adrenal insufficiency/alacrima/achalasia (3A) syndrome. *Archives of Disease in Childhood*, 68(6), 779–782.
- Gwynn, B., Smith, R. S., Rowe, L. B., Taylor, B. A., and Peters, L. L. (2006). A mouse TRAPP-related protein is involved in pigmentation. *Genomics*, 88(2), 196–203.
<https://doi.org/10.1016/j.ygeno.2006.04.002>
- Haase, G., and Rabouille, C. (2015). Golgi Fragmentation in ALS Motor Neurons. New Mechanisms Targeting Microtubules, Tethers, and Transport Vesicles. *Frontiers in Neuroscience*, 9, 448.
<https://doi.org/10.3389/fnins.2015.00448>
- Hamasaki, M., Furuta, N., Matsuda, A., Nezu, A., Yamamoto, A., Fujita, N., ... Yoshimori, T. (2013). Autophagosomes form at ER–mitochondria contact sites. *Nature*, 495(7441), 389–393.
<https://doi.org/10.1038/nature11910>
- Hamilton, G., Harris, S. E., Davies, G., Liewald, D. C., Tenesa, A., Starr, J. M., ... Deary, I. J. (2011). Alzheimer’s disease genes are associated with measures of cognitive ageing in the lothian birth cohorts of 1921 and 1936. *International Journal of Alzheimer’s Disease*, 2011, 505984.
<https://doi.org/10.4061/2011/505984>
- Higashio, H., and Kohno, K. (2002). A genetic link between the unfolded protein response and vesicle formation from the endoplasmic reticulum. *Biochemical and Biophysical Research Communications*, 296(3), 568–574.
- Hirose, H., Arasaki, K., Dohmae, N., Takio, K., Hatsuzawa, K., Nagahama, M., ... Tagaya, M. (2004). Implication of ZW10 in membrane trafficking between the endoplasmic reticulum and Golgi. *The EMBO Journal*, 23(6), 1267–1278. <https://doi.org/10.1038/sj.emboj.7600135>
- Houlden, H., Smith, S., De Carvalho, M., Blake, J., Mathias, C., Wood, N. W., and Reilly, M. M. (2002). Clinical and genetic characterization of families with triple A (Allgrove) syndrome. *Brain: A Journal of Neurology*, 125(Pt 12), 2681–2690.
- Humphries, W. H., Szymanski, C. J., and Payne, C. K. (2011). Endo-lysosomal vesicles positive for Rab7 and LAMP1 are terminal vesicles for the transport of dextran. *PloS One*, 6(10), e26626.
<https://doi.org/10.1371/journal.pone.0026626>

- Ishii, Y., Nakahara, T., Kataoka, M., Kusumoto-Matsuo, R., Mori, S., Takeuchi, T., and Kukimoto, I. (2013). Identification of TRAPPC8 as a Host Factor Required for Human Papillomavirus Cell Entry. *PLoS ONE*, 8(11), e80297. <https://doi.org/10.1371/journal.pone.0080297>
- Jeffery, C. J. (2003). Multifunctional proteins: examples of gene sharing. *Annals of Medicine*, 35(1), 28–35.
- Jeyabalan, J., Nesbit, M. A., Galvanovskis, J., Callaghan, R., Rorsman, P., and Thakker, R. V. (2010). SEDLIN forms homodimers: characterisation of SEDLIN mutations and their interactions with transcription factors MBP1, PITX1 and SF1. *PloS One*, 5(5), e10646. <https://doi.org/10.1371/journal.pone.0010646>
- Jiang, Y., Scarpa, A., Zhang, L., Stone, S., Feliciano, E., and Ferro-Novick, S. (1998). A high copy suppressor screen reveals genetic interactions between BET3 and a new gene. Evidence for a novel complex in ER-to-Golgi transport. *Genetics*, 149(2), 833–841.
- Jones, S., Newman, C., Liu, F., and Segev, N. (2000). The TRAPP complex is a nucleotide exchanger for Ypt1 and Ypt31/32. *Molecular Biology of the Cell*, 11(12), 4403–4411.
- Jones, T. A., Nikolova, L. S., Schjelderup, A., and Metzstein, M. M. (2014). Exocyst-mediated membrane trafficking is required for branch outgrowth in *Drosophila* tracheal terminal cells. *Developmental Biology*, 390(1), 41–50. <https://doi.org/10.1016/j.ydbio.2014.02.021>
- Jongen, P. J., Ter Laak, H. J., and Stadhouders, A. M. (1995). Rimmed basophilic vacuoles and filamentous inclusions in neuromuscular disorders. *Neuromuscular Disorders: NMD*, 5(1), 31–38.
- Joshi, G., Bekier, M. E., and Wang, Y. (2015). Golgi fragmentation in Alzheimer's disease. *Frontiers in Neuroscience*, 9, 340. <https://doi.org/10.3389/fnins.2015.00340>
- Kabeya, Y., Mizushima, N., Ueno, T., Yamamoto, A., Kirisako, T., Noda, T., ... Yoshimori, T. (2000). LC3, a mammalian homologue of yeast Apg8p, is localized in autophagosome membranes after processing. *The EMBO Journal*, 19(21), 5720–5728. <https://doi.org/10.1093/emboj/19.21.5720>
- Kaneda, D., Sugie, K., Yamamoto, A., Matsumoto, H., Kato, T., Nonaka, I., and Nishino, I. (2003). A novel form of autophagic vacuolar myopathy with late-onset and multiorgan involvement. *Neurology*, 61(1), 128–131.

- Katz, F. N., Rothman, J. E., Knipe, D. M., and Lodish, H. F. (1977). Membrane assembly: synthesis and intracellular processing of the vesicular stomatitis viral glycoprotein. *Journal of Supramolecular Structure*, 7(3–4), 353–370. <https://doi.org/10.1002/jss.400070308>
- Kawamura, N., Sun-Wada, G.-H., Aoyama, M., Harada, A., Takasuga, S., Sasaki, T., and Wada, Y. (2012). Delivery of endosomes to lysosomes via microautophagy in the visceral endoderm of mouse embryos. *Nature Communications*, 3, 1071. <https://doi.org/10.1038/ncomms2069>
- Kegel, K. B., Kim, M., Sapp, E., McIntyre, C., Castaño, J. G., Aronin, N., and DiFiglia, M. (2000). Huntingtin expression stimulates endosomal-lysosomal activity, endosome tubulation, and autophagy. *The Journal of Neuroscience: The Official Journal of the Society for Neuroscience*, 20(19), 7268–7278.
- Khattak, N., and Mir, A. (2014). Computational Analysis of TRAPPC9: Candidate Gene for Autosomal Recessive Non-Syndromic Mental Retardation. *CNS and Neurological Disorders - Drug Targets*, 13(4), 699–711. <https://doi.org/10.2174/18715273113129990105>
- Kim, J., Huang, W.-P., Stromhaug, P. E., and Klionsky, D. J. (2002). Convergence of multiple autophagy and cytoplasm to vacuole targeting components to a perivacuolar membrane compartment prior to de novo vesicle formation. *The Journal of Biological Chemistry*, 277(1), 763–773. <https://doi.org/10.1074/jbc.M109134200>
- Kim, Y.-G., Raunser, S., Munger, C., Wagner, J., Song, Y.-L., Cygler, M., ... Sacher, M. (2006). The architecture of the multisubunit TRAPP I complex suggests a model for vesicle tethering. *Cell*, 127(4), 817–830. <https://doi.org/10.1016/j.cell.2006.09.029>
- Kingsley, D. M., Kozarsky, K. F., Segal, M., and Krieger, M. (1986). Three types of low density lipoprotein receptor-deficient mutant have pleiotropic defects in the synthesis of N-linked, O-linked, and lipid-linked carbohydrate chains. *The Journal of Cell Biology*, 102(5), 1576–1585.
- Klionsky, D. J., Abdelmohsen, K., Abe, A., Abedin, M. J., Abeliovich, H., Acevedo Arozena, A., ... Zughair, S. M. (2016). Guidelines for the use and interpretation of assays for monitoring autophagy (3rd edition). *Autophagy*, 12(1), 1–222. <https://doi.org/10.1080/15548627.2015.1100356>
- Klumperman, J., Schweizer, A., Clausen, H., Tang, B. L., Hong, W., Oorschot, V., and Hauri, H. P. (1998). The recycling pathway of protein ERGIC-53 and dynamics of the ER-Golgi intermediate compartment. *Journal of Cell Science*, 111 (Pt 22), 3411–3425.

- Knipe, D. M., Baltimore, D., and Lodish, H. F. (1977). Maturation of viral proteins in cells infected with temperature-sensitive mutants of vesicular stomatitis virus. *Journal of Virology*, *21*(3), 1149–1158.
- Koehler, K., Milev, M. P., Prematilake, K., Reschke, F., Kutzner, S., Jühlen, R., ... Sacher, M. (2016). A novel TRAPPC11 mutation in two Turkish families associated with cerebral atrophy, global retardation, scoliosis, achalasia and alacrima. *Journal of Medical Genetics*. Online first. <https://doi.org/10.1136/jmedgenet-2016-104108> (KK, MPM and KP contributed equally)
- Kong, X., Qian, J., Chen, L.-S., Wang, Y.-C., Wang, J.-L., Chen, H., ... Fang, J.-Y. (2013). Synbindin in extracellular signal-regulated protein kinase spatial regulation and gastric cancer aggressiveness. *Journal of the National Cancer Institute*, *105*(22), 1738–1749. <https://doi.org/10.1093/jnci/djt271>
- Koreishi, M., Yu, S., Oda, M., Honjo, Y., and Satoh, A. (2013). CK2 Phosphorylates Sec31 and Regulates ER-To-Golgi Trafficking. *PLoS ONE*, *8*(1), e54382. <https://doi.org/10.1371/journal.pone.0054382>
- Kranz, C., Ng, B. G., Sun, L., Sharma, V., Eklund, E. A., Miura, Y., ... Freeze, H. H. (2007). COG8 deficiency causes new congenital disorder of glycosylation type IIIh. *Human Molecular Genetics*, *16*(7), 731–741. <https://doi.org/10.1093/hmg/ddm028>
- Kreis, T. E., and Lodish, H. F. (1986). Oligomerization is essential for transport of vesicular stomatitis viral glycoprotein to the cell surface. *Cell*, *46*(6), 929–937.
- Kubota, Y., Sano, M., Goda, S., Suzuki, N., and Nishiwaki, K. (2006). The conserved oligomeric Golgi complex acts in organ morphogenesis via glycosylation of an ADAM protease in *C. elegans*. *Development (Cambridge, England)*, *133*(2), 263–273. <https://doi.org/10.1242/dev.02195>
- Kudlyk, T., Willett, R., Pokrovskaya, I. D., and Lupashin, V. (2013). COG6 Interacts with a Subset of the Golgi SNAREs and Is Important for the Golgi Complex Integrity: COG6 and Golgi SNAREs. *Traffic*, *14*(2), 194–204. <https://doi.org/10.1111/tra.12020>
- Liang, W.-C., Zhu, W., Mitsuhashi, S., Noguchi, S., Sacher, M., Ogawa, M., ... Nishino, I. (2015). Congenital muscular dystrophy with fatty liver and infantile-onset cataract caused by TRAPPC11 mutations: broadening of the phenotype. *Skeletal Muscle*, *5*(1). <https://doi.org/10.1186/s13395-015-0056-4>

- Lipatova, Z., Belogortseva, N., Zhang, X. Q., Kim, J., Taussig, D., and Segev, N. (2012). Regulation of selective autophagy onset by a Ypt/Rab GTPase module. *Proceedings of the National Academy of Sciences*, 109(18), 6981–6986. <https://doi.org/10.1073/pnas.1121299109>
- Lipatova, Z., Majumdar, U., and Segev, N. (2016). Trs33-containing TRAPP IV: A Novel Autophagy-Specific Ypt1 GEF. *Genetics*. <https://doi.org/10.1534/genetics.116.194910>
- Lipatova, Z., Shah, A. H., Kim, J. J., Mulholland, J. W., and Segev, N. (2013). Regulation of ER-phagy by a Ypt/Rab GTPase module. *Molecular Biology of the Cell*, 24(19), 3133–3144. <https://doi.org/10.1091/mbc.E13-05-0269>
- Lodish, H. F., and Kong, N. (1983). Reversible block in intracellular transport and budding of mutant vesicular stomatitis virus glycoproteins. *Virology*, 125(2), 335–348.
- Lodish, H. F., and Weiss, R. A. (1979). Selective isolation of mutants of vesicular stomatitis virus defective in production of the viral glycoprotein. *Journal of Virology*, 30(1), 177–189.
- Loh, E., Peter, F., Subramaniam, V. N., and Hong, W. (2005). Mammalian Bet3 functions as a cytosolic factor participating in transport from the ER to the Golgi apparatus. *Journal of Cell Science*, 118(Pt 6), 1209–1222. <https://doi.org/10.1242/jcs.01723>
- Lord, C., Bhandari, D., Menon, S., Ghassemian, M., Nycz, D., Hay, J., ... Ferro-Novick, S. (2011). Sequential interactions with Sec23 control the direction of vesicle traffic. *Nature*, 473(7346), 181–186. <https://doi.org/10.1038/nature09969>
- Lünemann, J. D., Schmidt, J., Dalakas, M. C., and Münz, C. (2007). Macroautophagy as a pathomechanism in sporadic inclusion body myositis. *Autophagy*, 3(4), 384–386.
- Lupashin, V., and Sztul, E. (2009). Tethering Factors. In N. Segev, *Trafficking Inside Cells* (pp. 254–281). New York, NY: Springer New York. Retrieved from http://link.springer.com/10.1007/978-0-387-93877-6_13
- Lynch-Day, M. A., Bhandari, D., Menon, S., Huang, J., Cai, H., Bartholomew, C. R., ... Klionsky, D. J. (2010). Trs85 directs a Ypt1 GEF, TRAPP III, to the phagophore to promote autophagy. *Proceedings of the National Academy of Sciences of the United States of America*, 107(17), 7811–7816. <https://doi.org/10.1073/pnas.1000063107>
- Machamer, C. E. (2015). The Golgi complex in stress and death. *Frontiers in Neuroscience*, 9, 421. <https://doi.org/10.3389/fnins.2015.00421>

- MacKenzie, J. J., Fitzpatrick, J., Babyn, P., Ferrero, G. B., Ballabio, A., Billingsley, G., ... Costa, T. (1996). X linked spondyloepiphyseal dysplasia: a clinical, radiological, and molecular study of a large kindred. *Journal of Medical Genetics*, 33(10), 823–828.
- Malhotra, V., Orci, L., Glick, B. S., Block, M. R., and Rothman, J. E. (1988). Role of an N-ethylmaleimide-sensitive transport component in promoting fusion of transport vesicles with cisternae of the Golgi stack. *Cell*, 54(2), 221–227.
- Martínez-Menárguez, J. A., Geuze, H. J., Slot, J. W., and Klumperman, J. (1999). Vesicular Tubular Clusters between the ER and Golgi Mediate Concentration of Soluble Secretory Proteins by Exclusion from COPI-Coated Vesicles. *Cell*, 98(1), 81–90. [https://doi.org/10.1016/S0092-8674\(00\)80608-X](https://doi.org/10.1016/S0092-8674(00)80608-X)
- McCarthy, S. E., Gillis, J., Kramer, M., Lihm, J., Yoon, S., Berstein, Y., ... Corvin, A. (2014). De novo mutations in schizophrenia implicate chromatin remodeling and support a genetic overlap with autism and intellectual disability. *Molecular Psychiatry*, 19(6), 652–658. <https://doi.org/10.1038/mp.2014.29>
- Meijer, W. H., van der Klei, I. J., Veenhuis, M., and Kiel, J. A. K. W. (2007). ATG genes involved in non-selective autophagy are conserved from yeast to man, but the selective Cvt and pexophagy pathways also require organism-specific genes. *Autophagy*, 3(2), 106–116.
- Meiling-Wesse, K., Epple, U. D., Krick, R., Barth, H., Appelles, A., Voss, C., ... Thumm, M. (2005). Trs85 (Gsg1), a component of the TRAPP complexes, is required for the organization of the preautophagosomal structure during selective autophagy via the Cvt pathway. *The Journal of Biological Chemistry*, 280(39), 33669–33678. <https://doi.org/10.1074/jbc.M501701200>
- Messler, S., Kropp, S., Episkopou, V., Felici, A., Würthner, J., Lemke, R., ... Würthner, J. U. (2011). The TGF- β signaling modulators TRAP1/TGFBRAP1 and VPS39/Vam6/TLP are essential for early embryonic development. *Immunobiology*, 216(3), 343–350. <https://doi.org/10.1016/j.imbio.2010.07.006>
- Michele, D. E., Barresi, R., Kanagawa, M., Saito, F., Cohn, R. D., Satz, J. S., ... Campbell, K. P. (2002). Post-translational disruption of dystroglycan–ligand interactions in congenital muscular dystrophies. *Nature*, 418(6896), 417–421. <https://doi.org/10.1038/nature00837>
- Milev, M. P., Hasaj, B., Saint-Dic, D., Snounou, S., Zhao, Q., and Sacher, M. (2015). TRAMM/TrappC12 plays a role in chromosome congression, kinetochore stability, and CENP-E

- recruitment. *The Journal of Cell Biology*, 209(2), 221–234.
<https://doi.org/10.1083/jcb.201501090>
- Misgar, R. A., Pala, N. A., Ramzan, M., Wani, A. I., Bashir, M. I., and Laway, B. A. (2015). Allgrove (Triple A) Syndrome: A Case Report from the Kashmir Valley. *Endocrinology and Metabolism (Seoul, Korea)*, 30(4), 604–606. <https://doi.org/10.3803/EnM.2015.30.4.604>
- Miyazaki, K., and Horio, T. (1989). Growth inhibitors: molecular diversity and roles in cell proliferation. *In Vitro Cellular and Developmental Biology: Journal of the Tissue Culture Association*, 25(10), 866–872.
- Mizushima, N., Yamamoto, A., Matsui, M., Yoshimori, T., and Ohsumi, Y. (2004). In vivo analysis of autophagy in response to nutrient starvation using transgenic mice expressing a fluorescent autophagosome marker. *Molecular Biology of the Cell*, 15(3), 1101–1111.
<https://doi.org/10.1091/mbc.E03-09-0704>
- Morozova, N., Liang, Y., Tokarev, A. A., Chen, S. H., Cox, R., Andrejic, J., ... Segev, N. (2006). TRAPPII subunits are required for the specificity switch of a Ypt-Rab GEF. *Nature Cell Biology*, 8(11), 1263–1269. <https://doi.org/10.1038/ncb1489>
- Nascimbeni, A. C., Fanin, M., Tasca, E., and Angelini, C. (2008). Molecular pathology and enzyme processing in various phenotypes of acid maltase deficiency. *Neurology*, 70(8), 617–626.
<https://doi.org/10.1212/01.wnl.0000299892.81127.8e>
- Nazarko, T. Y., Huang, J., Nicaud, J.-M., Klionsky, D. J., and Sibirny, A. A. (2005). Trs85 is required for macroautophagy, pexophagy and cytoplasm to vacuole targeting in *Yarrowia lipolytica* and *Saccharomyces cerevisiae*. *Autophagy*, 1(1), 37–45.
- Nelson, D. S., Alvarez, C., Gao, Y. S., García-Mata, R., Fialkowski, E., and Sztul, E. (1998). The membrane transport factor TAP/p115 cycles between the Golgi and earlier secretory compartments and contains distinct domains required for its localization and function. *The Journal of Cell Biology*, 143(2), 319–331.
- Ng, B. G., Kranz, C., Hagebeuk, E. E. O., Duran, M., Abeling, N. G. G. M., Wuyts, B., ... Freeze, H. H. (2007). Molecular and clinical characterization of a Moroccan Cog7 deficient patient. *Molecular Genetics and Metabolism*, 91(2), 201–204.
<https://doi.org/10.1016/j.ymgme.2007.02.011>

- Nishino, I., Fu, J., Tanji, K., Yamada, T., Shimojo, S., Koori, T., ... Hirano, M. (2000). Primary LAMP-2 deficiency causes X-linked vacuolar cardiomyopathy and myopathy (Danon disease). *Nature*, *406*(6798), 906–910. <https://doi.org/10.1038/35022604>
- Nishino, I., Malicdan, M. C. V., Murayama, K., Nonaka, I., Hayashi, Y. K., and Noguchi, S. (2005). Molecular pathomechanism of distal myopathy with rimmed vacuoles. *Acta Myologica: Myopathies and Cardiomyopathies: Official Journal of the Mediterranean Society of Myology / Edited by the Gaetano Conte Academy for the Study of Striated Muscle Diseases*, *24*(2), 80–83.
- Paesold-Burda, P., Maag, C., Troxler, H., Foulquier, F., Kleinert, P., Schnabel, S., ... Hennet, T. (2009). Deficiency in COG5 causes a moderate form of congenital disorders of glycosylation. *Human Molecular Genetics*, *18*(22), 4350–4356. <https://doi.org/10.1093/hmg/ddp389>
- Pattingre, S., Tassa, A., Qu, X., Garuti, R., Liang, X. H., Mizushima, N., ... Levine, B. (2005). Bcl-2 antiapoptotic proteins inhibit Beclin 1-dependent autophagy. *Cell*, *122*(6), 927–939. <https://doi.org/10.1016/j.cell.2005.07.002>
- Peplowska, K., Markgraf, D. F., Ostrowicz, C. W., Bange, G., and Ungermann, C. (2007). The CORVET tethering complex interacts with the yeast Rab5 homolog Vps21 and is involved in endo-lysosomal biogenesis. *Developmental Cell*, *12*(5), 739–750. <https://doi.org/10.1016/j.devcel.2007.03.006>
- Pérez-Victoria, F. J., Abascal-Palacios, G., Tascón, I., Kajava, A., Magadán, J. G., Pioro, E. P., ... Hierro, A. (2010). Structural basis for the wobbler mouse neurodegenerative disorder caused by mutation in the Vps54 subunit of the GARP complex. *Proceedings of the National Academy of Sciences of the United States of America*, *107*(29), 12860–12865. <https://doi.org/10.1073/pnas.1004756107>
- Pérez-Victoria, F. J., and Bonifacino, J. S. (2009). Dual roles of the mammalian GARP complex in tethering and SNARE complex assembly at the trans-golgi network. *Molecular and Cellular Biology*, *29*(19), 5251–5263. <https://doi.org/10.1128/MCB.00495-09>
- Pongor, L., Kormos, M., Hatzis, C., Pusztai, L., Szabó, A., and Györffy, B. (2015). A genome-wide approach to link genotype to clinical outcome by utilizing next generation sequencing and gene chip data of 6,697 breast cancer patients. *Genome Medicine*, *7*(1). <https://doi.org/10.1186/s13073-015-0228-1>

- Prescott, A. R., Lucocq, J. M., James, J., Lister, J. M., and Ponnambalam, S. (1997). Distinct compartmentalization of TGN46 and beta 1,4-galactosyltransferase in HeLa cells. *European Journal of Cell Biology*, 72(3), 238–246.
- Presley, J. F., Cole, N. B., Schroer, T. A., Hirschberg, K., Zaal, K. J., and Lippincott-Schwartz, J. (1997). ER-to-Golgi transport visualized in living cells. *Nature*, 389(6646), 81–85.
<https://doi.org/10.1038/38001>
- Raben, N., Takikita, S., Pittis, M. G., Bembi, B., Marie, S. K. N., Roberts, A., ... Plotz, P. H. (2007). Deconstructing Pompe disease by analyzing single muscle fibers: to see a world in a grain of sand. *Autophagy*, 3(6), 546–552.
- Ren, Y., Yip, C. K., Tripathi, A., Huie, D., Jeffrey, P. D., Walz, T., and Hughson, F. M. (2009). A structure-based mechanism for vesicle capture by the multisubunit tethering complex Dsl1. *Cell*, 139(6), 1119–1129. <https://doi.org/10.1016/j.cell.2009.11.002>
- Reynders, E., Foulquier, F., Leão Teles, E., Quelhas, D., Morelle, W., Rabouille, C., ... Matthijs, G. (2009). Golgi function and dysfunction in the first COG4-deficient CDG type II patient. *Human Molecular Genetics*, 18(17), 3244–3256. <https://doi.org/10.1093/hmg/ddp262>
- Richardson, B. C., Smith, R. D., Ungar, D., Nakamura, A., Jeffrey, P. D., Lupashin, V. V., and Hughson, F. M. (2009). Structural basis for a human glycosylation disorder caused by mutation of the COG4 gene. *Proceedings of the National Academy of Sciences*, 106(32), 13329–13334. <https://doi.org/10.1073/pnas.0901966106>
- Rothman, J., and Lenard, J. (1977). Membrane asymmetry. *Science*, 195(4280), 743–753. <https://doi.org/10.1126/science.402030>
- Roy, D., Sin, S.-H., Damania, B., and Dittmer, D. P. (2011). Tumor suppressor genes FHIT and WWOX are deleted in primary effusion lymphoma (PEL) cell lines. *Blood*, 118(7), e32-39. <https://doi.org/10.1182/blood-2010-12-323659>
- Sacher, M., Barrowman, J., Schieltz, D., Yates, J. R., and Ferro-Novick, S. (2000). Identification and characterization of five new subunits of TRAPP. *European Journal of Cell Biology*, 79(2), 71–80. [https://doi.org/10.1078/S0171-9335\(04\)70009-6](https://doi.org/10.1078/S0171-9335(04)70009-6)
- Sacher, M., Barrowman, J., Wang, W., Horecka, J., Zhang, Y., Pypaert, M., and Ferro-Novick, S. (2001). TRAPP I implicated in the specificity of tethering in ER-to-Golgi transport. *Molecular Cell*, 7(2), 433–442.

- Sacher, M., and Ferro-Novick, S. (2001). Purification of TRAPP from *Saccharomyces cerevisiae* and identification of its mammalian counterpart. *Methods in Enzymology*, 329, 234–241.
- Sacher, M., Jiang, Y., Barrowman, J., Scarpa, A., Burston, J., Zhang, L., ... Ferro-Novick, S. (1998). TRAPP, a highly conserved novel complex on the cis-Golgi that mediates vesicle docking and fusion. *The EMBO Journal*, 17(9), 2494–2503. <https://doi.org/10.1093/emboj/17.9.2494>
- Sadler, K. C. (2005). A genetic screen in zebrafish identifies the mutants vps18, nf2 and foie gras as models of liver disease. *Development*, 132(15), 3561–3572. <https://doi.org/10.1242/dev.01918>
- Sambrook, J., and Russel, D. W. (2001). *Molecular cloning: A laboratory manual* (III). Cold spring harbor, New York: Cold spring laboratory press.
- Sato, K., and Nakano, A. (2005). Dissection of COPII subunit-cargo assembly and disassembly kinetics during Sar1p-GTP hydrolysis. *Nature Structural and Molecular Biology*, 12(2), 167–174. <https://doi.org/10.1038/nsmb893>
- Scales, S. J., Pepperkok, R., and Kreis, T. E. (1997). Visualization of ER-to-Golgi transport in living cells reveals a sequential mode of action for COPII and COPI. *Cell*, 90(6), 1137–1148.
- Schonthaler, H. B., Fleisch, V. C., Biehlmaier, O., Makhankov, Y., Rinner, O., Bahadori, R., ... Dahm, R. (2008). The zebrafish mutant lbk/vam6 resembles human multisystemic disorders caused by aberrant trafficking of endosomal vesicles. *Development (Cambridge, England)*, 135(2), 387–399. <https://doi.org/10.1242/dev.006098>
- Schou, K. B., Morthorst, S. K., Christensen, S. T., and Pedersen, L. B. (2014). Identification of conserved, centrosome-targeting ASH domains in TRAPP II complex subunits and TRAPPC8. *Cilia*, 3(1), 6. <https://doi.org/10.1186/2046-2530-3-6>
- Schwake, M., Schröder, B., and Saftig, P. (2013). Lysosomal membrane proteins and their central role in physiology. *Traffic (Copenhagen, Denmark)*, 14(7), 739–748. <https://doi.org/10.1111/tra.12056>
- Schworer, C. M., Shiffer, K. A., and Mortimore, G. E. (1981). Quantitative relationship between autophagy and proteolysis during graded amino acid deprivation in perfused rat liver. *The Journal of Biological Chemistry*, 256(14), 7652–7658.
- Scrivens, P. J., Noueihed, B., Shahrzad, N., Hul, S., Brunet, S., and Sacher, M. (2011). C4orf41 and TTC-15 are mammalian TRAPP components with a role at an early stage in ER-to-Golgi trafficking. *Molecular Biology of the Cell*, 22(12), 2083–2093. <https://doi.org/10.1091/mbc.E10-11-0873>

- Scrivens, P. J., Shahrzad, N., Moores, A., Morin, A., Brunet, S., and Sacher, M. (2009). TRAPPC2L is a Novel, Highly Conserved TRAPP-Interacting Protein. *Traffic*, *10*(6), 724–736. <https://doi.org/10.1111/j.1600-0854.2009.00906.x>
- Shestakova, A., Suvorova, E., Pavliv, O., Khaidakova, G., and Lupashin, V. (2007). Interaction of the conserved oligomeric Golgi complex with t-SNARE Syntaxin5a/Sed5 enhances intra-Golgi SNARE complex stability. *The Journal of Cell Biology*, *179*(6), 1179–1192. <https://doi.org/10.1083/jcb.200705145>
- Shestakova, A., Zolov, S., and Lupashin, V. (2006). COG complex-mediated recycling of Golgi glycosyltransferases is essential for normal protein glycosylation. *Traffic (Copenhagen, Denmark)*, *7*(2), 191–204. <https://doi.org/10.1111/j.1600-0854.2005.00376.x>
- Shirahama-Noda, K., Kira, S., Yoshimori, T., and Noda, T. (2013). TRAPPIII is responsible for vesicular transport from early endosomes to Golgi, facilitating Atg9 cycling in autophagy. *Journal of Cell Science*, *126*(Pt 21), 4963–4973. <https://doi.org/10.1242/jcs.131318>
- Spaapen, L. J. M., Bakker, J. A., van der Meer, S. B., Sijstermans, H. J., Steet, R. A., Wevers, R. A., and Jaeken, J. (2005). Clinical and biochemical presentation of siblings with COG-7 deficiency, a lethal multiple O- and N-glycosylation disorder. *Journal of Inherited Metabolic Disease*, *28*(5), 707–714. <https://doi.org/10.1007/s10545-005-0015-z>
- Starai, V. J., Hickey, C. M., and Wickner, W. (2008). HOPS proofreads the trans-SNARE complex for yeast vacuole fusion. *Molecular Biology of the Cell*, *19*(6), 2500–2508. <https://doi.org/10.1091/mbc.E08-01-0077>
- Suzuki, K. (2001). The pre-autophagosomal structure organized by concerted functions of APG genes is essential for autophagosome formation. *The EMBO Journal*, *20*(21), 5971–5981. <https://doi.org/10.1093/emboj/20.21.5971>
- Tan, D., Cai, Y., Wang, J., Zhang, J., Menon, S., Chou, H.-T., ... Walz, T. (2013). The EM structure of the TRAPPIII complex leads to the identification of a requirement for COPII vesicles on the macroautophagy pathway. *Proceedings of the National Academy of Sciences of the United States of America*, *110*(48), 19432–19437. <https://doi.org/10.1073/pnas.1316356110>
- Taussig, D., Lipatova, Z., Kim, J. J., Zhang, X., and Segev, N. (2013). Trs20 is required for TRAPP II assembly. *Traffic (Copenhagen, Denmark)*, *14*(6), 678–690. <https://doi.org/10.1111/tra.12065>

- Taussig, D., Lipatova, Z., and Segev, N. (2014). Trs20 is required for TRAPP III complex assembly at the PAS and its function in autophagy. *Traffic (Copenhagen, Denmark)*, *15*(3), 327–337. <https://doi.org/10.1111/tra.12145>
- Tokarev, A. A., Alfonso, A., and Segev, N. (2009). Overview of Intracellular Compartments and Trafficking Pathways. In N. Segev, *Trafficking Inside Cells* (pp. 3–14). New York, NY: Springer New York. Retrieved from http://link.springer.com/10.1007/978-0-387-93877-6_1
- Venditti, R., Scanu, T., Santoro, M., Di Tullio, G., Spaar, A., Gaibisso, R., ... De Matteis, M. A. (2012). Sedlin controls the ER export of procollagen by regulating the Sar1 cycle. *Science (New York, N.Y.)*, *337*(6102), 1668–1672. <https://doi.org/10.1126/science.1224947>
- Wang, N., Lee, I.-J., Rask, G., and Wu, J.-Q. (2016). Roles of the TRAPP-II Complex and the Exocyst in Membrane Deposition during Fission Yeast Cytokinesis. *PLoS Biology*, *14*(4), e1002437. <https://doi.org/10.1371/journal.pbio.1002437>
- Wang, W., Sacher, M., and Ferro-Novick, S. (2000). TRAPP stimulates guanine nucleotide exchange on Ypt1p. *The Journal of Cell Biology*, *151*(2), 289–296.
- Wen, J., Hanna, C. W., Martell, S., Leung, P., Lewis, S., Robinson, W. P., ... Rajcan-Separovic, E. (2015). Functional consequences of copy number variants in miscarriage. *Molecular Cytogenetics*, *8*(1), 6. <https://doi.org/10.1186/s13039-015-0109-8>
- Wendler, F., Gillingham, A. K., Sinka, R., Rosa-Ferreira, C., Gordon, D. E., Franch-Marro, X., ... Munro, S. (2010). A genome-wide RNA interference screen identifies two novel components of the metazoan secretory pathway. *The EMBO Journal*, *29*(2), 304–314. <https://doi.org/10.1038/emboj.2009.350>
- Weng, Y.-R., Kong, X., Yu, Y.-N., Wang, Y.-C., Hong, J., Zhao, S.-L., and Fang, J.-Y. (2014). The role of ERK2 in colorectal carcinogenesis is partly regulated by TRAPPC4: TRAPPC4 PARTLY REGULATE ERK2 IN CRC. *Molecular Carcinogenesis*, *53*(S1), E72–E84. <https://doi.org/10.1002/mc.22031>
- Williams, B. C., Karr, T. L., Montgomery, J. M., and Goldberg, M. L. (1992). The *Drosophila* l(1)zw10 gene product, required for accurate mitotic chromosome segregation, is redistributed at anaphase onset. *The Journal of Cell Biology*, *118*(4), 759–773.
- Wu, X., Steet, R. A., Bohorov, O., Bakker, J., Newell, J., Krieger, M., ... Freeze, H. H. (2004). Mutation of the COG complex subunit gene COG7 causes a lethal congenital disorder. *Nature Medicine*, *10*(5), 518–523. <https://doi.org/10.1038/nm1041>

- Xiang, Y., Zhang, X., Nix, D. B., Katoh, T., Aoki, K., Tiemeyer, M., and Wang, Y. (2013). Regulation of protein glycosylation and sorting by the Golgi matrix proteins GRASP55/65. *Nature Communications*, 4, 1659. <https://doi.org/10.1038/ncomms2669>
- Xiao, J., Liu, C.-C., Chen, P.-L., and Lee, W.-H. (2001). RINT-1, a Novel Rad50-interacting Protein, Participates in Radiation-induced G2/M Checkpoint Control. *Journal of Biological Chemistry*, 276(9), 6105–6111. <https://doi.org/10.1074/jbc.M008893200>
- Yamasaki, A., Menon, S., Yu, S., Barrowman, J., Meerloo, T., Oorschot, V., ... Ferro-Novick, S. (2009). mTrs130 is a component of a mammalian TRAPP-II complex, a Rab1 GEF that binds to COPI-coated vesicles. *Molecular Biology of the Cell*, 20(19), 4205–4215. <https://doi.org/10.1091/mbc.E09-05-0387>
- Yen, W.-L., Shintani, T., Nair, U., Cao, Y., Richardson, B. C., Li, Z., ... Klionsky, D. J. (2010). The conserved oligomeric Golgi complex is involved in double-membrane vesicle formation during autophagy. *The Journal of Cell Biology*, 188(1), 101–114. <https://doi.org/10.1083/jcb.200904075>
- Yu, S., Satoh, A., Pypaert, M., Mullen, K., Hay, J. C., and Ferro-Novick, S. (2006). mBet3p is required for homotypic COPII vesicle tethering in mammalian cells. *The Journal of Cell Biology*, 174(3), 359–368. <https://doi.org/10.1083/jcb.200603044>
- Zanetti, G., Prinz, S., Daum, S., Meister, A., Schekman, R., Bacia, K., and Briggs, J. A. (2013). The structure of the COPII transport-vesicle coat assembled on membranes. *eLife*, 2. <https://doi.org/10.7554/eLife.00951>
- Zeevaert, R., Foulquier, F., Jaeken, J., and Matthijs, G. (2008). Deficiencies in subunits of the Conserved Oligomeric Golgi (COG) complex define a novel group of Congenital Disorders of Glycosylation. *Molecular Genetics and Metabolism*, 93(1), 15–21. <https://doi.org/10.1016/j.ymgme.2007.08.118>
- Zhang, Y., Liu, S., Wang, H., Yang, W., Li, F., Yang, F., ... Hu, W. (2015). Elevated NIBP/TRAPPC9 mediates tumorigenesis of cancer cells through NFκB signaling. *Oncotarget*, 6(8), 6160–6178. <https://doi.org/10.18632/oncotarget.3349>
- Zhao, S.-L., Hong, J., Xie, Z.-Q., Tang, J.-T., Su, W.-Y., Du, W., ... Fang, J.-Y. (2011). TRAPPC4-ERK2 interaction activates ERK1/2, modulates its nuclear localization and regulates proliferation and apoptosis of colorectal cancer cells. *PLoS One*, 6(8), e23262. <https://doi.org/10.1371/journal.pone.0023262>

- Zink, S., Wenzel, D., Wurm, C. A., and Schmitt, H. D. (2009). A link between ER tethering and COP-I vesicle uncoating. *Developmental Cell*, 17(3), 403–416.
<https://doi.org/10.1016/j.devcel.2009.07.012>
- Zong, M., Satoh, A., Yu, M. K., Siu, K. Y., Ng, W. Y., Chan, H. C., ... Yu, S. (2012). TRAPPC9 mediates the interaction between p150 and COPII vesicles at the target membrane. *PloS One*, 7(1), e29995. <https://doi.org/10.1371/journal.pone.0029995>
- Zong, M., Wu, X., Chan, C. W. L., Choi, M. Y., Chan, H. C., Tanner, J. A., and Yu, S. (2011). The adaptor function of TRAPPC2 in mammalian TRAPPs explains TRAPPC2-associated SEDT and TRAPPC9-associated congenital intellectual disability. *PloS One*, 6(8), e23350.
<https://doi.org/10.1371/journal.pone.0023350>

6 APPENDIX I

ORIGINAL ARTICLE

A novel TRAPPC11 mutation in two Turkish families associated with cerebral atrophy, global retardation, scoliosis, achalasia and alacrima

Katrin Koehler,¹ Miroslav P. Milev,² Keshika Prematilake,² Felix Reschke,¹ Susann Kutzner,¹ Ramona Jühlen,¹ Dana Landgraf,¹ Eda Utine,³ Filiz Hazan,⁴ Gulden Diniz,⁵ Markus Schuelke,⁶ Angela Huebner,¹ Michael Sacher^{2,7}

• Additional material is published online only. To view please visit the journal online (<http://dx.doi.org/10.1136/jmedgenet-2016-104108>).

For numbered affiliations see end of article.

Correspondence to Dr Katrin Koehler, Division of Paediatric Endocrinology and Diabetology, Department of Paediatrics, Clinical Research, Technical University Dresden, Fetscherstrasse 74, 01307 Dresden, Germany; katrin.koehler@uniklinikum-dresden.de

KK, MPM and KP contributed equally.

Received 16 June 2016
 Revised 2 September 2016
 Accepted 10 September 2016

To cite: Koehler K, Milev MP, Prematilake K, et al. *J Med Genet* Published Online First: [please include Day Month Year] doi:10.1136/jmedgenet-2016-104108

ABSTRACT

Background Triple A syndrome (MIM #231550) is associated with mutations in the AAAS gene. However, about 30% of patients with triple A syndrome symptoms but an unresolved diagnosis do not harbour mutations in AAAS.

Objective Search for novel genetic defects in families with a triple A-like phenotype in whom AAAS mutations are not detected.

Methods Genome-wide linkage analysis, whole-exome sequencing and functional analyses were used to discover and verify a novel genetic defect in two families with achalasia, alacrima, myopathy and further symptoms. Effect and pathogenicity of the mutation were verified by cell biological studies.

Results We identified a homozygous splice mutation in TRAPPC11 (c.1893+3A>G, [NM_021942.5], g.4:184,607,904A>G [hg19]) in four patients from two unrelated families leading to incomplete exon skipping and reduction in full-length mRNA levels. TRAPPC11 encodes for trafficking protein particle complex subunit 11 (TRAPPC11), a protein of the transport protein particle (TRAPP) complex. Western blot analysis revealed a dramatic decrease in full-length TRAPPC11 protein levels and hypoglycosylation of LAMP1. Trafficking experiments in patient fibroblasts revealed a delayed arrival of marker proteins in the Golgi and a delay in their release from the Golgi to the plasma membrane. Mutations in TRAPPC11 have previously been described to cause limb-girdle muscular dystrophy type 2S (MIM #615356). Indeed, muscle histology of our patients also revealed mild dystrophic changes. Immunohistochemically, β -sarcoglycan was absent from focal patches.

Conclusions The identified novel TRAPPC11 mutation represents an expansion of the myopathy phenotype described before and is characterised particularly by achalasia, alacrima, neurological and muscular phenotypes.

INTRODUCTION

Triple A syndrome (MIM #231550) is an autosomal recessive disease characterised by adrenocorticotrophic hormone-resistant adrenal insufficiency, achalasia and alacrima.¹ In addition to the three main features, patients often present with a variety of dermatological features and progressive neurological symptoms involving the central, peripheral and autonomic nervous systems. Some patients also

display intellectual disabilities. The phenotype is highly variable with regard to severity, age of onset and manifestation of all main symptoms. In addition, adrenal failure may occur later in life or may not arise at all.² Classical triple A syndrome is caused by homozygous or compound heterozygous mutations in the achalasia-addisonianism-alacrima syndrome (AAAS) gene on chromosome 12q13.³⁻⁴ This gene encodes a protein of the nuclear pore complex (NPC) named ALADIN (ALacrima Achalasia aDrenal Insufficiency Neurologic disorder).⁵ While most ALADIN mutants fail to localise to the NPC,⁶⁻⁷ mutations in this protein result in dysregulation of cellular redox homeostasis in vitro, suggesting a role in the progressive degeneration of affected tissues.⁸⁻⁹

Recently, a triple A-like disease, the alacrima, achalasia and mental retardation (AAMR) syndrome (MIM #615510) was described to be caused by mutations in the GDP-mannose pyrophosphorylase A (GMPPA) gene on chromosome 2q35.¹⁰ These patients presented at birth or in the first years of life with alacrima, achalasia and psychomotor developmental delay with speech delay, but without clinical symptoms of adrenal insufficiency. Most patients also had muscular hypotonia and share aspects with hereditary sensory and autonomic neuropathies.¹⁰ Although the underlying cellular mechanism of GMPPA dysfunction is not fully known, a loss of function of GDP-mannose pyrophosphorylase, consisting of the regulatory subunit GMPPA and the catalytic subunit GMPPB, is assumed.¹⁰ Interestingly, about 30% of the patients with a suspected triple A syndrome due to a combination of typical symptoms do not harbour any mutations in AAAS or GMPPA suggesting that triple A syndrome is a genetically heterogeneous disorder.¹¹ To date, the intriguing combination of achalasia and alacrima is caused only by mutations in AAAS or GMPPA, whereby hitherto the specific mechanism is obscure. It is assumed that neural degeneration plays a role.

Muscular dystrophy encompasses a large group of muscular disorders with limb-girdle muscular dystrophies (LGMD) accounting for up to one-third of muscular dystrophy cases. The LGMD phenotype has been associated with mutations in 30 different protein-coding genes.¹² The combination of myopathy with mental retardation occurs more frequently in muscular dystrophy-dystroglycanopathy

Genome-wide studies

(MDDG), for example, MDDGB1 (POMT1), MDDGB2 (POMT2), MDDGB3 (POMGNT1), MDDGB5 (FKRP), MDDGB6 (LARGE) and MDDGB14 (GMPPB) mostly affecting O-mannosyl glycosylation of dystroglycans.^{13–19} There are overlapping phenotypes, for example, mutations in GMPPB also cause LGMD2T with mental retardation.¹⁹

Here, we report the discovery of a novel mutation in the trafficking protein particle complex subunit 11 (TRAPPC11) gene in two unrelated consanguineous Turkish families each with two patients suffering from myopathy and intellectual disability including cerebral atrophy, scoliosis, achalasia and alacrima, thus expanding the clinical phenotype of TRAPPC11 mutations.

PATIENTS

The study was approved by the local ethics review board (Medical Faculty, Technical University Dresden; EK820897). All subjects or their legal representatives gave written informed consent to the study. The study was performed in accordance with the Declaration of Helsinki. The two unrelated consanguineous families (F1 and F2) originated from Turkey. The parents are each first-degree cousins. An overview of the symptoms of all patients is given in table 1. Patients' case presentations are reported in detail in the online supplementary information section.

MATERIALS AND METHODS

Homozygosity mapping

Blood samples from patients for DNA analysis were collected after obtaining written informed consent. DNA preparation was

performed according to standard protocols using the QIAamp DNA Mini Kit (Qiagen). Homozygosity mapping was done with DNA samples of three affected patients of both families (F1.II.2, F2.II.2, F2.II.3) using the GeneChip Human Mapping 6.0 SNP array (Affymetrix), as described.²⁰ HomozygosityMapper 2012 (<http://www.homozygositymapper.org>) was used to delineate genetic intervals that were homozygous for 400 SNPs in succession in the affected individuals.²¹ Both families were analysed separately.

Whole exome sequencing

Exonic sequences were enriched from patient F2.II.2 using NimbleGen SeqCap EZ human exome library V2.0 and sequenced on a HiSeq2000 (Illumina) with read length of paired-end 2×100 bp and average coverage of >50-fold. FASTQ files (FASTA format sequences bundled with their quality data) were aligned to the human GRCh37.p11 (hg19) reference sequence using the BWA-MEM V0.7.1 aligner. A variant file was generated for all exons ±20 bp flanking regions using the GATK V3.3 software package and sent to MutationTaster2 (<http://www.mutationtaster.org>) for the assessment of potential pathogenicity.²² Filtering options were used as described.²⁰ All relevant variants were inspected visually using the Integrative Genomics Viewer (<http://www.broadinstitute.org/igv>).

Sanger sequencing and microsatellite analysis

Cosegregations of the TRAPPC11 mutation in families F1 and F2 were verified by automatic Sanger sequencing using an ABI 3130xL genetic analyser and BigDye Terminator Cycle Sequencing Kit 1.1 (Applied Biosystems). Exon 18 and flanking intronic regions were amplified with primer pair 5'-TAA GTG CAG AAG TCA GTA AGA ATG-3' and 5'-ATT TGT TAC TAT GAA ACC ATT AAG AC-3'. Primer pairs for sequencing of coding regions and all exon/intron junctions of the TRAPPC11 gene are listed in online supplementary table S1.

Haplotype analysis was performed with M13-labelled primers by standard semi-automated methods using an ABI 3130xL Genetic Analyzer.²³ Marker information and primer sequences are listed in online supplementary tables S2 and S3. Allele calling was performed using GeneScan Software, V3.7.1 and GeneMapper 4.0 (Applied Biosystems).

RT-PCR analysis

Total RNA from blood was collected into a PAXgene Blood RNA Tube (BD) and prepared using PAXgene Blood RNA Kit (Qiagen). After reverse transcription of messenger RNA (mRNA) with Go Script Reverse Transcription System (Promega), the sequences of exons 17–19 of TRAPPC11 were amplified using the following primers: 5'-ATG AAA GTC CTG ATC CAG AAC-3' (forward primer exon 17) and 5'-GGC ACA TCT TTC CTT GAG TC-3' (reverse primer exon 19).

Fibroblast RNA was isolated using the Nucleospin RNAII kit (Macherey-Nagel) with on-column DNase treatment. Quantitative RT-PCR on cDNA from patients (F1.II.1, F1.II.2, F2.II.3) and two control fibroblasts were set up in triplicates from three independent RNA preparations per sample on a 7300 Real-Time PCR system (ABI) using GoTaq Probe qPCR Master Mix (Promega). Sequences of the wild-type TRAPPC11 allele (exons 17–18) were amplified using oligonucleotide primers 5'-GCT GTG AAA ACT GCT CAG AAG CT-3' (forward primer exon 17), 5'-GGC TTT GCA CTG CAC AAA TG-3' (reverse primer exon 17/18) and probe 5'-FAM TTT CTC TGG CTG GCA GCA ATA TTT TCA CAA TAMRA-3' (exon 17). Sequences of the mutant TRAPPC11 allele (exons 17–19 without exon 18)

Table 1 Clinical presentation of the affected individuals

Patient	F1.II.1	F1.II.2	F2.II.2	F2.II.3
Consanguinity	Yes	Yes	Yes	Yes
Sex	Male	Female	Male	Female
Age	16	12	15	13
Cardinal symptoms of triple A syndrome				
Achalasia	Yes	No	Yes	Yes
Achalasia age of onset (years)	0.5	–	2.5	2
Alacrima	Yes	Yes	Yes	Yes
Alacrima age of onset (years)	Birth	0.5	Birth	Birth
Adrenal insufficiency	No	No	No	No
Epidermal symptoms				
Hyperkeratosis	Yes	Yes	No	No
Neurological and muscular symptoms				
Intellectual disability	Yes	Yes	Yes	Yes
Milestones delay	Yes	Yes	Yes	Yes
Muscular weakness/dystrophy	Weakness	Weakness	Dystrophy	Atrophy
Gait abnormalities	Yes	No gait	No gait	No gait
Cerebral atrophy in MRI	Yes	Yes	Yes	Yes
Speech delay (few words)	Yes	Yes	Yes	Yes
Nasal speech	No	Yes	No	No
Other symptoms				
Short stature	Yes	Yes	Yes	Yes
Dystrophy: body weight <10 percentile	Yes	Yes	Yes	Yes
Epilepsy/seizures	Yes	Yes	–	–
Caries	Yes	Yes	No	No
Nephrolithiasis	Yes	No	No	No
Undescended testis	Yes	–	No	–
Scoliosis	Yes	Yes	Yes	Yes

were amplified in a second reaction using the same forward primer and probe from exon 17 and an artificial reverse primer Ex17/19-R 5'-CAG AAC TGG TTG TAT TCC AAA TGG-3'. Gene transcription was normalised in relation to the transcription of the housekeeping gene β -actin with the following primers: 5'-GCA CCC AGC ACA ATG AAG ATC-3', 5'-CGC AAC TAA GTC ATA GTC CGC-3' and the β -actin-probe 5'-FAM TGC TCC TCC TGA GCG CAA GTA CTC C TAMRA-3'.

Western blot

Lysates of cultured fibroblasts from control individuals or patients were prepared by harvesting cells in lysis buffer (20 mM HEPES, pH 7.4, 0.1 M KCl, 0.5% Triton X-100, 5 mM MgCl₂ with protease inhibitors). A total of 30 μ g of protein was fractionated on an sodium dodecyl sulfate (SDS)-polyacrylamide gel. The fractionated proteins were transferred to a nitrocellulose membrane, blocked for 1 hour with 5% skim milk in 1 \times PBS-T (PBS with 0.1% Tween 20) and then incubated for 1 hour with primary antibody. The primary antibodies used were anti-green fluorescence protein (GFP) (Roche), anti-tubulin (Sigma), anti-LAMP1 (H4A3, Santa Cruz Biotechnology) and anti-TrappC11.²⁴ The appropriate secondary antibodies (anti-rabbit-horseradish peroxidase (HRP) or anti-mouse-HRP) (KPL) were then added in 1 \times PBS-T for 45 min. After washing the membrane, the signal was developed using enhanced chemiluminescence (ECL) western blotting detection reagents (GE Amersham) and visualised on a GE Amersham Imager 600.

VSVG-GFP ts045 assay

Fibroblast cells were infected with virus encoding vesicular stomatitis virus glycoprotein (VSVG)-GFP ts045 for 1 hour at 37°C. The cells were then incubated for ~18 hours at 40°C. Prior to a shift to 32°C, cycloheximide was added to a final concentration of 10 μ g/mL. At various time points, cells were either fixed in 3% paraformaldehyde for 20 min and processed for immunofluorescence microscopy (see below) or quickly harvested in ice-cold lysis buffer (20 mM HEPES, pH 7.4, 0.1 M KCl, 0.5% Triton X-100, 5 mM MgCl₂ with protease inhibitors). For endoglycosidase H (endo H) treatment, 5–20 μ g of total cell lysate was denatured at 100°C for 10 min before the addition of 10 U of endo H. Treated samples were incubated for 1 hour at 37°C. Western blot analysis was used to detect the fusion protein using mouse anti-GFP (Roche). Quantitation of western blots scanned on a GE Amersham Imager 600 was performed using the ImageJ V1.48 program (National Institutes of Health (NIH)) after background subtraction and are expressed as endo H-resistant pixels/(endo H-resistant + endo H-sensitive pixels) at each time point.

Fluorescence microscopy

Following fixation in paraformaldehyde, samples for immunofluorescence microscopy were first quenched with 0.1 M glycine for 10 min, permeabilised in 0.2% Triton X-100 for 5 min and then blocked with 5% normal goat serum (NGS, Cell Signaling Technology) for 40 min. Primary (mouse antibody anti-GFP (Sigma) and rabbit anti-mannosidase II (kind gift from Kelley Moreman, University of Georgia)) were diluted in 5% NGS and incubated overnight at 4°C. After washing with PBS, secondary antibodies (antimouse AlexaFluor-488 and antirabbit AlexaFluor-647) and DAPI were applied for 1 hour at room temperature. Images of 1024 \times 1024 pixel resolution were captured on a Nikon C2 laser scanning confocal microscope fitted with a 63 \times Plan Apo I, NA1.4 objective (Nikon) controlled by

NIS Elements C 4.4 software. Optical sections of 0.2 mm increments were acquired.

Time-lapse microscopy

Fibroblast cells were treated as described for the VSVG-GFP assay except they were plated on glass-bottom dishes (14 mm diameter, thickness of 1.5; MafTek). Immediately after the 40°C incubation, the dishes were placed in the temperature-controlled chamber of the microscope heated to 32°C with 5% CO₂. Time-lapse microscopy was performed beginning at 3 min after the temperature shift (a time necessary to select the cells for imaging) using a 40 \times oil objective (NA 1.3), no binning, on an inverted confocal microscope (LiveScan Swept Field; Nikon), Piezo Z stage (Nano-Z100N; Mad City Labs) and an electron-multiplying charge-coupled device camera (512 \times 512, iXon X3; Andor Technology). Images were acquired with NIS-Elements V4.0 acquisition software every 30 s using a 0.7 s exposure at 0.2 mm increments with a slit size of 50 nm for up to 3 hours. Images were viewed and analysed on ImageJ V1.48 (NIH). Montages of images from the videos with corresponding time points were plotted in Illustrator CS6 (Adobe).

Immunohistochemistry

Muscle biopsy was performed on patient F2.II.3. The muscle biopsy sample from the gastrocnemius muscle was frozen in isopentane precooled in liquid nitrogen and 8–12 mm sections were cut using a cryostat. These sections were stained with routine histochemical and enzyme histochemical stains, such as H&E, modified Gomori's trichrome and Masson's trichrome. A rich panel of antibodies against structural proteins of muscle fibre was performed immunohistochemically. These included antispectrin (Novocastra, NCL-spec1), antidyostrophin N-terminus (Novocastra, NCL-dys3), antiadhalin (Novocastra, NCL- α -sarc) and other antisarcoglycans (Novocastra, NCL- β - δ - γ -sarc) antibodies. In addition, antimyosin heavy chain fast and slow (Novocastra, NCL-MHCf/MHCs) antibodies were used for discriminating between fibre type, and antimyosin heavy chain neonatal (Novocastra, NCL-MHCn) antibody was used for identification of pathological immature fibres.

Statistical analyses

All data sets were shown as means \pm SEM. Statistical significance was assessed using an unpaired two-tailed Student's t-test using the GraphPad Prism software statistical package 6.0 (GraphPad Software). The significance level was set to $p < 0.05$.

RESULTS

Molecular genetics

In the present study, we investigated two consanguineous Turkish families (F1 and F2) each with two affected siblings, who suffer from a triple A-like syndrome with alacrima and achalasia, but without signs of adrenal insufficiency (for laboratory findings, see online supplementary table S4). The parents and three siblings were unaffected, consistent with an autosomal-recessive mode of inheritance. Autozygosity mapping delineated various regions in both families (see online supplementary figures S2 and S3 and table S5), but only one region of 2.7 Mbp on chromosome 4 that was shared by both families and that was flanked by the SNPs rs6854653 and rs9685847 (figure 1A). Whole exome sequencing was performed on patient F2.II.2. In order to identify the common disease gene for both families as well as further potential disease-causing mutations in other genes that were only located in the autozygous regions of family 2 in the potential case of a

Genome-wide studies

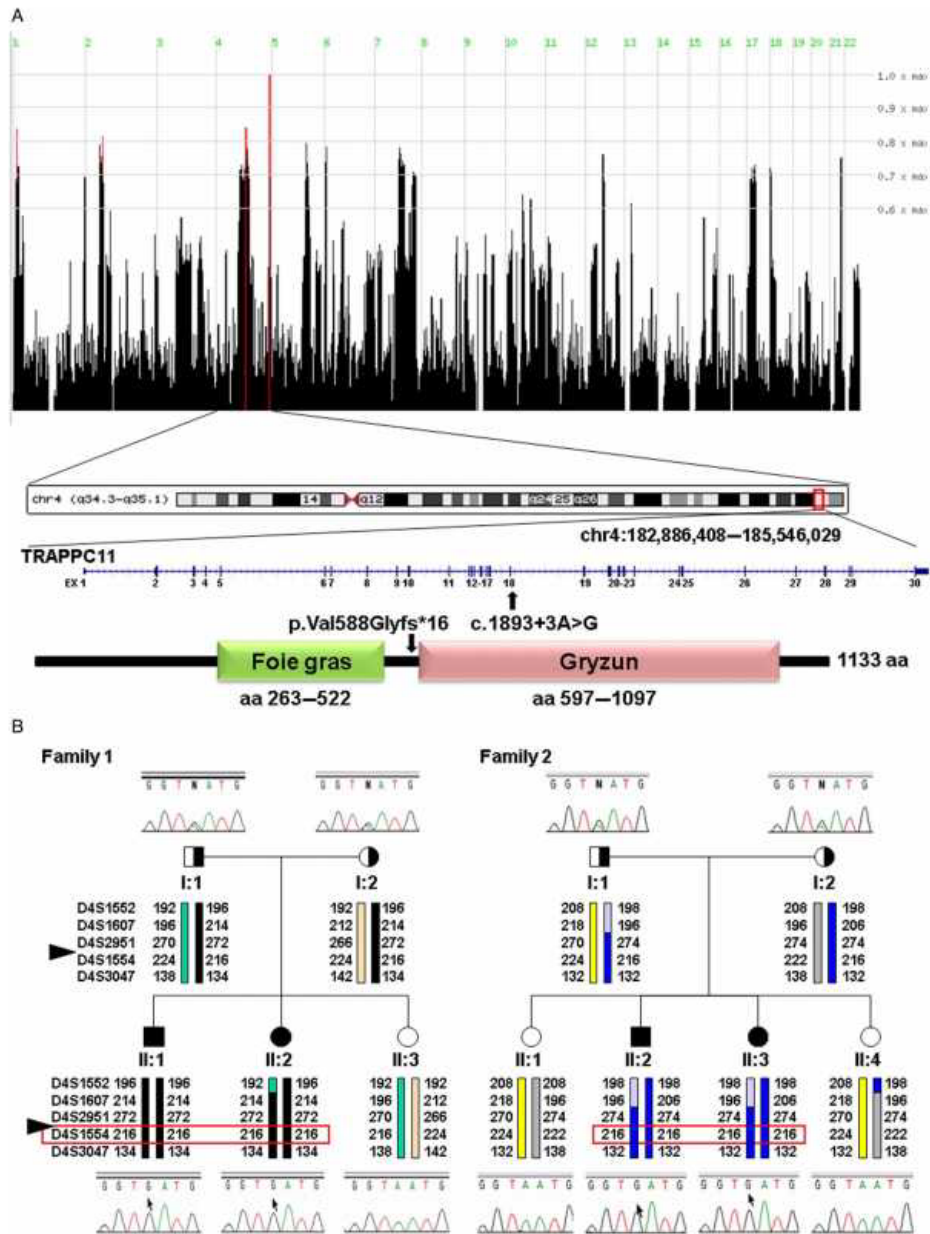


Figure 1 Affected individuals carry a homozygous trafficking protein particle complex subunit 11 (TRAPPC11) mutation. (A) HomozygosityMapper2012 analysis revealed one locus on chromosome 4 with the highest score that was homozygous in all three investigated patients. This locus comprised 2.7 Mbp and covered 30 protein-coding genes. The TRAPPC11 gene is located among them, and the identified DNA alteration and the predicted change at the protein level is indicated. (B) Haplotype analysis using microsatellite markers of the chromosomal TRAPPC11 region revealed a shared haplotype of the TRAPPC11 flanking marker D4S1554 (highlighted by the red square). The sequencing electropherograms at the genomic DNA level of all family members shows the segregation of the mutation in both families.

two-gene disorder,²⁵ we subjected all variants found in all the autozygous regions (corresponding to 548 protein-coding genes) to a MutationTaster2 analysis. Using this approach, we only identified a single homozygous variant in TRAPPC11 (c.1893+3A>G, [NM_021942.5], g.4:184,607,904A>G [hg19]) at the splice donor site of exon 18 that was predicted to affect splicing. The coverage of this position was 132×. The variant was neither listed in the 1000 genome (<http://www.1000genomes.org>) nor in the 5000 exome (<https://http://www.genomeweb.com/sequencing/baylor-sequence-more-5000-exomes-human-disease-studies>) projects or in the dbSNP (<http://www.ncbi.nlm.nih.gov/SNP>) and Exome Aggregation Consortium (ExAC) databases (<http://exac.broadinstitute.org>). The genotype-phenotype segregation in the family was verified by Sanger sequencing. The same mutation could be identified in the second apparently unrelated family (F1), which also segregated with the phenotype (figure 1B). Having identified the mutation in TRAPPC11 as the likely underlying genetic defect in these two families, we screened 56 additional patients affected by triple A syndrome or a triple A-like disorder. These patients were selected since they carry no mutation in AAS or GMPPA. None of these patients revealed a TRAPPC11 mutation in any of the 29 coding exons (exons 2–30) and exon-intron boundaries.

To clarify whether the two families would be closely related, we performed a haplotype analysis using microsatellite markers of the chromosomal TRAPPC11 region. We found a shared haplotype of the TRAPPC11 flanking marker D4S1554 in families F1 and F2 (figure 1B). In the affected patients of family F1, we found a homozygous haplotype over nearly the entire region. Although the two patients of family F2 show a homozygous region around the TRAPPC11 gene, they shared only one flanking microsatellite marker with family F1, indicating that the families are not closely related but the mutation might be a founder mutation.

Consequences of the TRAPPC11 mutation on the transcript level

The c.1893+3A>G mutation was further qualitatively and quantitatively investigated on the mRNA level. After

amplification of exon 17 to exon 19 of reverse transcribed TRAPPC11 mRNA from patients F1.II.1 and F1.II.2, we found that patient cells produced an out-of-frame aberrant splice product in which the 131 bp of exon 18 is missing. Patient cells also produced the regular splice product that includes exon 18 (figure 2A). Quantitative measurements (qRT-PCR with TaqMan) revealed that patient fibroblasts had only 20% of the regular splice product as compared with control fibroblasts (100%) (figure 2B), suggesting an incomplete splicing defect due to the mutation. The aberrant splice product of patient cells was calculated to be only about 12% of the quantity in comparison with the regular splicing product of the control cells. From this, we conclude that a loss of 80% of the intact TRAPPC11 transcripts in combination with an aberrant splicing product causes the phenotype of the patients. Quantitative measurements of mRNA from parent's blood cells revealed comparable levels of the regular splice product in heterozygous carriers of the c.1893+3A>G mutation compared with controls without this mutation. The levels of the aberrant splice product were only about half as high as those of the homozygotes (see online supplementary figure S4).

Western blot analysis of TRAPPC11 and LAMP1

We next sought to determine the consequences on the cellular level of the c.1893+3A>G mutation. The splicing defect that deletes exon 18 is predicted to result in the mutant protein p.Val588Glyfs16*, resulting in a truncation of the protein just prior to the conserved glycosyl domain (figure 1A). Lysates prepared from fibroblasts derived from two affected individuals (F1.II.1 and F1.II.2) were subjected to western blot analysis using rabbit antiserum raised against the human TRAPPC11 protein²⁴ and against the human LAMP1 protein. Since this TRAPPC11 antiserum was raised against an epitope in the extreme carboxy portion of the protein, a truncated product, as expected for this mutation, would not be detected. Rather, we detected a dramatic decrease in the levels of full-length TRAPPC11 in both affected individuals (figure 3A). Small amounts of full-length TRAPPC11 in the lysates from the affected individuals are consistent with the incomplete splicing

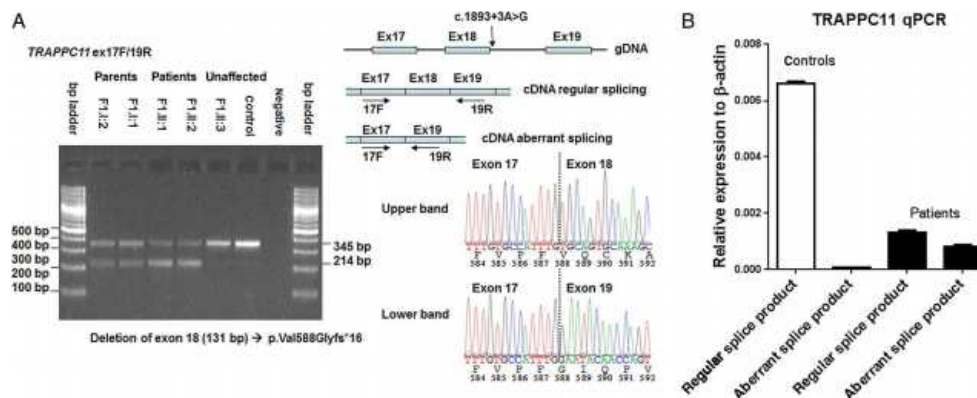


Figure 2 Affected individuals have reduced levels of trafficking protein particle complex subunit 11 (TRAPPC11) transcript as well as a novel splice variant. (A) Agarose gel electrophoresis and sequencing chromatograms of cDNA-derived PCR products using PAXgene blood RNA and primers amplifying exons 17–19. PCR-amplified cDNA fragments were analysed by electrophoresis on a 2% agarose gel and by sequencing. The 345 bp amplicon represents the regular splice product and the 214 bp amplicon represents the aberrant splicing product; control=pooled cDNA; negative=water control. (B) TRAPPC11 mRNA expression analysis performed by TaqMan PCR on fibroblast cDNA. A reduction of ~80% TRAPPC11 expression in affected individuals compared with control was shown.

Genome-wide studies

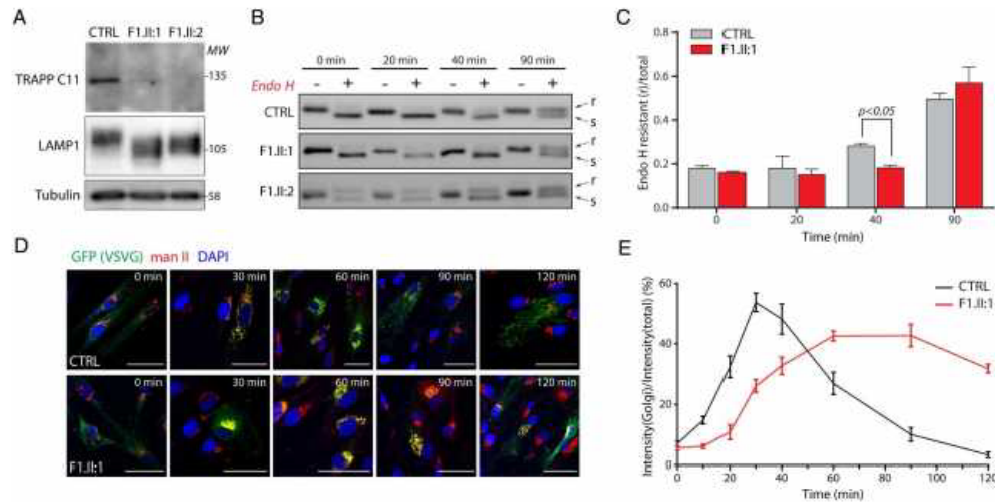


Figure 3 The affected individuals showed a delay in endoglycosidase H resistance and an accumulation of vesicular stomatitis virus glycoprotein (VSVG)-GFP ts045 in the Golgi. (A) Lysates prepared from control, F1.II:1 and F1.II:2 fibroblasts were probed for trafficking Protein Particle Complex subunit 11 (TRAPP C11), LAMP1 and tubulin as a loading control. (B) Fibroblasts were infected with virus encoding VSVG-GFP ts045. The fusion protein was retained in the endoplasmic reticulum (ER) at 40°C overnight. The cells were then treated with cycloheximide and shifted to 32°C to release a synchronised wave of protein from the ER. Samples were collected at the indicated time points and a portion of the lysate was treated with endoglycosidase H (endo H). The protein was visualised by western blot analysis using an anti-GFP antibody. A representative blot is shown. (C) The data from these independent experiments described in (B) were quantitated and are displayed as \pm SEM. Statistical significance was assessed using a Student's t-test. (D) The VSVG-GFP ts045 assay was performed as described in (B) except that the cells were fixed and stained for mannosidase II (man II) and GFP at the indicated time points. Scale bars are 50 μ m. (E) Cells at the time points in (D) were quantified by measuring GFP immunoreactivity intensity in the Golgi region (defined by man II staining) compared with the total GFP immunoreactivity in the cell. For each time point, N ranges from 5 to 15.

defect and reduced mRNA levels of the regular splice product described above. In a previous study characterising the TRAPP C11 mutations p.G980R and p.A372_S429del, hyperglycosylation of lysosomal-associated membrane protein 1 (LAMP1) was demonstrated.²⁴ In contrast to that study we found that LAMP1 was hypoglycosylated in both F1.II:1 and F1.II:2 (figure 3A). This result could reflect a membrane trafficking defect or a role for TRAPP C11 in protein glycosylation as recently reported.²⁷

VSVG-GFP ts045 assay for monitoring the transport along the secretory pathway

Since TRAPP C11 has been implicated in endoplasmic reticulum (ER)-to-Golgi transport,²⁴⁻²⁸ we next used an established assay to follow the movement of a protein from the ER, through the Golgi and on to its final destination, the plasma membrane.²⁹ The marker protein is a temperature-sensitive form of VSVG fused to GFP (VSVG-GFP ts045). At restrictive temperature, the protein is retained in the ER and as the temperature is lowered, in the presence of the protein synthesis inhibitor cycloheximide, there is a synchronised release of the protein from this compartment. Upon reaching the Golgi, the protein is eventually processed such that it becomes resistant to endoglycosidase H (endo H). Fibroblasts from unaffected and affected individuals were infected with a virus expressing VSVG-GFP ts045 and held at restrictive temperature overnight to allow accumulation of the protein in the ER. Samples were collected prior to the downshift in temperature and at time points up to 90 min after downshifting. A portion of the sample was treated

with endo H to assess the location of the protein within the cell. As shown in figure 3B and C, at 40 min post-downshift, there was a slight delay in the acquisition of endo H resistance of the protein in the fibroblasts of affected individuals, suggesting a delay in the exit of the protein from the ER or a delay in traffic through the Golgi complex.

To distinguish between these two possibilities, cells were fixed at the same time points and the location of VSVG-GFP ts045 was assessed by immunofluorescence microscopy (figure 3D). Before downshifting of the temperature in the culture, the marker protein stains the cells in a diffuse reticular pattern consistent with ER localisation. By 20 and 40 min post-downshift, the marker protein colocalised with the Golgi marker mannosidase II in both affected and unaffected individuals. At the later time points, while the marker protein in unaffected individuals clearly separated from the Golgi marker and was found at the cell surface, a significant amount was retained in the Golgi in affected individuals. It is noteworthy that not all fibroblasts in the culture from affected individuals showed this phenotype. In fact, there were a number of cells that failed to show colocalisation between the Golgi marker and VSVG-GFP ts045 at the later time points (see below). Quantitation of the phenotype demonstrated a delay in the exit of the protein from the Golgi in affected individuals (figure 3E).

Time-lapse fluorescence microscopy to investigate dynamic events at the single-cell level

Since each time point in figure 3E represents a population of different cells at a given time point, we used time-lapse

microscopy to follow the movement of VSVG-GFP ts045 within the same cell over time (figure 4A–C and online supplementary movie 1). Consistent with the fixed cell data above, there was a clear delay in the release of the marker protein from the Golgi (quantified in figure 4D). In addition, we noted a slight delay in the arrival of the VSVG-GFP ts045 protein in the Golgi, suggesting there may either be two affected steps in membrane traffic or the delayed arrival in the Golgi may be a secondary consequence of reduced transport through the Golgi. Importantly we identified two populations of cells within the culture from affected individuals: one showing the delays described above, representing ~70% of the cells, and a second with kinetics that were intermediate to those of unaffected cells, representing ~30% of the cells (figure 4C and online supplementary movie 2). This is consistent with the incomplete splicing defect suggested above and indicates that some cells may produce sufficient full-length TRAPPC11 to support near-normal membrane traffic.

Muscle biopsy

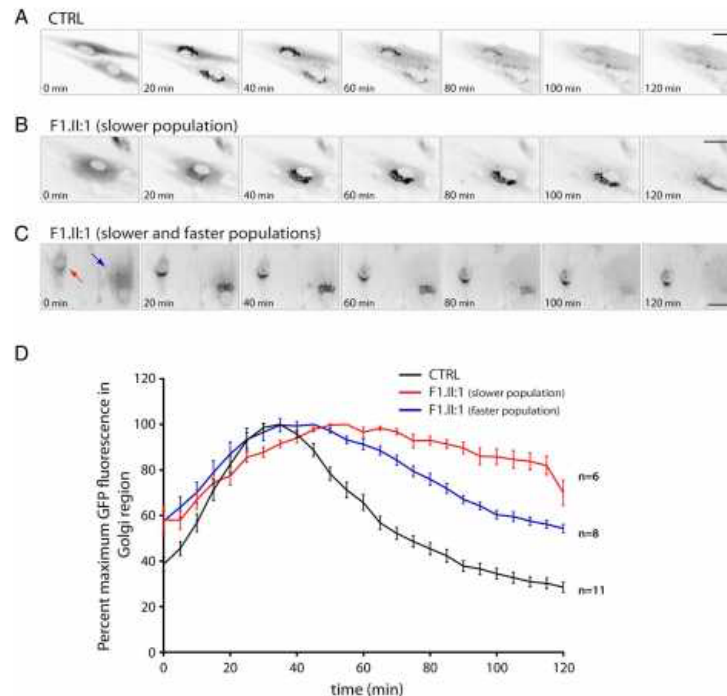
Histopathological evaluation of the muscle biopsy of patient F2.II:3 revealed mild dystrophic changes (figure 5A) like contraction, regeneration, degeneration, nuclear internalisation and fibrosis (figure 5B). In addition, many pathological immature myofibres were seen using the neonatal myosin staining (figure 5C). Based on immunostaining, α -sarcoglycan (α -SGC), delta-sarcoglycan (δ -SGC) and gamma-sarcoglycan (γ -SGC) were present at normal levels (figure 5D), whereas β -sarcoglycan (β -SGC) was deficient and conspicuously absent from focal patches (figure 5E). Other common structural proteins of muscle cell showed normal expression patterns and levels. Interestingly there was also fibre-type grouping (figure 5F), which is specific for denervation with

reinnervation seen in neuropathies and spinal muscular atrophy.³⁰

DISCUSSION

Here, we investigated two apparently unrelated Turkish families each with two patients suffering from cerebral atrophy, global retardation, scoliosis, achalasia and alacrima. All patients have the same novel homozygous splice site mutation in TRAPPC11. The presence of a second mutation was excluded with MutationTaster2 analysis of all further variants found in the autozygous regions of family 2, although the possibility of an additional phenotype-influencing mutation cannot be completely ruled out. Triple A syndrome was initially assumed because the two symptoms alacrima and achalasia of this disease were present. In addition to these symptoms, patients showed more clinical abnormalities that are not described for triple A syndrome patients, although the missing feature of classical triple A syndrome (ie, adrenal insufficiency) may also develop at a later age.³¹ We categorise this phenotype not as a new cause of triple A syndrome but rather as an expansion of the known TRAPPC11 phenotype with myopathy, intellectual disability, alacrima and achalasia. Our patients carry the mutation c.1393+3A>G, which leads to a partial loss of exon 18 (131 bp) resulting in a frameshift mutation (p.Val588Glyfs16*). The predicted shorter protein is estimated to be ~70 kDa in contrast to the full-length protein of ~130 kDa. mRNA quantification and western blot results suggest that the very low amount of intact TRAPPC11 transcript in combination with an aberrant splicing product leads to the dysfunction of the protein and results in the observed phenotype of our patients. The reduced levels of

Figure 4 Live-cell imaging reveals two populations of fibroblasts derived from affected individuals. The vesicular stomatitis virus glycoprotein (VSVG)-GFP ts045 assay was performed as described in the legend to figure 3B except during the shift to 32°C, the cells were imaged every 30 s over a period of 120 min. Still images from the movies at the indicated time points are shown for control (A) and F1.II:1 (B and C). Scale bars are 50 μ m. The full movies are shown in online supplementary movies 1 and 2. (D) The data from the live-cell imaging were quantified (n=6–11) by identifying the Golgi region at the time when the Golgi had a maximum fluorescence intensity (~30 min for the control and ~50 min for F1.II:1) and monitoring GFP fluorescence in the Golgi region for 120 min after the temperature shift. Data are shown as \pm SEM.



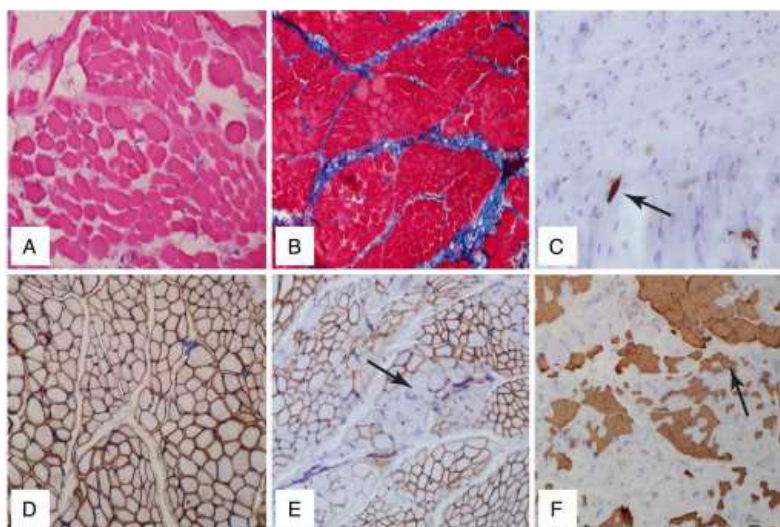


Figure 5 Immunohistochemical analyses reveal dystrophic changes in the affected individual F2II.3. (A) A muscle biopsy from patient F2II.3 was sectioned and stained with H&E to reveal the muscle fibres. Note the marked variation in fibre size and shape (200 \times magnification). (B) Muscle biopsy sections were stained with Masson's trichrome and photographed at 100 \times magnification. There is marked fibrosis as seen by the distended blue-stained portions between the red-stained muscle fibres. (C) Muscle biopsy sections were stained with antibody against neonatal myosin and photographed at 200 \times magnification after 3,3'-diaminobenzidine (DAB) staining. There are a few immature fibres seen in the field (arrow). (D) Staining with anti- β -sarcoglycan revealed normal sarcolemmal expression in muscle biopsy sections following DAB staining (200 \times magnification). (E) Staining with anti- β -sarcoglycan revealed the absence of focal sarcolemmal localisation of the protein following DAB staining (200 \times magnification) (arrow). (F) Staining of muscle biopsy sections with anti-MHCf showed marked fibre type grouping instead of the normal checkboard pattern following DAB staining (100 \times magnification) (arrow).

mutant TRAPPC11 transcript are most likely due to nonsense-mediated RNA decay.³²

The transport protein particle (TRAPP) is a multiprotein complex with several related but compositionally distinct forms. In yeast, these complexes function in a number of processes including ER-to-Golgi transport (TRAPP I), intra-Golgi and endosome-to-Golgi transport (TRAPP II) and autophagy (TRAPP III).³³ TRAPPC11 was identified as a component of the mammalian TRAPP III complex and has no recognisable yeast homologue.²⁴ The disruption of TRAPPC11 by viral insertional mutagenesis in zebrafish resulted in steatosis and cataracts, while RNAi depletion in HeLa cells and *Drosophila* S2 cells resulted in partial disassembly of the TRAPP complex and a defect in membrane transport in the early secretory pathway.^{24 28 34}

Recently a homozygous mutation in the TRAPPC11 gene on chromosome 4q35 was identified in patients with autosomal recessive limb-girdle muscular dystrophy type 2S (LGMD2S) (MIM #615356), characterised by proximal muscle weakness resulting in gait abnormalities, scoliosis and scapular winging. A second homozygous mutation in which a small portion of the protein is deleted resulted in myopathy ataxia, hyperkinetic movements and intellectual disability.²⁴ Furthermore, one Asian patient carrying a compound heterozygous mutation in TRAPPC11 was described with congenital muscular dystrophy (CMD), progressive fatty liver and infantile-onset cataract.³⁵ From these reported cases, it can be concluded that the phenotype caused by TRAPPC11 mutations includes myopathy and some variable accompanying features. Our patients differ from the other published cases in that they also have achalasia and alacrima, two typical symptoms of triple A syndrome. Usually

achalasia is an expression of neurological malfunction (loss of ganglion cells and myenteric nerves). Congenital alacrima is characterised by aplasia or hypoplasia of the lacrimal gland and can be depicted in MRI as bilateral lacrimal gland agenesis.³⁶

We found that LAMP1 was hypoglycosylated in our patients' cells. This result may reflect the recently reported role of TRAPPC11 in protein glycosylation.²⁷ The glycoproteins LAMP1 and LAMP2 provide 50% of lysosomal membrane proteins.³⁷ They are coreponsible for maintaining lysosomal integrity pH and catabolism of lysosomes and play an important role in the function of lysosomes. They are also involved in lysosomal exocytosis, movement of the lysosomes along microtubules and the fusion of phagosomes with lysosomes.³⁸ Acid hydrolases contained in the lysosomes mediate the degradation of cellular components and the defence against bacteria, viruses and toxic substances. Disturbances in these processes can have dramatic effects on cell metabolism. In contrast to our observation of LAMP1 hypoglycosylation, a previous study describing another TRAPPC11 mutation demonstrated not only a reduction in the cellular levels of LAMP1 and LAMP2, but the proteins were observed in a higher molecular size region of the gel as compared with controls, suggesting that they might have a higher degree of glycosylation.²⁴ Taken together with these previous studies, our data suggest that the type of mutation, and not necessarily the cellular levels of TRAPPC11, can influence protein glycosylation. Alternatively the defect in glycosylation may be related to a defect in membrane trafficking processes as was shown by the results in figures 3 and 4.

Disruption of Golgi structure has been reported in other neurodegenerative disorders such as amyotrophic lateral sclerosis,

Alzheimer's disease and Parkinson's disease.^{39–41} It has been suggested that cellular stresses can affect Golgi morphology, possibly through a signalling pathway such as autophagy.⁴¹ Thus, the connection between TRAPPC11 mutations and the observed phenotypes may indeed be complex and need further investigation. Our results extend the cellular, phenotypic and genetic spectrum of TRAPPC11-related disorders and underline the essential role of TRAPPC11 in human physiology and cell homeostasis.

Author affiliations

¹Klinik und Poliklinik für Kinder- und Jugendmedizin, Universitätsklinikum Carl Gustav Carus, Technische Universität Dresden, Dresden, Germany
²Department of Biology, Concordia University, Montreal, Quebec, Canada
³Pediatric Genetics Department, İhsan Doğramacı Children's Hospital, Hacettepe University, Ankara, Turkey
⁴Department of Medical Genetics, Dr. Behçet Uz Children's Hospital, Izmir, Turkey
⁵Neuromuscular Diseases Centre, Tepecik Research Hospital, Izmir, Turkey
⁶Department of Neuropediatrics and NeuroCare Clinical Research Center, Charité-Universitätsmedizin Berlin, Berlin, Germany
⁷Department of Anatomy and Cell Biology, McGill University, Montreal, Quebec, Canada

Acknowledgements We are grateful to Kelley Moreman for providing the antimannosidase II antibody.

Contributors EU and FH phenotyped the patients. MSch and KK processed, analysed and validated the whole exome sequencing data. SK, DL and FR performed the Sanger sequencing. DL performed RNA and microsatellite analysis. MPM and KP performed western blotting. VSVG-GFP ts045 assay, fluorescence and time-lapse microscopy. GD performed the immunohistochemistry. KK, MPM, KP, RJ and MSA analysed and interpreted the data. AH, MSA and KK supervised the work and obtained funding support. KK and MSA wrote the manuscript. All authors read the final version of the manuscript and gave their permission for publication.

Funding This work was supported by a DFG grant HU 895/5-1 and HU 895/5-2 (Clinical Research Unit 252) to AH, SFB 665 TP C4 to MSch, a Canadian Institutes for Health Research grant and a Natural Sciences and Engineering Research Council grant to MSA.

Competing interests None declared.

Patient consent Parental consent obtained.

Ethics approval Local ethics review board (Medical Faculty, Technical University Dresden; EK820897).

Provenance and peer review Not commissioned; externally peer reviewed.

REFERENCES

- Allgrove J, Clayden GS, Grant DB, Macaulay JC. Familial glucocorticoid deficiency with achalasia of the cardia and deficient tear production. *Lancet* 1978;1:1284–6.
- Huebner A, Kaindl AM, Braun R, Handschug K. New insights into the molecular basis of the triple A syndrome. *EndocrRes* 2002;28:733–9.
- Tullio-Pelet A, Salomon R, Hady-Rabia S, Mignier C, De Laet MH, Chouachi B, Bakiri F, Brotier P, Cattolico L, Penet C, Begeot M, Naville D, Nicolino M, Chaussain JL, Weissenbach J, Munnich A, Lyonnet S. Mutant WD-repeat protein in triple-A syndrome. *Nat Genet* 2000;26:332–5.
- Handschug K, Sperling S, Yoon SJ, Hennig S, Clark AJ, Huebner A. Triple A syndrome is caused by mutations in AAA3, a new WD-repeat protein gene. *Hum Mol Genet* 2001;10:283–90.
- Cronshaw JM, Kutchinsky AN, Zhang W, Chait BT, Matunis MJ. Proteomic analysis of the mammalian nuclear pore complex. *J Cell Biol* 2002;158:915–27.
- Cronshaw JM, Matunis MJ. The nuclear pore complex protein ALADIN is mislocalized in triple A syndrome. *Proc Natl Acad Sci USA* 2003;100:5823–7.
- Krumholz M, Koehler K, Huebner A. Cellular localization of 17 natural mutant variants of ALADIN protein in triple A syndrome—shedding light on an unexpected splice mutation. *Biochem Cell Biol* 2006;84:243–9.
- Kind B, Koehler K, Krumholz M, Landgraf D, Huebner A. Intracellular ROS level is increased in fibroblasts of triple A syndrome patients. *J Mol Med* 2010;88:1233–42.
- Jöhlen R, Idkowiak J, Taylor AE, Kind B, Arlt W, Huebner A, Koehler K. Role of ALADIN in human adrenocortical cells for oxidative stress response and steroidogenesis. *PLoS ONE* 2015;10:e0124582.
- Koehler K, Malik M, Mahmood S, Giesselmann S, Beetz C, Hennings JC, Huebner AK, Grahn A, Reunert J, Nüberg G, Thiele H, Altmüller J, Nürnberg P, Müntz R, Babovic-Vuksanovic D, Basel-Vanagaitte L, Borck G, Bramswig J, Mühlberg R, Sarda P, Sikiric A, nyane-Yeboah K, Zeharia A, Ahmad A, Coubes C, Wada Y,

- Marquardt T, Vanderschaeghe D, Van SE, Kurth I, Huebner A, Hubner CA. Mutations in GMPPA cause a glycosylation disorder characterized by intellectual disability and autonomic dysfunction. *Am J Hum Genet* 2013;93:727–34.
- Reschke F, Köhler K, Landgraf D, Susann K, Utine E, Hazan F, Hübner A. A novel mutation of the TRAPPC11 gene causes a disease with cerebral atrophy, global retardation, therapy refractory seizures, achalasia, and alacrima: a triple A-like syndrome. *Neuropediatrics* 2014;45:fp020.
- Vissing J. Limb girdle muscular dystrophies: classification, clinical spectrum and emerging therapies. *Curr Opin Neurol* 2016;29:635–41.
- Vuillaumier-Barrot S, Quijano-Roy S, Bouchet-Seraphin C, Maugeen S, Peudenier S, Van den Bergh P, Marcorelles P, Avila-Smirnow D, Chelbi M, Romero NB, Carlier RY, Estoumet B, Guicheney P, Seta N. Four Caucasian patients with mutations in the fukutin gene and variable clinical phenotype. *Neuromuscul Disord* 2009;19:182–8.
- Balci B, Uyanik G, Dincer P, Gross C, Willer T, Talim B, Haliloglu G, Kale G, Hehr U, Winkler J, Topaloglu H. An autosomal recessive limb girdle muscular dystrophy (LGMD2) with mild mental retardation is allelic to Walker-Warburg syndrome (WWS) caused by a mutation in the POMT1 gene. *Neuromuscul Disord* 2005;15:271–5.
- van Reeuwijk J, Janssen M, van den Elzen C, Beltran-Valero de Bernabé D, Sabatelli P, Merlini L, Boon M, Scheffer H, Brockington M, Muntoni F, Huynen MA, Verrips A, Walsh CA, Barth PG, Brunner HG, van Bokhoven H. POMT2 mutations cause alpha-dystroglycan hypoglycosylation and Walker-Warburg syndrome. *J Med Genet* 2005;42:907–12.
- Clement E, Mercuri E, Godfrey C, Smith J, Robb S, Kinali M, Straub V, Bushby K, Manzur A, Talim B, Cowan F, Quinlivan R, Klein A, Longman C, McWilliam R, Topaloglu H, Mein R, Abbs S, North K, Barkovich AJ, Rutherford M, Muntoni F. Brain involvement in muscular dystrophies with defective dystroglycan glycosylation. *Ann Neurol* 2008;64:573–82.
- Brockington M, Blake DJ, Prandini P, Brown SC, Torelli S, Benson MA, Ponting CP, Estoumet B, Romero NB, Mercuri E, Voit I, Sewry CA, Guicheney P, Muntoni F. Mutations in the fukutin-related protein gene (FKRP) cause a form of congenital muscular dystrophy with secondary lamin alpha2 deficiency and abnormal glycosylation of alpha-dystroglycan. *Am J Hum Genet* 2001;69:1198–209.
- Longman C, Brockington M, Torelli S, Jimenez-Mallebrera C, Kennedy C, Khalil N, Feng L, Saran RK, Voit I, Merlini L, Sewry CA, Brown SC, Muntoni F. Mutations in the human LARGE gene cause MDC1D, a novel form of congenital muscular dystrophy with severe mental retardation and abnormal glycosylation of alpha-dystroglycan. *Hum Mol Genet* 2003;12:2853–61.
- Cars J, Stevens E, Foley AR, Cimk S, Riemersma M, Torelli S, Hoischen A, Willer T, van Scherpenzeel M, Moore SA, Messina S, Bertini E, Bönnemann CG, Abdemur JB, Grossman CM, Kesari A, Punetha J, Quinlivan R, Waddell LB, Young HK, Wraige E, Yau S, Brodd L, Peng L, Sewry C, MacArthur DG, North KN, Hoffman E, Stemple DL, Hurler ME, van Bokhoven H, Campbell KP, Lefeber DJ, UK10K Consortium, Lin Y-Y, Muntoni F. Mutations in GDP-mannose pyrophosphorylase B cause congenital and limb-girdle muscular dystrophies associated with hypoglycosylation of alpha-dystroglycan. *Am J Hum Genet* 2013;93:29–41.
- von Renesse A, Petkova MV, Lützkendorf S, Heinemeyer J, Gill E, Hübner C, von Moers A, Stenzel W, Schuelke M. POMK mutation in a family with congenital muscular dystrophy with merosin deficiency, hypomyelination, mild hearing deficit and intellectual disability. *J Med Genet* 2014;51:275–82.
- Seelow D, Schuelke M. HomozygosityMapper2012—bridging the gap between homozygosity mapping and deep sequencing. *Nucleic Acids Res* 2012;40:W516–20.
- Schwarz JM, Cooper DN, Schuelke M, Seelow D. MutationTaster2: mutation prediction for the deep-sequencing age. *Nat Methods* 2014;11:361–2.
- Schuelke M. An economic method for the fluorescent labeling of PCR fragments. *Nat Biotechnol* 2000;18:233–4.
- Scrivens PJ, Nouchet B, Shahzad N, Hul S, Brunet S, Sacher M. C4orf41 and TTC-15 are mammalian TRAPP components with a role at an early stage in ER-to-Golgi trafficking. *Mol Biol Cell* 2011;22:2083–93.
- Lal D, Neubauer BA, Toliat MR, Altmüller J, Thiele H, Nürnberg P, Kamrath C, Schänzer A, Sander T, Hahn A, Nothnagel M. Increased Probability of Co-Occurrence of Two Rare Diseases in Consanguineous Families and Resolution of a Complex Phenotype by Next Generation Sequencing. *PLoS ONE* 2016;11:e0146040.
- Bögershausen N, Shahzad N, Chong JX, von Kleist-Retzow J-C, Stanga D, Li Y, Bernier FP, Loucks CM, Wirth R, Puffenberger EG, Hegele RA, Schreml J, Lapointe G, Keupp K, Brett CL, Anderson R, Hahn A, Innes AM, Suchowersky O, Mets MB, Nürnberg G, McLeod DR, Thiele H, Waggoner D, Altmüller J, Boycott KM, Schoser B, Nürnberg P, Ober C, Heller R, Parboosingh JS, Wolnik B, Sacher M, Lamont RE. Recessive TRAPPC11 Mutations Cause a Disease Spectrum of Limb Girdle Muscular Dystrophy and Myopathy with Movement Disorder and Intellectual Disability. *Am J Hum Genet* 2013;93:181–90.
- DeRossi C, Vacaru A, Rafiq R, Cinaroglu A, Imrie D, Nayar S, Baryshnikova A, Milev MP, Stanga D, Kadakia D, Gao N, Chu J, Freeze HH, Lehman MA, Sacher M, Sadler KC. trappc11 is required for protein glycosylation in zebrafish and humans. *Mol Biol Cell* 2016;27:1220–34.

Genome-wide studies

- 28 Wendler F, Gillingham AK, Sinka R, Rosa-Ferreira C, Gordon DE, Franch-Marro X, Peden AA, Vincent J-P, Munro S. A genome-wide RNA interference screen identifies two novel components of the metazoan secretory pathway. *EMBO J* 2010;29:304–14.
- 29 Scales SJ, Pepperkok R, Kreis TE. Visualization of ER-to-Golgi transport in living cells reveals a sequential mode of action for COPII and COPI. *Cell* 1997;90:1137–48.
- 30 Hefner RR, Moore D, Balos LL. Muscle Biopsy in Neuromuscular Diseases. In: Mills SE, ed. *Stenberg's diagnostic surgical pathology*. 6th edition. Philadelphia, PA: Wolters Kluwer, 2015:117–118.
- 31 Huebner A, Kaindl AM, Knobloch KP, Petzold H, Mann P, Koehler K. The triple A syndrome is due to mutations in ALADIN, a novel member of the nuclear pore complex. *Endocr Res* 2004;30:891–9.
- 32 Khajavi M, Inoue K, Lupski JR. Nonsense-mediated mRNA decay modulates clinical outcome of genetic disease. *Eur J Hum Genet* 2006;14:1074–81.
- 33 Brunet S, Sacher M. In sickness and in health: the role of TRAPP and associated proteins in disease. *Traffic Cph Den* 2014;15:803–18.
- 34 Sadler KC, Amsterdam A, Soroka C, Boyer J, Hopkins N. A genetic screen in zebrafish identifies the mutants vps18, nf2 and foie gras as models of liver disease. *Dev Camb Engl* 2005;132:3561–72.
- 35 Liang WC, Zhu W, Mitsuhashi S, Noguchi S, Sacher M, Ogawa M, Shih H-H, Jong Y-J, Nishino I. Congenital muscular dystrophy with fatty liver and infantile-onset cataract caused by TRAPPC11 mutations: broadening of the phenotype. *Skelet Muscle* 2015;5:29.
- 36 Li W, Gong C, Qi Z, Wu DI, Cao B. Identification of AAAS gene mutation in Allgrove syndrome: A report of three cases. *Exp Ther Med* 2015;10:1277–82.
- 37 Eskelinen EL. Roles of LAMP-1 and LAMP-2 in lysosome biogenesis and autophagy. *Mol Aspects Med* 2006;27:495–502.
- 38 Schwake M, Schröder B, Saftig P. Lysosomal membrane proteins and their central role in physiology. *Traffic Cph Den* 2013;14:739–48.
- 39 Haase G, Rabouille C. Golgi Fragmentation in ALS Motor Neurons. New Mechanisms Targeting Microtubules, Tethers, and Transport Vesicles. *Front Neurosci* 2015;9:448.
- 40 Joshi G, Bekier ME, Wang Y. Golgi fragmentation in Alzheimer's disease. *Front Neurosci* 2015;9:340.
- 41 Machamer CE. The Golgi complex in stress and death. *Front Neurosci* 2015;9:421.



A novel **TRAPPC11** mutation in two Turkish families associated with cerebral atrophy, global retardation, scoliosis, achalasia and alacrims

Katrin Koehler, Miroslav P. Milev, Keshika Prematilake, Felix Reschke, Susann Kutzner, Ramona Jühlen, Dana Landgraf, Eda Utine, Filiz Hazan, Gulden Diniz, Markus Schuelke, Angela Huebner and Michael Sacher
J Med Genet published online October 5, 2016

Updated information and services can be found at:
<http://jmg.bmj.com/content/early/2016/10/05/jmedgenet-2016-104108>

These include:

References

This article cites 40 articles, 10 of which you can access for free at:
<http://jmg.bmj.com/content/early/2016/10/05/jmedgenet-2016-104108#B1BL>

Email alerting service

Receive free email alerts when new articles cite this article. Sign up in the box at the top right corner of the online article.

Topic Collections

Articles on similar topics can be found in the following collections

[Calcium and bone](#) (305)
[Genetic screening / counselling](#) (879)
[Immunology \(including allergy\)](#) (601)
[Molecular genetics](#) (1249)
[Muscle disease](#) (146)
[Neuromuscular disease](#) (257)

Notes

To request permissions go to:
<http://group.bmj.com/group/rights-licensing/permissions>

To order reprints go to:
<http://journals.bmj.com/cgi/reprintform>

To subscribe to BMJ go to:
<http://group.bmj.com/subscribe/>